Universidade de Aveiro Departamento de Química

Ano 2012/2013

LILIANA DOMINGUES PEDRO

SILÍCIO E SAÚDE VASCULAR

Em colaboração com:

MRC Human Nutrition Research

Universidade de Aveiro Departamento de Química

Ano 2012/2013

LILIANA DOMINGUES PEDRO

SILÍCIO E SAÚDE VASCULAR

Dissertação apresentada à Universidade de Aveiro para cumprimento dos requisitos necessários à obtenção do grau Mestre em Biotecnologia Molecular, realizada sob a orientação científica do Doutor Ravin Jugdaohsingh, investigador sénior do grupo Biomeral Research no Medical Research Council – Human Nutrition Research, Reino Unido; e do Doutor Jorge Saraiva, investigador auxiliar do Departamento de Química da Universidade de Aveiro.

Em colaboração com:

MRC Human Nutrition Research

O júri

presidente

Prof. Doutor João Coutinho
professor associado com agregação da Universidade de Aveiro

Prof. Doutor Jorge Saraiva
investigador auxiliar da Universidade de Aveiro

Prof. Doutora Teresa Santos
professor auxiliar da Universidade de Aveiro

Doutor Nuno Faria
investigador sénior do MRC – Human Nutrition Research, RU

Acknowledgments

I am grateful to my supervisor Dr. Ravin Jugdaohsingh, who supported and helped me throughout this work.
I also wish to thank all lab members in the BMR group, without the help of whom this thesis would not have been possible.
My very special thanks to all the people that made Cambridge and especially MRC a great place to work and learn, and have fun at the same time. This includes more people than I can name in this thesis, but that I will always remember dearly.

Be true to your work, your word, and your friend.
Henry Thoreau

Keywords

Silicon, aorta, cardiovascular health, ageing, extracellular matrix, elastin

Abstract

The involvement of Si in cardiovascular diseases has been suggested by several authors. However, only a small number of studies have investigated the Si content of human aortic tissue. The aim of this study was to investigate age- and gender-related changes in silicon levels of the human aorta. Moreover, associations were sought between silicon and structural components, e.g. elastin of the aortic wall, as to enlighten possible associations between silicon and aortic health.

Forty thoracic aortas, obtained *post-mortem* from female and male subjects between 45 and 83 years old, were analysed for Si content and other elements (Al, B, Cu, Fe, Mn, Zn, Ca, K, Mg, Na and P) by ICP-OES. Elastin was quantified using a colorimetric dye-binding method Fastin™ Elastin assay.

Silicon levels in the aorta samples did not vary significantly with age or gender. Relevant correlations with the Si concentration in the aorta were observed for (1) Cu in the female samples with a significant positive correlation, and (2) a negative correlation with P levels, although this was not significant. Analysis of the elastin concentration in the aorta samples revealed no gender- or age-related changes, although a trend for a decrease in older subjects (< 66 years) was observed. Elastin levels did not correlate with the Si concentrations in the aorta samples, but a negative correlation was observed with Cu in samples from female donors and with K (male and female). Additionally, Si levels in the aorta were also similar to levels analysed in skin biopsy samples (male and female: n = 47, age range = 19 – 72), where a trend for increasing Si levels with ageing was observed in female subjects.

Results from the present study could be used to support the suggestion that silicon affects factors that are involved in progression of aortic stiffness, including the utilization of copper, essential in preventing oxidative damage to adult elastin fibres, and decreasing the adsorption of phosphorus to the matrix proteins and thereby prevent the calcification of the aortic wall.

Palavras-chave

Silício, aorta, saúde cardiovascular, envelhecimento, matrix extracellular, elastina

Resumo

O envolvimento do silício em doenças cardiovasculares, particularmente aterosclerose, foi sugerido por vários autores. No entanto, apenas um número reduzido de estudos investigaram a concentração de Si em aortas humanas. Este estudo teve como objectivo investigar alterações no conteúdo de Si e elastina com a idade e sexo em amostras de aortas humanas. Foram também investigadas correlações entre as concentrações de silício e elastina.

Silício e outros elementos (Al, B, Cu, Fe, Mn, Zn, Ca, K, Mg, Na e P) foram quantificados, através de ICP-OES, em 40 aortas torácicas, obtidas *post-mortem* de indivíduos de sexo masculino e feminino com idades compreendidas entre os 54 e 83 anos. O conteúdo de elastina destas amostras foi determinado através do método colorimétrico Fastin™ Elastin assay.

Não foram observadas correlações significativas entre a concentração de Si nas amostras de aorta com a idade ou sexo dos indivíduos. Correlações entre a concentração de Si e outros elementos foram também investigadas e, para além de uma correlação positiva e significativa, observada entre Si e Cu em amostras provenientes de indivíduos do sexo feminino, foi também identificada uma correlação negativa entre Si e P, embora não significantiva. A quantificação de elastina nas amostras de aorta não demonstrou alterações significantivas com a idade ou sexo dos pacientes, no entanto foi observado um decréscimo na concentração de elastina em individuos de idade avançada (< 66 anos). Correlações negativas relevantes foram observadas entre a elastina e K, e entre elastina e Cu em amostras de indivíduos do sexo feminino. Não foram identificadas correlações significativas entre a concentração de elastina e Si nas amostras de aorta analisadas. Adicionalmente, a concentração de Si na aorta humana foi semelhante à quantidade determinada em amostras de biópsias da pele humana (indivíduos do sexo feminino e masculino: n = 47, faixa etária = 19 – 72), onde foi observada uma tendência para o aumento da concentração de Si com o envelhecimento em indivíduos do sexo feminino.

Os resultados deste estudo poderão ser usados para apoiar a hipótese de que o Si interage com factores que estão envolvidos no envelhecimento vascular e progressivo aumento da rigidez da aorta. Estes incluém a utilização de cobre, essencial na prevenção de danos oxidativos em fibras elásticas maduras (elastina), e também a diminuição da absorção de fósforo em proteínas da matriz extracelular, consequentemente, impedindo a calcificação da parede da aorta.

INDEX

INDEX OF FIGURES

INDEX OF TABLES

ABBREVIATIONS/ACRONYMS

BMI	Body Mass Index: calculate as a function of weight per square of the height (kg/m^2)
BMR	BoneMineral Research group
DMAB	4-(Dimethylamino)benzaldehyde, also known as Erlich's Reagent
ECM	Extracellular Matrix
HNO_3	Nitric Acid
ICP-OES	Inductively Coupled Plasma – Optical Emission Spectrometry
IP	Immunoprecipitation
LOX	Lysyl oxidase
MMP	Matrix metalloproteinase
MRC-HNR	Medical Research Council – Human Nutrition Research
MWAD	Microwave Assisted Digestion
NIPA	Non-Interfering Protein Assay
OAE	Oxalic Acid Extract
OAE*p*	Pooled Oxalic Acid Extracts
OH-Pro	Hydroxyproline
PSBS	Pooled-Sample Based Standards
PTFE	Polytetrafluoroethylene
ROS	Reactive oxygen species
SD	Standard Deviation
SDS PAGE	Sodium Dodecyl Sulfate Polyacrylamide Gel Electrophoresis
$Si(OH)_4$	Orthosalicic acid
SOD	Superoxide dismutase
STD	Standard
TB	Skin tissue bank samples
TPPS	5,10,15,20-tetraphenyl-21H,23H-phorphine tetra-sulfonate (dye)
UK	United Kingdom
UPPA™	Universal Protein Precipitation Agent
VMS	Punch skin biopsies collected by Dr. Ian Wilkinson and Dr. Viknesh Selvarajah
VSMC	Vascular Smooth Muscle Cells
wt	weight

1 MRC – Human Nutrition Research

1.1 BioMineral Research Group

Since the 20th century, scientists have identified different food nutrients and defined nutritional standards and recommendations in order to prevent deficiencies and promote human health. The BioMineral Research (BMR) group concentrates on the role of minerals in health and disease, and focuses particularly in nano-mineral synthesis to help provide new solutions for more bioavailable mineral supplements.

Silicon is not yet generally accepted as an essential nutrient for humans, although numerous studies suggest an important role in bone formation, blood vessels and brain health[1]. In 1972 Carlisle and, Schwarz & Milne first reported that silicon deficiency in chicks and rats, respectively, led to severe bone and connective tissue defects (cartilage and joints) and that these abnormalities could be corrected by silicon supplementation[2]. In the same decade other reports appeared suggesting that, in addition to the aging process, inadequate dietary silicon intake may contribute to some cases of atherosclerosis and hypertension[3, 4]; hypothesizing a preventive role for silicon in cardiovascular health.

Total dietary silicon intake varies greatly between cultures and feeding habits, as it is related to the amounts and proportions of food consumed from animal (low silicon) and plant (high silicon) origin, and the amounts of refined and processed foods in the diet[5]. Bioavailable dietary silicon supplements can be used to optimize dietary silicon intake and consequently improved quality of life.

Focusing on human clinical data, this project proposed to evaluate the possible link between cardiovascular health and nutrition, particularly the silicon content of the ageing aortas and ultimately to provide clues of the biological role of silicon in cardiovascular health and inform upon dietary silicon requirements for a healthy aorta.

1.2 Aims and scopes

The distribution of silicon in animal tissues, the nature of the Si interactions with connective tissues and their components has led to the supposition of an essential if not, an important role for Si in the maintenance of the architecture and resilience of the aortic wall. Not considering the positive results published by Loeper in 1979, on the effect of silicon in cardiovascular diseases, namely atherosclerosis, only a small number of studies have investigated the effect of Si on aortic health. The data currently available is not enough to reach any firm conclusions. Results vary greatly and most were obtained before the development of suitable and accurate methods for trace element analysis/quantification.

The BMR group hypothesized that the Si concentration of the human aorta decreases with ageing and that this reduction correlates with the decrease in elastin content and the decrease in mechanical performance, e.g. elasticity, of the ageing aorta. The aim of this project was to investigate age- and gender-related changes in silicon levels of human aortas, obtained from male and female organ donors of different ages. Moreover, associations were sought between silicon content and elastin concentrations of the aorta. The content of other physiological important elements in the human aorta were also investigated to determine the specificity of the associations with silicon.

A secondary objective was the development of a biochemical assay that would allow the accurate measurement of the total collagen and elastin contents in human aortas using a single sample for both assays.

The research project was divided into two parts: I. Mineral and biochemical study of human aortas: via multi-element quantification by ICP-OES and elastin measurement by colorimetric assays; and II. Method development for elastin and collagen quantification using a single specimen for both analyses.

2 Introduction

2.1 Silicon

Silicon (Si) is ubiquitous element in our environment found mainly as solid phase silicates in rocks (quartz) and soil minerals. The process of weathering gradually releases soluble silicates, mainly orthosilicic acid (or silicic acid), $Si(OH)_4$, a highly bioavailable Si source, into natural water bodies (Figure 1). For years, Si was considered a non-essential trace element, a "fortuitous reminder of our geochemical origins". Only now this element is being recognized as an important trace element for the normal growth and development and, general health of higher animals[6].

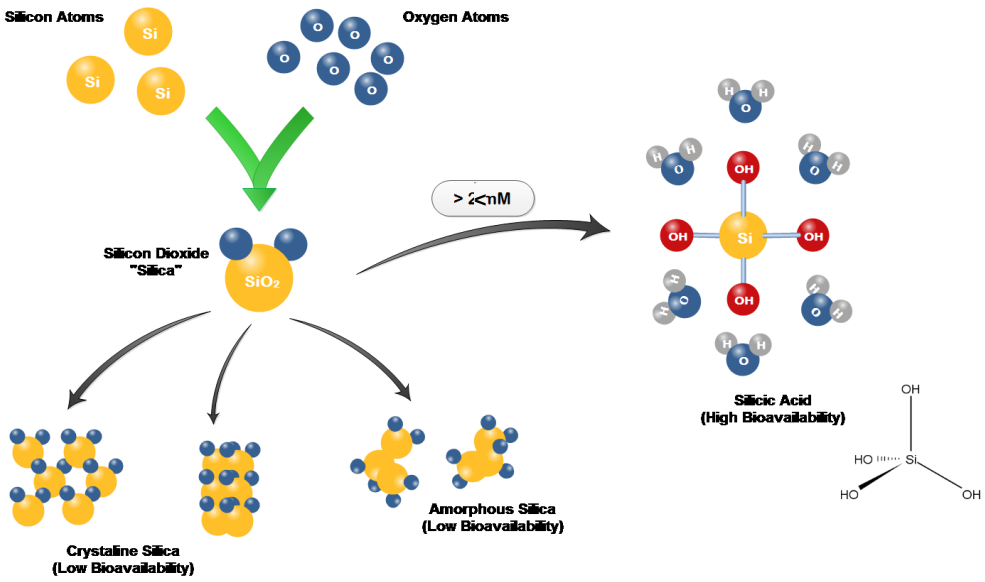

Figure 1 - Silicon and silica chemistry. Silicic acid: soluble molecule with high bioavailability, at concentrations above 2mM Si, $Si(OH)_4$ starts to polymerise towards insoluble polymer/colloidal species. Crystalline and amorphous silica: forms of silicon dioxide or silicates with low bioavailability, most commonly found as quartz and soil minerals. Adapted from Martin, 2007 [7].

2.1.1 *Dietary intake and food sources*

Total dietary silicon intake varies greatly between cultures and feeding habits, as it is related to the amounts and proportions of food consumed from animal (low silicon) and plant (high silicon) origin and the amounts of refined and processed foods in the diet. Dietary intake of Si is between 20-50 mg Si/day

for most Western populations[8] (Figure 2). The highest levels (and sources) of Si are found amongst plant-based foods, especially whole grains, oats, barley, rice and wheat. Likewise, products made from grains are also high in Si, such as breakfast cereals, bread, pasta, biscuits and beer[8, 9]. Although tap water has a relatively low Si content, it has the potential to be a major source to overall Si intake due to the amount normally consumed directly or as an ingredient and/or diluent, e.g. in the preparation of foods and beverages. Manufacturing processes may also affect the Si content of foods. For example dry fruits have relatively high Si levels, since the drying process further increases their Si content due to water loss[9].

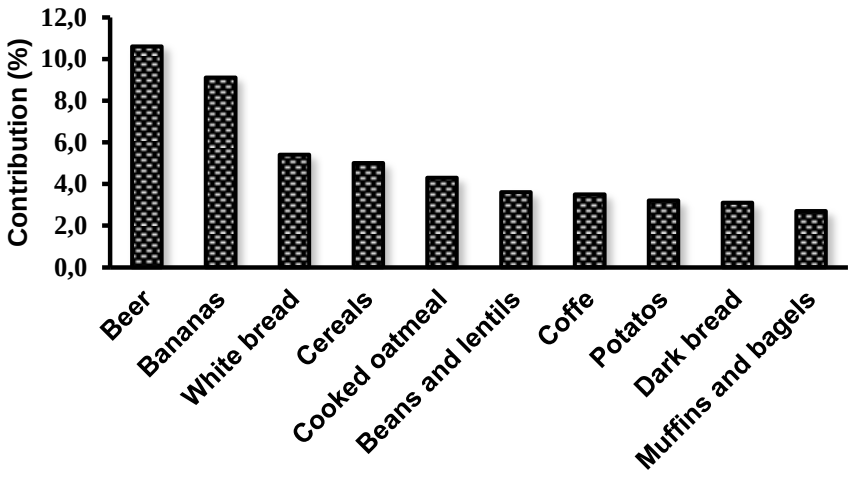

Figure 2 - Major (top 10) food sources that contribute to the total silicon intake in the male population of the Framingham cohort study (USA). Adapted from Jugdaohsingh, 2002 [8].

2.1.2 *Silicon absorption and excretion*

The mechanism of absorption and excretion of Si is still poorly understood. Nonetheless, it is known that the orthosilicic acid in foods and beverages is readily and rapidly absorbed in the proximal small intestine. Other forms (species) of silica need to be broken down to $Si(OH)_4$ prior to absorption in the gastrointestinal tract[10]. The silicon is absorbed across the intestinal mucosa reaches the blood circulation, where it is found virtually non-protein bound[11], and then is readily excreted by the kidneys[10]. Renal function appears to have an

important role in the maintenance of the baseline serum Si concentrations after food ingestion (Figure 3). Moreover it was verified that with any impairment in renal function (e.g. uraemic patients), urinary elimination of silicon decreases and serum silicon concentration increases[12].

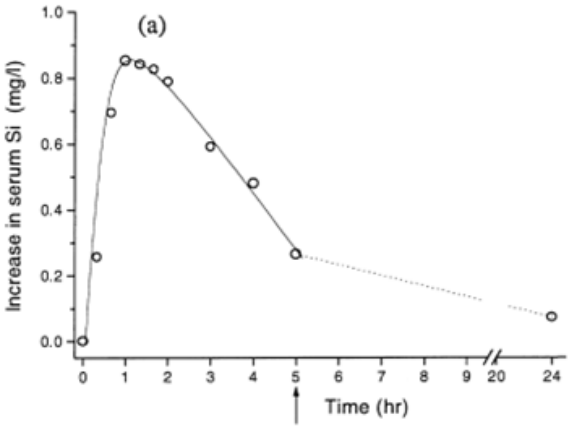

Figure 3 - Silicon uptake and excretion. Uptake of Si into serum, following ingestion (at t=0 h) of an orthosilicic acid solution (of 55.2 mg/L Si) in a healthy fasted volunteer. Ingestion of orthosilicic acid markedly increased serum Si levels and peak concentration was observed between 60 and 84 min. Silicon was rapidly cleared from serum and levels quickly returned to baseline level. Adapted from Reffitt, 1999[10].

2.1.3 *Tissue distribution and metabolism*

Data on silicon concentrations in living tissues is very limited and varies greatly and are generally higher in earlier reports (pre 1980's). Moreover, most of the studies were perform in animals (Figure 4) and, although a similar tissue distribution of Si is expected in humans, this has not been investigated[12]. The development of new and more accurate analytical methods, such as atomic emission spectroscopy techniques, as well as the increasing awareness for environmental sample contaminations, are the most plausible explanations for the more recent lower levels reported[13].

Normal fasting serum Si levels in adults are between 70 – 150 µg/L and increase up to 800 µg/L with ingestion of foods-containing silicon[8].

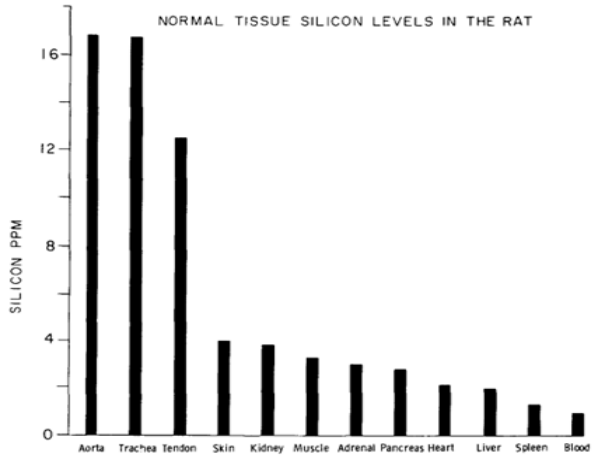

Figure 4 - Normal tissue silicon levels in the rat, expressed in mg/kg (ppm) of wet weight of tissue. Carlisle, 1978[14].

In the rat the highest silicon levels are found in aorta and other connective tissues such as bone, tendon, trachea and skin[14] (Figure 4). Amongst human tissues besides the connective tissues previously mentioned, e.g. aorta, tendon and bone, higher levels of Si were localized in skin and, hair, and lower levels were reported in soft tissues such as liver, heart, adrenals and brain[3]. The reasons behind the high silicon content in connective tissues are suggested to be linked with the association of this element with the glycosaminoglycan and polyuronides fractions, contributing to the structural framework and resilience of connective tissues[15].

Several investigators have postulated that sex and endocrine hormones may regulate the tissue distribution of Si in tissues and its utilization at the cellular level[16, 17]. In a cross-sectional population based study, dietary Si intake was found to be positively and significantly correlated with bone mineral density at the hip site in men and pre-menopausal women; but not in post-menopausal women[18] (Figure 5). A subsequent women only study confirmed the association in pre-menopausal women and showed a restoration of Si bone mineral correlation in post-menopausal women who were taking or had previously taken hormone replacement therapy[19]. The difference in the magnitude of the silicon effect between post-menopausal women and men and pre-menopausal women led to

the conclusion that hormonal factors may be involved. In post-menopausal women circulating estrogen levels are markedly reduced compared to pre-menopausal women, while in men levels are slightly higher than post-menopausal women and little change occurs in estrogen metabolism with ageing[18].

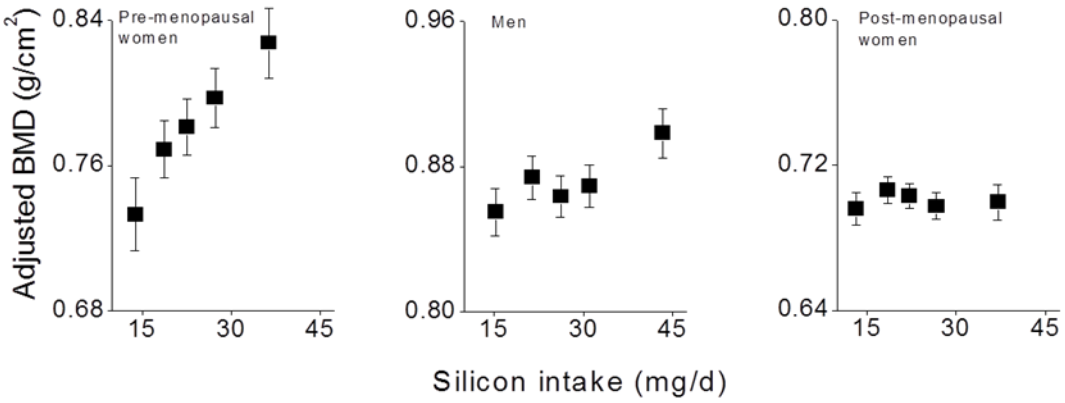

Figure 5 - Correlations between dietary silicon intake and adjusted bone mineral density at the total hip in pre-menopausal, post-menopausal women and mean. Jugdaohsingh, 2004[18].

2.2 Silicon and aortic health

Silicon is not yet generally accepted as an essential nutrient for humans, although numerous studies suggest an important role in bone formation, blood vessels and brain health[12].

In 1972 Carlisle and, Schwarz & Milne first reported that silicon deficiency in chicks and rats, respectively, led to severe bone and connective tissue defects (cartilage and joints) and that these abnormalities could be corrected by silicon supplementation[14] (Figure 6). In the same decade, Loeper and colleagues reported that the silicon content of normal human aorta decreases markedly with ageing and that the concentration of silicon in the arterial wall decreases with the development of atherosclerosis. Furthermore, they stated that "Si partially inhibits lipid deposition by maintaining the normal calibre of elastic fibres, with occasional thickening and proliferation of these fibres"[3] (Figure 7).

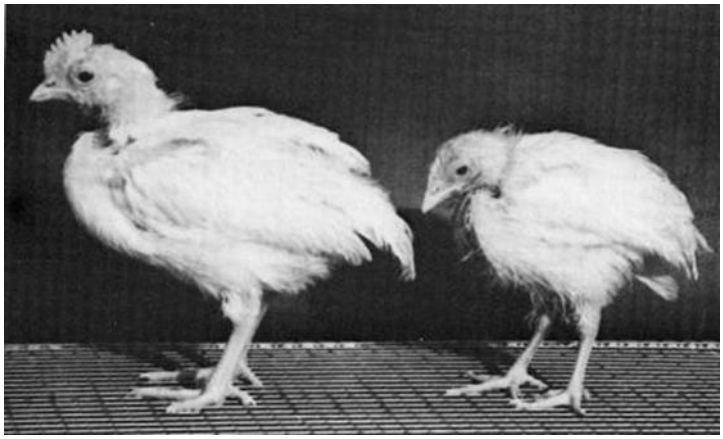

Figure 6 - Carlisle Si deprivation study in chicks. Four week old chicks maintained on a silicon-replete (left) and silicon-deficient (right) diet. Chicks on a silicon-depleted diet had depressed growth, retardation in skeletal development and, skull and connective tissue (combs, wattles and joints) deformations. Carlisle, 1978[14].

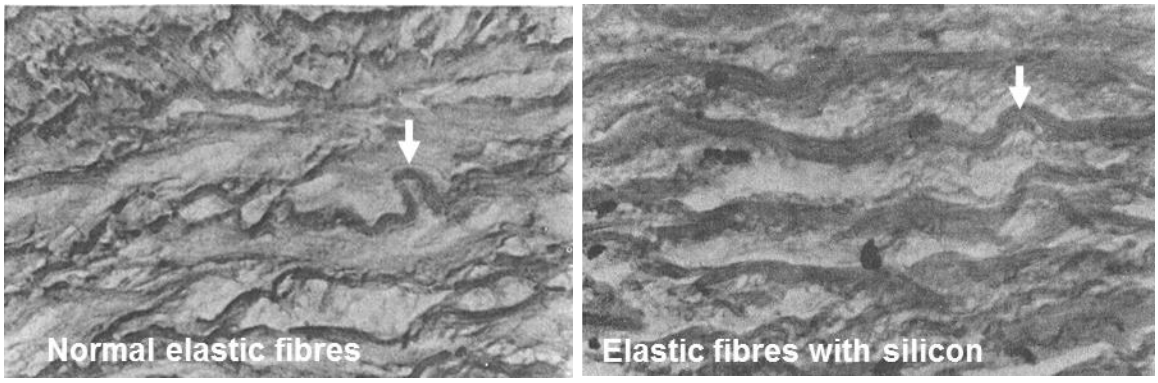

Figure 7 - Effect of silicon on rabbit elastic aortic tissues. Left image: The elastic fibres (white arrows) of a rabbit that received only a cholesterol diet. The fibres are mostly depleted, thin and fragmented. Right image: the elastic fibres of rabits that received a cholesterol diet with silicon are dense, regular and often thickened. Loeper, 1978[3].

2.2.1 *Aorta and aortic stiffness*

The aorta is one of the largest elastic arteries and has two main functions; firstly to carry oxygenated blood to the tissues of the body for their nutrition; and secondly to cushion the blood flow transforming the periodical left ventricular ejection into a continuous flow[20]. The cushioning function is only possible due to the arterial wall structure, which allows the vessel to act like an elastic buffer. Thus the structure of the aortic wall and its elastic behaviour is vital for cardiovascular performance[21].

Aortic stiffness describes the reduce capability and capacity of the aorta to expand and contract in response to pressure changes, and therefore is closely

related to the mechanical properties (e.g. elasticity) of the arterial wall[22] (Figure 8 (b)). With aging, the aortic wall thickness and stiffness are increased due to structural changes in the intima and media layers, these include alterations in the elastin and collagen compositions, calcium deposition and increase of the intima-media thickness[22] (Figure 8 (a))[21].

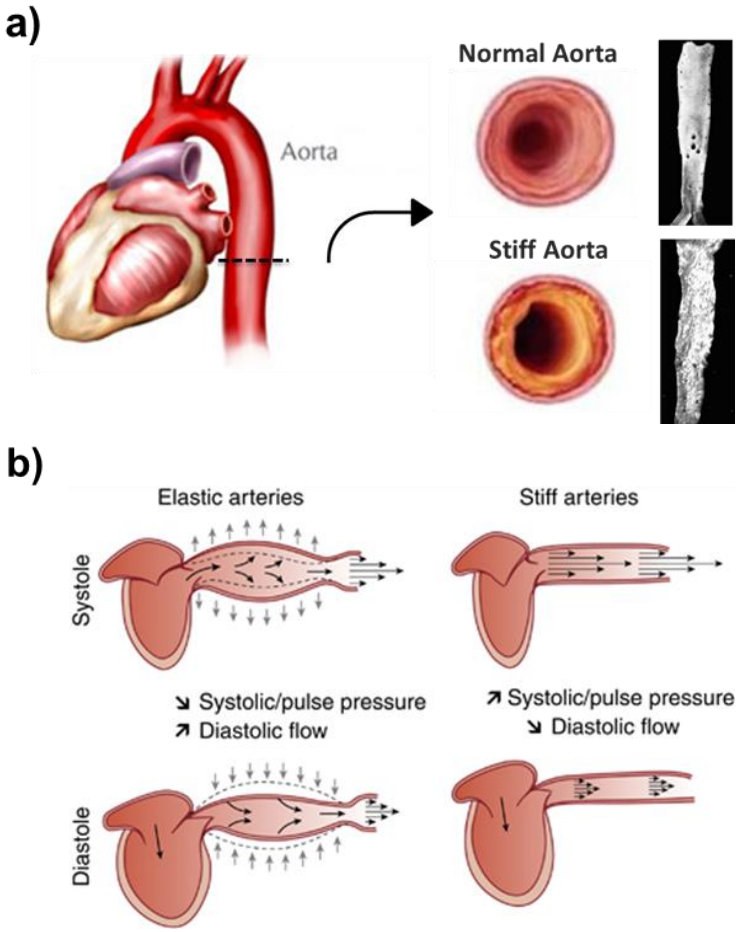

Figure 8 - Aortic stiffness. a) Representation of a normal (upper) and stiff aorta (lower). Note the perfectly smooth appearance of the intima in the normal aorta, compared to the irregular nodules and the rough appearance of the stiff aorta. Adapted from Warfield, 1920[23]. b) Schematic representation of the role of arterial stiffness in decreasing blood flow through the peripheral circulation. Briet, 2012[24].

2.2.2 *Aortic extracellular matrix (ECM) and ageing*

Connective tissues are characterised by the amount, type and arrangement of their ECM components. In addition to providing the architectural framework for the arterial wall that imparts mechanical support and viscoelasticity, the ECM

plays an essential role in the development, remodelling and signalling in the cardiovascular system[22].

The ECM of the aortic wall is composed of two main classes of macromolecules, fibrous proteins and glycoproteins, closely associated with the vascular smooth muscle cells (VSMC) that produce them. These molecules are organized into highly ordered networks that vary within the different layers of the aortic wall, intima, media and adventitia[25]. The tunica media is organized into lamellar units, which consists of concentric layers of elastic fibres, VSMC and interlamellar matrix[25]. Elastic fibres are composed predominantly of elastin, whereas the interlamellar matrix includes type I collagen, type III collagen and other ECM molecules such as glycoproteins, proteoglycans and glycosaminoglycans (or mucopolysaccharides)[22, 25] (Figure 9).

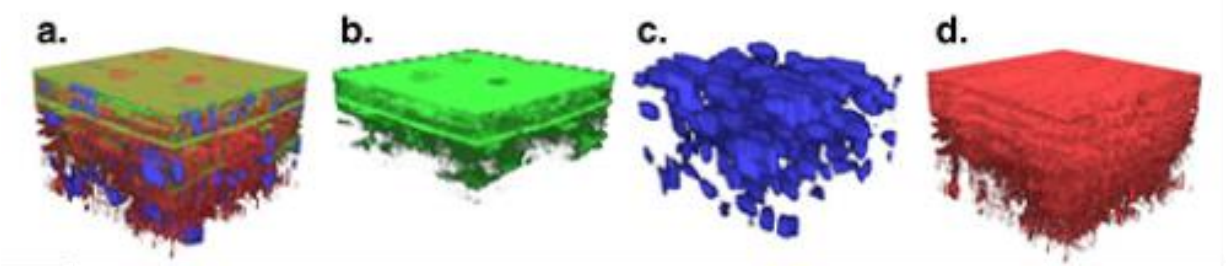

Figure 9 - In vivo arrangement of combined and individual constituents of the aortic ECM. 3D confocal images showing in vivo microstructure (a), in green: elastin (b), blue: VSMC nuclei (c) and red: collagen (d). Lumen surface located at top and aortic layers distributed from top to bottom: tunica intima, tunica media and tunica adventitia. O'Connell, 2008[26].

The two main components that account for the majority of aortic wall mechanical properties are the collagen and elastin fibres[25].

Collagen type I and type III are the most abundant in the mature aorta. These collagen fibrils are known for their ability to self-assemble into highly orientated supramolecular aggregates forming a three-dimensional meshwork in the ECM that provides strength and resilience to the artery wall[25, 27] (Figure 10).

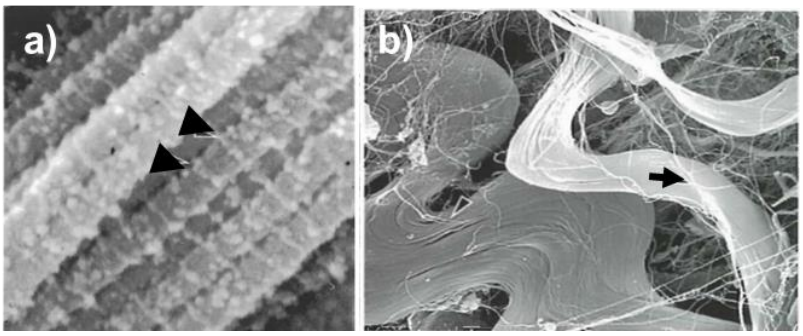

Figure 10 - Collagen fibres in rat aorta. (a) Closer view of a collagen bundle in the rat aortic adventitia. Thin filamentous structures form the characteristic quarter-staggered appearance of collagen type I fibrils with the gaps separating consecutive tropocollagen monomers (arrow heads). (b) Tape-shaped collagen fibres in the rat aortic adventitia with thinner bundles or single collagen fibrils marked with the black arro**w.** Ushiki, 2002[27].

Elastin is the major protein that imparts elasticity to the aortic wall and confers reversible extensibility during cyclic loading[25]. Elastin is a cross-linked polymer of the tropoelastin monomeric form of the protein. Elastin has an amorphous appearance by transmission electron microscopy and is the major component of mature elastic fibres[27] (Figure 11 (b – c)). Elastin is formed through a highly complex process called elastogenesis (Figure 11 (a)). Inside the VSMCs, the elastin gene is activated and the protein tropoelastin is synthesized and released in the extracellular space. Once the tropoelatin is aligned with the microfibriliar lattice, most of the lysil residues will be deaminated and oxidized to allysine by the copper (Cu^{2+}) requiring lysyl oxidase (LOX)[25, 27]. These allysine side chains can subsequently react with adjacent allysil or lysyl residues to form the elastin characteristic tetra-functional desmosine and isodesmosine cross-links, leading to the formation of an insoluble polymer that is the functional form of the elastin protein[27].

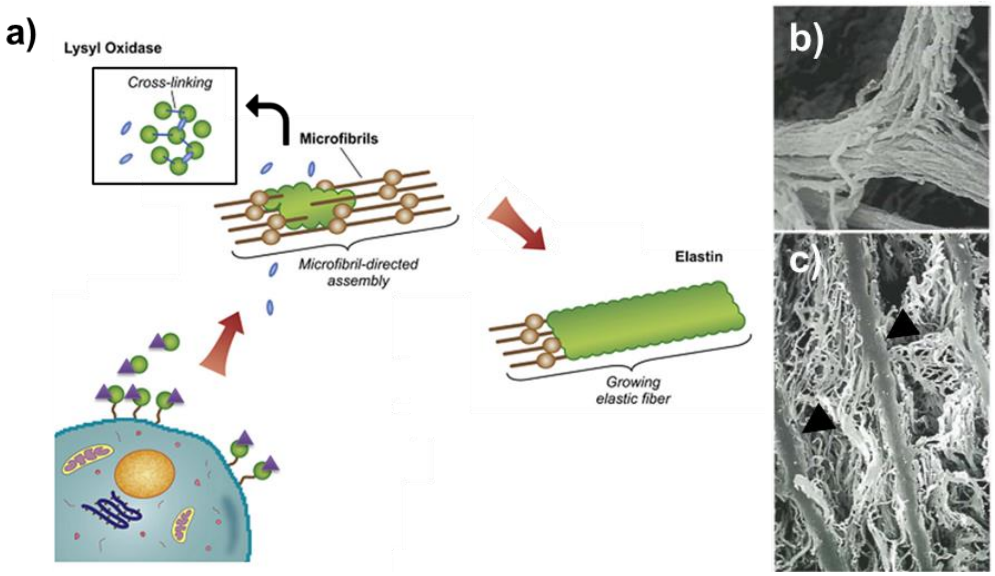

Figure 11 - Elastic fibres synthesis and elastin network. (a) Schematic representation of elastogenesis. Tropoelastin molecules (green spheres) are released into the extracellular space and chaperoned (purple triangles) to the microfibrillar scaffold site. This association prevents the premature aggregation of tropoelastin. When it comes in contact with the microfibrillar structure the tropoelastin molecule is aligned correctly and modified by lysyl oxidase (blue cylinders) and incorporated in the elastic network by irreversible polymerization. Elastin, together with the microfibrils creates the elastic fibre. Adapted from Moore, 2012[28]. (b) Closer view of an elastic fibre in the rat's adventitia. The elastic fibre is seen as a bundle of fine fibrils. (c) Transverse section of the rat aortic media. The media elastic laminae (arrow heads) and interlaminar elastin fibres can be observed. Ushiki, 2002[27].

Mature elastin and collagen are extremely stable, and their turnover rates are so low that they are considered to last for the entire lifespan of the host[25, 29]. However, during aging and during the occurrence of vascular pathologies, the balance between proteases and their inhibitors is temporally destroyed[29]. Increased oxidative stress and expression of matrix metalloproteinases (MMP), such as MMP-2 and MMP-9, and proteolytic enzymes with "elastase-like" activity, have been reported to be involved in the thinning and degradation of vascular elastin and collagen fibres in ageing[29, 30] (Table 1).

Table 1 - Proteinases and metalloproteinases (MMP) detected in vascular and inflammatory cells that participate in vascular ECM remodelling. Jacob, 2003[29].

Proteinases produced by vascular cells	Proteinases produced by inflammatory cells	Inhibitors
MMPs:	MMPs:	TIMPs,
Collagenases: MMP-1 [a]	Collagenases: MMP-1 (MΦ), MMP-8 (PMN), MMP-13 (MΦ)	α2-macroglobulin
Gelatinases: MMP-2, MMP-9 [a]	Gelatinases: MMP-2 (MΦ, lymphocytes), MMP-9 (MΦ, PMN)	
"Elastases": MMP-7	"Elastases": MMP-7 (MΦ), MMP-12 (MΦ)	
Stromelysins: MMP-3 [a]	Stromelysins: MMP-3 (MΦ)	
MT-MMPs: MMP-14		
Serine proteases:	Serine proteases:	α1-Antitrypsin,
SMC elastase	Leukocyte elastase (PMN)	α2-macroglobulin, elafin
	Cathepsin G (PMN)	
Cysteine proteases:	Cysteine proteases:	
Cathepsin S [a]	Cathepsin S (MΦ)	Cystatin
	Cathepsin K (MΦ)	

[a] Enzymes not expressed in basal conditions

Elastin expression, in most tissues, occurs only during late gestation until the end of childhood with negligible synthesis in adulthood. Thus, when the elastic fibres are damage during aging (or as a result of tissue injury); they are generally not repaired or replaced. Instead, more collagen is produced, decreasing the amount of elastin compared to collagen and shifting the arterial mechanical properties into the stiffer (100-1,000 times stiffer) range of collagen fibres[27, 29].

The cumulative effects of the enzymatic degradation plus the structural and functional modifications of ECM components of the aortic wall during ageing, result in the degeneration and thinning of the elastin fibres with a gradual transfer of mechanical loading to collagen and in the increase of the microscopic calcification of the aortic media[22, 25].

2.2.3 *Silicon in the maintenance of aortic ECM*

The arterial wall is considered to be the main site of action for silicon in the aortic health. The potential involvement of Si in atherosclerosis was suggested

based on the remarks that the Si content in the aorta is higher than in other tissues and it decreases with ageing and the development of atherosclerosis and hypertension[3, 13] (Figure 12 & Table 2).

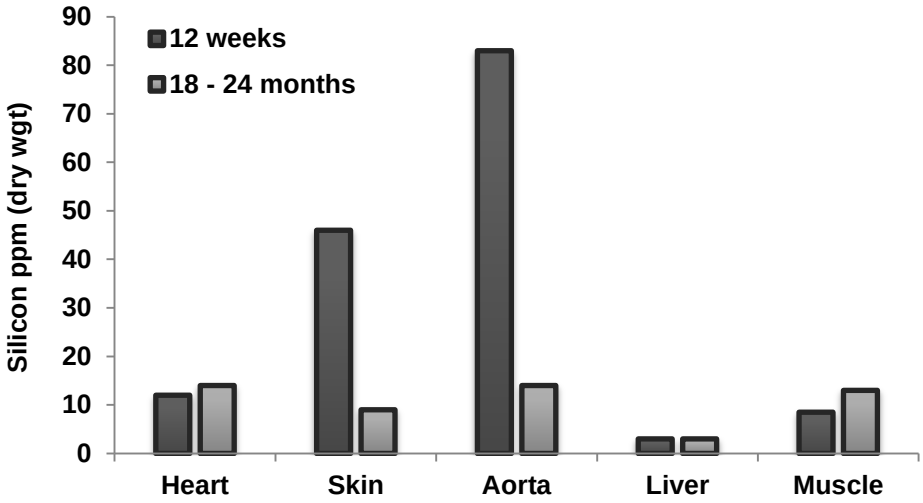

Figure 12 - Effect of age on rabbit tissue silicon levels. Values represent mean silicon levels of 18 rabbits expressed as part per million (ppm) dry weight of tissue. Carlisle, 1975[2].

Table 2 - Silicon and cardiovascular diseases.

Author	Publication Year	Species	Cardiovascular disease	Study Findings
Loeper[3]	1974	Humans	Atherosclerosis	Silicon concentration decreases in direct proportion to the severity of the atheromatous lesion
Schwarz[13]	1975	Humans	Coronary heart disease	Inverse relation between silicic acid in drinking water and the prevalence of coronary heart disease in Finland
Dawson[31]	1978	Humans	Hypertension, Atherosclerosis	Significant negative correlations between silicon levels in drinking water and mortality rates for hypertension and atherosclerosis.
Nakashima[32]	1984	Humans	Atherosclerosis	Increase in arterial silicon content is related to the occurrence and/or progression of atherosclerosis
Najda[33]	1991	Rats	Atherosclerosis	Increase in HDL-cholesterol and HDL-phospholipid concentrations and, decrease in LDL-cholesterol and triglyceride levels in the silicon supplemented group.
Maehira[34]	2011	Rats	Hypertension	Silicon reduces hypertension in spontaneously hypertensive rats by stimulating intracellular Mg uptake and antihypertensive and anti-atherogenic gene expressions.

Loeper and Fragny observed that Si partially inhibits lipid deposition through the preservation of elastin fibres (Figure 7) and mucopolysaccharides integrity which enhances the impermeability of the vessel wall to lipid and calcium deposition[3]. Conversely, Nakashima measured the Si content of normal (healthy), fatty streaks and atheroma of human aortic intima and found an increased in the aortic intima Si content with the development of atherosclerosis, although no correlation was found between Si content and ageing[32] (Table 2). The differences between these reports may originate from the different aortic tissue used for Si measurement. As only the intima layer was analysed in the studies by Nakashima, it is still possible that the Si content of the aorta as a whole, could decrease with the development of atherosclerosis as found by Loeper's original study.

A structural role for silicon has also been proposed, mainly supported by the findings that in connective tissues, silicon is integrally associated with glycosaminoglycans and polysaccharides fractions, especially hyaluronic acid, chondroitin 4-sulfate and dermatan sulphate[15, 35]. The metabolic processes by which Si is assimilated and incorporated within glycosaminoglycans is not understood, but in a stereochemical point of view, it is plausible that Si may be incorporated as a mono- or disaccharide derivative during the polysaccharide synthesis[15]. Additionally, Si has been shown to play a role in the formation of the cross-links between collagen and proteoglycans, thus stabilizing the matrix molecules and preventing its enzymatic degradation[36]. These findings lead to the proposal that Si is covalently bound to the carbohydrate matrix, where it may play an important role in the structural organization of these molecules, functioning as a biological cross-linking agent and holding the glycosaminoglycans and proteins together in an organized fashion[15, 36].

The biochemical role of silicon in the connective tissue synthesis and maintenance of cardiovascular health has also been associated with in its aptitude to influence the biological availability, uptake, utilization, distribution and excretion of

metals, essential and toxic[37]. The metabolism of the different minerals are highly interdependent of each other, so it's not surprising that Si, by affecting the uptake of one mineral, may promote major changes in the organism's metabolic functions. Recent work have suggested that the association between silicon and connective tissue synthesis and function, including its effects on the integrity of the elastin and collagen fibres in the artery wall, may be due to the ability of Si to influence the metabolism of other essential metals, such as copper, iron and manganese, that are vital co-factors in enzymes involved in connective tissue synthesis and structure[37, 38].

Silicon facilitates copper utilization and iron absorption and transportation[38, 39]. Copper and iron are crucial in the synthesis of elastin and collagen fibrils, acting as essential co-factors for the enzymes involved in the cross-link formation (LOX) and hydroxylation of proline residues (prolyl 4-hydroxylase) during collagen and elastin synthesis[40] (Figure 11). Experimental and epidemiological studies on animals and man, have shown that Cu deficiency leads to the abnormal synthesis of elastin and collagen in arteries, thus damaging the elastic properties of the vessel wall[41]. Moreover, Si supplementation in calves and quails led to marginal increase in the calcium and phosphorous content of the tibia. It seems that silicon affects ECM in both tissues (bone and vascular tissues). In bone, which is naturally calcified interacts with Ca and P favouring the calcium incorporation into the bone, but in the aorta it prevents damage of the wall and prevents subsequent calcification[42].

Aluminium accumulation influences the pathogenesis of Alzheimer's disease and also interferes with the intracellular calcium homeostasis and enzymatic activity of several Mg and Fe dependent enzymes. Silicon interacts with aluminium species to form aluminosilicates reducing its gastro-intestinal absorption and enhancing its excretion via kidneys and therefore reducing its potential toxicity[37].

2.3 Analytical techniques

Earlier studies investigating the silicon content of human aortas used colorimetric assays[3, 32] that are prone to interference and it is unlikely that environmental contaminations were assessed[13].

2.3.1 *Total elemental analysis*

Silicon and other trace-elements concentration in the aorta were evaluated by inductively coupled plasma – optical emission spectrometry (ICP-OES); an analytical technique that is highly suitable for biological samples and one can obtain multi-element information rapidly and accurately. The BMR group have extensive experience with this technique/method particularly for Si analysis. Prior to analysis the samples were converted into the liquid state through a digestion procedure: closed-vessel microwave assisted digestion (MWAD).

2.3.1.1 Closed-Vessel MWAD

Biological samples, such as aortic tissue, have a very complex matrix composed of carbohydrates, proteins and lipids; and thus, not completely soluble in water or organic solvents. Sample digestion methods must therefore efficiently decompose the sample matrix to allow complete solubility of the biological matrix and the release the analyte(s) of interest.

Microwave-assisted acid digestion has become the favour method of preparation of samples for total elemental analysis. Some of the advantages of this technique include a higher temperature and pressure, which reduces the digestion time, use of ultra clean plastic ware (PTFE), which reduces the potential contaminants, reduction in acid volume and sample mass and a reduction in the loss of volatile species[43]. The single reaction chamber features a large, pressurized reaction chamber into which all samples were placed simultaneously for microwave digestion. The sample vials sit in a hydrogen peroxide solution that provides a consistent load for the delivered microwave energy. This insures even heating and

consistent conditions in all the sample vials, but it also soaks up energy from exothermic reactions. The chamber is pressurized with nitrogen to prevent the boiling of samples and to eliminate possible cross contamination[43] (Figure 13).

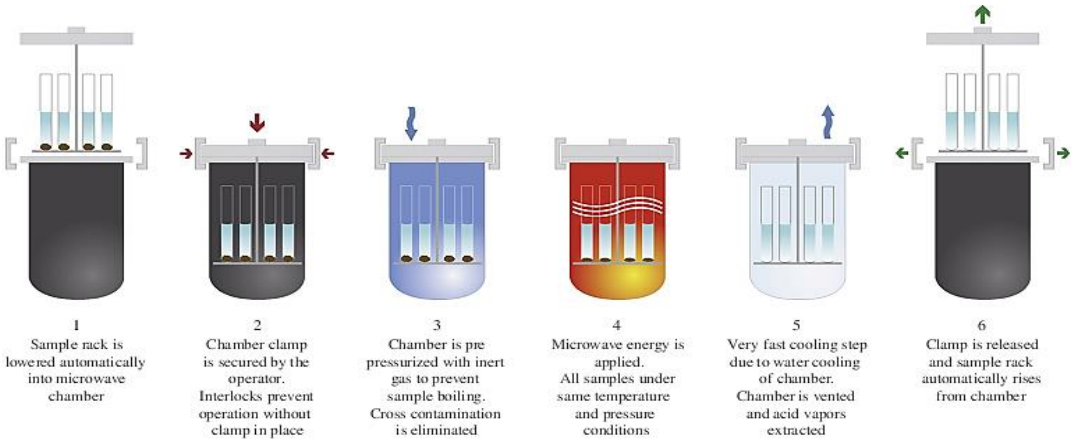

Figure 13 - Flow diagram of the single reaction chamber operation in the UltraWAVE™ microwave digestion system. Nóbrega, 2012[43].

2.3.1.2 ICP-OES

ICP-OES is one of the most common techniques for elemental analysis. A plasma source is used to vaporise the sample into its constituent atoms or ions, further collisional excitation within the plasma promotes the transition of the outer electrons to a higher energy level. The energy absorbed by the electrons is released on return to the resting state by emitting photons of a characteristic wavelength depending on the element present (qualitative information) (Figure 14). The intensity of the radiation (energy) released is related to the number of transitions, which is proportional to the element concentration in the sample (quantitative information)[44].

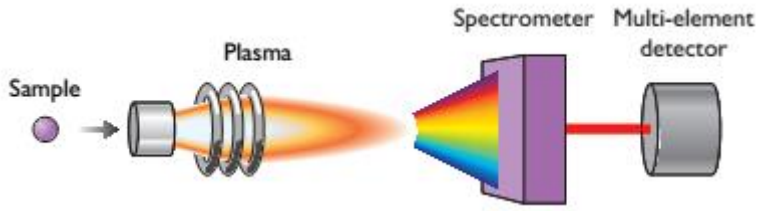

Figure 14 - Schematic of an ICP-OES. A plasma source is used to excite the sample atoms to excite states; the intensity of the radiation emitted at specific wavelengths is measured and used to determine the concentrations of the elements of interest.

One of the major advantages of ICP-OES is its capability for multi-element analysis. The ICP-OES at MRC-HNR has a polychromator attached for simultaneous analysis of up to ten elements, which can be analysed in the same amount of sample that is required to determine one element using a monochromator. This is ideal for biological samples, like the aorta specimens analysed in this work, where sample volume is limited.

2.3.2 *Biochemical Assays for the Aortic Matrix*

The elastin content of the aortic specimens was analysed using a quantitative dye-binding method, developed based on the Fastin™ Elastin Assay. Collagen was determined using a colorimetric assay for hydroxyproline, after the removal of the elastin peptides present in the matrix by immunoprecipitation (IP).

2.3.2.1 Elastin Quantification

Experimental procedures reported in literature were compared for elastin quantification. The following criteria were considered: I. Type of elastin measured (cross-linked and/or soluble); II. Detection limit; III. Accuracy of method; IV. Sample preparation; V. Interfering agents; and VI. Cost per analysis. The *Fastin™ Elastin Assay* was selected as a suitable method for elastin measurement in human aortic tissue.

The Fastin™ Elastin Assay is a quantitative dye-binding method for the analysis of soluble elastin peptides. Insoluble cross-linked elastin can also be measured by the extraction and reduction of this protein in the form of soluble cross-linked polypeptide elastin fragments (α-elastin) by hot oxalic acid treatment. The quantification of soluble α-elastin is based on the release of a bound elastin-specific dye, 5,10,15,20-tetraphenyl-21H,23H-porphine tetra-sulfonate (TPPS), that is firmly retained by the basic amino acid side chain residues of elastin (Figure 15). The presence of other soluble proteins or complex carbohydrates does not interfere with this assay.

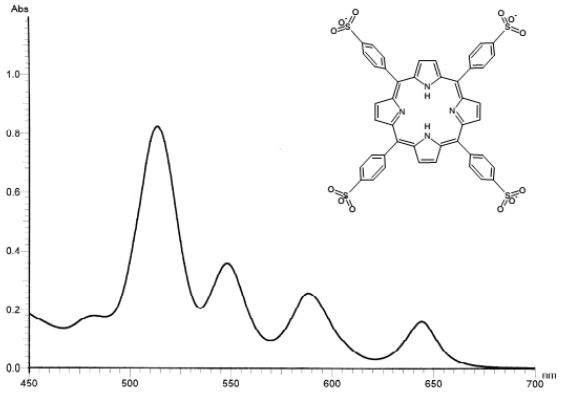

Figure 15 - The visible absorbance spectrum and structural form of TPPS.

2.3.2.2 Collagen Quantification

Hydroxyproline (OH-Pro) is an imino acid that is unique to collagen and elastin[45], and is widely used as a factor to estimate the collagen content in biological samples. An immunoprecipitation step was combined with OH-Pro amino acid quantification assay to remove the elastin present the aortic ECM and accurately quantify the collagen content.

The determination of the hydroxyproline composition of a polypeptide consists of two steps: I. Complete hydrolysis of the tissue lysate proteins to liberate the residues; and II. Quantification of the free OH-Pro amino acids.

2.3.2.2.1 Immunoprecipitation

Immunoprecipitation is a method that enables the purification of a protein from a complex mixture using a protein specific antibody immobilized on a solid support. The antibody is pre-immobilized onto an insoluble support, such as agarose beads, and then incubated with the tissue lysate containing the target protein. The immobilized immune complexes are collected from the lysate, eluted from the support and finally analysed.

For this project the elastin was immobilized using the Thermo Scientific Pierce Classic IP kit, via Protein A/G agarose beaded support coupled with a monoclonal anti-Elastin antibody (Figure 16).

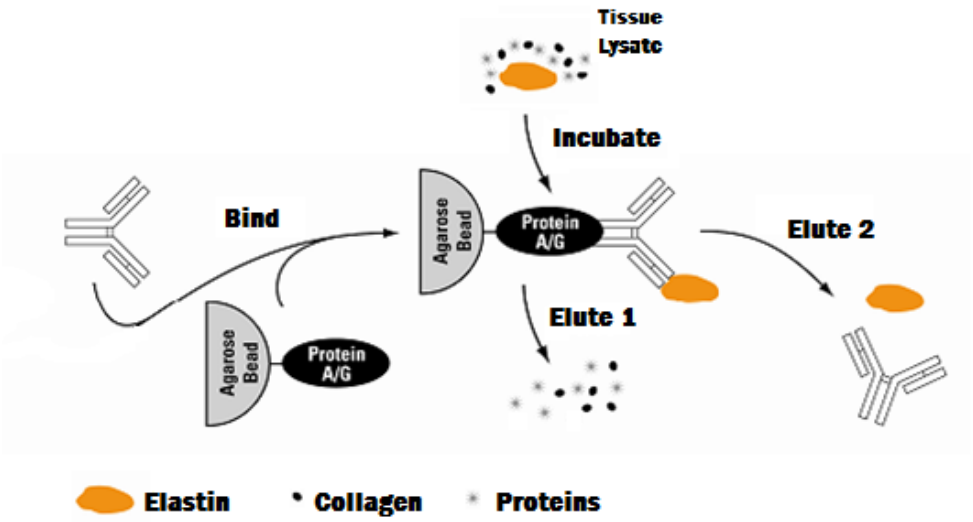

Figure 16 - Diagram of the immunoprecipitation procedure. The antibody is captured in the agarose affinity beads. The incubation with the tissue lysate promotes the formation of the immune complex. Non-bound proteins, including collagen are eluted first, and finally the antibody and antigen are eluted with a low-pH buffer.

2.3.2.2.2 Hydroxyproline composition assay

Microwave-radiation induced hydrolysis

Microwave hydrolysis of proteins and peptides represent an accurate and convenient alternative to conventional methods. The microwave hydrolysis system at MRC-HNR is design to perform rapid, vapour phase acid hydrolysis of protein/peptide samples under inert, anaerobic conditions to prevent oxidative degradation of amino acids. Vapour-phase hydrolysis involves hydrolysis of a sample in a sealed, evacuated container also containing the hydrolysing acid (usually HCl), but where the sample is not place directly in the acid. The vacuum reduces the vapour pressure of the HCl, and thus resulting vapour that envelops the sample (Figure 17)[46].

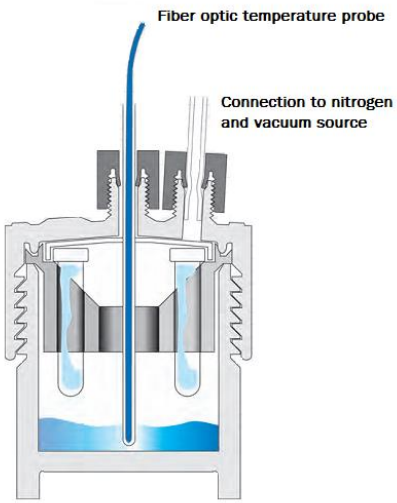

Figure 17 - Diagram of the hydrolysis reaction in the vessel for vapour-phase microwave hydrolysis. The sealed sample vessel containing the hydrolysing acid and the sample vials is alternately vacuum evacuated and purged with nitrogen. The acid vapour envelops the sample hydrolysing the peptides/proteins and liberating the amino acid residues.

Hydroxyproline assay

The hydroxyproline is released upon acid digestion of the collagen containing tissue lysate. In the hydroxyproline assay, the free amino acid concentration is determined by the reaction of oxidized hydroxyproline with 4-(Dimethylamino)benzaldehyde (DMAB), which results in a colorimetric (560 nm) product, proportional to the hydroxyproline content in the tissue lysate (Figure 18).

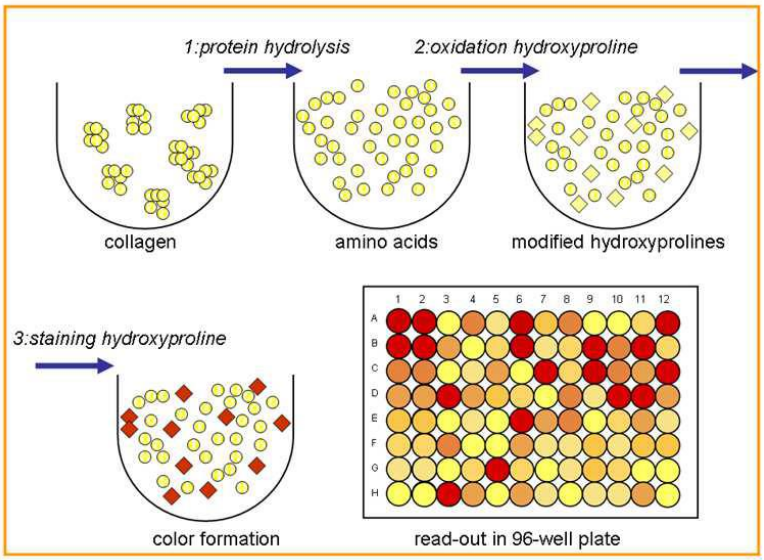

Figure 18 - Diagram of the OH-Pro procedure. 1. Collagen was digested to free amino acids. 2. & 3. OH-Pro residues were oxidised with buffered chloramine-T reagent & the chromophore developed upon the addition of the Erlich's Reagent. The hydroxyproline content was determined upon the absorbance measurement.

The assay does not discriminate between types of collagen, pro-collagen or mature collagen. Note that proteoglycans do not interfere with the analysis because they only react with Erlich's reagent after pre-treatment with acetyl acetone[47]. The total collagen content of the tissue lysate is determined assuming that this protein contains an average of 13.5% w/w of OH-Pro[48].

3 Materials and Methods

3.1 Materials

Unless stated otherwise all water used was ultra-high purity (UHP; 18.2 $^{M\Omega}/_{cm}$) from a Sartorius Stedim Biotech arium® pro ultrapure water system.

High purity nitric acid, ≥69% (w/v) HNO_3 (puriss. p.a., ACS reagent) was purchase from Sigma-Aldrich Company Ltd., Dorset, UK.

Samples were weight accurately on a four decimal place, top pan balance (Sartorius Ltd).

Atomic spectroscopy single elemental standard solutions were obtained from PerkinElemer Life and Analytical Sciences, Connecticut, USA (Pure Plus grade: Al, Ca, Cu, Fe, K, Mg, Mn and Zn; and Pure grade: B, P and Si) and SPEX CertiPrep, Inc., New Jersey, USA (Assurance grade: Na).

1.1 Tissue samples

The tissue samples were obtained from Dr. Ian Wilkinson (Addenbrooke's Hospital) through collaborations and he obtained the tissues from Addenbrooke's Hospital and other hospitals in the East Anglia Region, UK. Ethic approval number MREC 03/2/074.

Aorta samples were selected from any patient deemed suitable for organ retrieval and where consent was obtained from the families. All specimens had grossly normal internal appearances except for a minority where calcification or plaques were clearly visible. Moreover, less than 5% had a diagnosed cardiovascular disease. The total number of the aortic wall samples collected amounted to 40, 21 men and 19 females, with age ranged between 25 and 83 years, although the majority were within 45 – 79 years age range.

3.2 Tissue collection/acquisition

Tissue samples where were obtained from cadaveric donors or beating heart donors through transplant co-ordinators at Addenbrooke's Hospital (Cambridge,

UK). The aorta samples were cut lengthwise and carefully divided into smaller pieces/sections, preserved in tissue preservation fluid or available medium, and stored temporarily at -80ºC. Upon ethical aproval, the samples were sent to MRC-HNR for multi-element analysis and for biochemical analysis (collagen and elastin contents).

3.3 Subsampling in the MRC-HNR laboratory

On receipt at the MRC-HNR laboratory the aorta samples were stored at -80ºC until subsampling. All further sample preparation was carried out entirely in a laminar flow-hood cabinet (Class II Safety Cabinet, Walker, Glossop, UK). All metal and plastic surfaces were decontaminated and sterilized with Distel High Level Laboratory Disinfectant (Tristel Solutions limited, Snailwell, UK).

After thawing, the aorta samples where thoroughly rinsed with water to remove the preservative solution and remaining blood and if present, the surrounding adipose tissue was removed. The cleaned aortas were divided into small pieces: approximately 40 mg in weight for multi-element analysis and 10 mg in weight for biochemical testing, and stored at -80ºC until analysis. All aliquots were carefully sliced so as to maintain all three aortic layers, tunica intima, tunica media and tunica adventitia, intact in all samples. The aorta samples with visible lesions, i.e. calcified plaques or wall thickening, where removed and aliquots of the normal and lesion areas analysed separately.

In a few cases the sample size was insufficient for the biochemical analysis of the ECM components, therefore analysis for elastin content was not carried out.

3.4 Elemental Analysis

The aortic wall element concentrations of Al, B, Ca, Cu, Fe, K, Mg, Mn, Na, P, Si and Zn in the aortic samples was determined by inductively coupled plasma optical emission spectrometry (ICP-OES) using the multi-element analysis mode (Jobin Yvon Horiba – ULTIMA 2000-2 with a polychromator attached).

For element determination, samples were decomposed according to the following procedure: 40 mg of wet samples were freeze dried overnight (Mini Lyotrap, LTE scientific Ldt, Greenfield, Oldham, UK) until reached constant weight. The freeze dried samples were accurately weighed to determine the water content and then digested using a closed-vessel microwave assisted acid digestion (MWAD) system (Milestone *UltraWAVE™*) and Si-free, pre-cleaned standard polytetrafluoroethylene (PTFE) vials with 400 µL 35% (v/v) nitric acid (HNO_3). The microwave heating program was performed in three steps: (1) 5 min ramp from 23ºC to 120ºC; (2) 5 min ramp from 120ºC to 230ºC; and (3) 10 min at 230ºC; followed by a cooling step for 20 min. The microwave power was limited to a max of 1000 W and pressure was limited to a maximum of 150 bar. All samples were digested to completeness and then diluted 1:2 with UHP water for the quantification of Al, B, Cu, Fe, Mn, Si and Z; and 1:10 in UHP water for the quantification of the remaining elements: Ca, K, P, Mg and Na. Blanks for the control of the digestion process and a certified reference material (Seronorm™ Trace Elements Serum L-1) for quality control were prepared in a similar manner and analysed collectively with the samples. The ICP-OES running conditions for the digested aorta sample analysis are summarized in Table 3.

Table 3 - Running conditions of ICP-OES for the analysis of aorta samples.

Analytical Conditions	
RF power (W)	1000
Plasma gas (L min^{-1})	10
Sheath gas (L min^{-1})	2
Auxiliary gas (L min^{-1})	0.0
Speed pump (rates min^{-1})	8
Nebulisation flow rate (L min^{-1})	0.02
Plasma stabilization time (s)	10
Number of replicates	3

Multi-element standards were prepared from individual 1,000 ppm aqueous stock solutions, with final concentrations for each element ranging from 0 to 10 ppm in an acid solution matched to the digested samples, i.e. 17% (v/v) HNO_3 for the 1:2

diluted digest samples and 0.17% (v/v) HNO_3 for the 1:10 diluted digest samples (Table 2). Peak profiles were used for each measurement run and the polychromator was centred in the Mg wavelength. Drift check solutions were carried out after every block of approximately 10 samples.

Table 4 - Atomic spectroscopic information for the multi-element analysis of aorta samples by ICP-OES. Description of the chromator type, the measured emission wavelength, diluent type and standard range used in the analysis of each element.

Element	Chromator Type	Wavelength (nm)	Diluent type (% HNO_3)	Standard range (ppm)
Al	Polychromator	396.152	0.17	0-10
B	Polychromator	208.959	0.17	0-5
Ca	Polychromator	317.933	17	0-10
Cu	Polychromator	324.754	0.17	0-5
Fe	Polychromator	259.940	0.17	0-5
Mg	Polychromator	279.079†	17	0-10
Mn	Polychromator	257.610	0.17	0-4
Zn	Polychromator	206.191	0.17	0-5
P	Polychromator/Monochromator‡	213.618/177.440	17	0-10
Si	Monochromator	251.611	0.17	0-5
K	Monochromator	766.490	17	0-10
Na	Monochromator	589.592	17	0-10

†Polychromator centring wavelength.

‡ Due to peak shift problems for the P peak when using the polychromator, some samples were analysed using the monochromator system for this element.

Matrix effect was corrected using pooled sample-based standards (PSBS)[49]. Briefly, after elemental analysis the remaining volume of the digested samples were pooled into a new tube. Aliquots of the pooled samples were spiked with different concentrations of the multi-element standard solutions, previously prepared, maintaining a sample dilution of 1:2.

As a ubiquitous element, and despite the careful sample handling, diluent (HNO_3) and environmental contamination with Si and some other trace elements is highly likely and it may vary between batches[49]. Thus, the limits of quantification for the samples were restricted by the background levels of the elements analysed in each batch: $\mathrm{LOQ} = \mathrm{mean}_{\mathrm{Blank}} + 3\mathrm{SD}_{\mathrm{Blank}}$.

Element concentration was measured in mg or μg of dry sample mass and corrected for matrix effect.

3.5 Biochemical assays

3.5.1 *Elastin solubilisation and protein extraction*

For the method development work, see chapter 4.II Method development for "combined" elastin and collagen quantification.

The insoluble matrix elastin in the aorta sample was solubilized to α-elastin[50] and the collagenous protein extracted as gelatine[51] by hot oxalic acid treatment. The 10 mg aorta aliquots previously prepared (see section 3.4) were freeze dried overnight (Mini Lyotrap, LTE scientific Ldt, Greenfield, Oldham, UK) until reached constant weight. The dried material was accurately weight and homogenized with an electric homogenizer (Tissue Tearor Homogenizer 120 VAC), speed 4 for 1 min at room temperature in 1 mL 0.25 M oxalic acid. The suspension was further incubated in a heating plate at 98ºC for 1h. The supernatant (OAE) containing solubilized α-elastin and collagen as gelatine was collected by centrifugation at 11,000xg for 20 minutes. The residual tissue in the tube was further incubated with 0.5 mL 0.25 M oxalic acid, at 98ºC for 1h. Up to three extractions were required to completely solubilize the insoluble elastin present in the aortic ECM. The first, second and third OAEs were pooled together (OAE*p*); a fourth extract was analysed separately to establish if the solubilisation was complete, i.e. the absence of (or negligible levels of) elastin in the fourth extract using the Fastin™ Elastin Assay (see below, section 3.6.2).

Aliquots of the pooled extracts, OAE*p*, were analysed for total elastin and protein contents (see below, section 3.6.2 & section 3.6.3). An additional aliquot of the OAE*p* was immunoprecipitated to separate the elastin and collagen components and re-analysed for elastin and collagen contents (see below).

3.5.2 *Elastin Quantification*

The OAE*p* solutions obtained in section 3.6.1 were analysed for aorta total elastin content, i.e. soluble tropoelastin and mature insoluble elastin; using the Fastin™ Elastin Assay kit (Biocolor Ltd, Antrim, UK)[52]. This assay only detects elastin and is unaffected by collagen present in the OAE*p*. 50 µL aliquot of the pooled OAE and 500 µL aliquots of for the fourth OAE were incubated for 10 minutes in an ice bath and then treated with an equal volume of elastin precipitating reagent containing trichloroacetic acid and hydrochloric acid, for 15 min at 4ºC. Following precipitation of the elastin peptides, the mixture was centrifuged at 10,000xg for 10 min and the supernatant discarded. The recovered sample was incubated with 1.0 mL of Fastin™ dye reagent, containing TPPS, for 90 min at room temperature with constant agitation. The elastin-dye complex was then precipitated via centrifugation at 10,000xg for 10 min. The supernatant was discarded and the dye released by adding 250 µL of dissociation reagent containing guanidine-HCL and propan-1-ol. The final dye solution was placed in a 96-well plate and the optical density was measured at 540 nm using a microplate reader (Labsystems Multiskan RC, Artisan Scientific, Champaign, IL, USA).

The elastin content was calculated from a standard curve produced with α-elastin standards (elastin from bovine neck ligament; Sigma-Aldrich Company Ltd., Dorset, UK), with concentrations between 5 to 70 µg, treated with the same method as the samples. Elastin content was expressed as mg elastin/g dry tissue weight.

3.5.3 *Protein Quantification*

Total protein concentration was determined using the Non-interfering Protein Assay™ Kit (NIPA) (Calbiochem®, Merck KGaA, Darmstadt, Germany). Total protein content was used to calculate the volume of OAE*p* to be loaded in the immunoprecipitation column (see below, section 3.6.1). The assay was performed according to the manufacturer's protocol with minimal alterations. Briefly, the interfering agents were removed by adding 500 µL UPPA-I and 500 µL UPPA-II

reagents to a 50 µL aliquot of OAE*p*. The precipitated protein was immobilized by 2 cycles of centrifugation at 11,000xg for 5 minutes each, and the interfering agents in the supernatant were discarded. The pellet was dissolved with 400 µL UHP water and the protein content was assayed by mixing the sample with 100 µL of an alkaline solution containing a known concentration of copper salt (Reagent-I). The unbound copper in solution (unbound to the protein backbone) was rapidly mixed with 1.0 mL of a colouring reagent (Reagent-II) and incubated in the dark for 15 min at room temperature. Finally, 250 µL of the solution were transferred to a 96-well plate and the optical density measured at 490 nm, against water, in a microplate reader.

A series of Bovine Serum Albumin protein standards (STD) were prepared in a similar manner, with a protein content ranging from 0 to 50 µg. A standard curve and corresponding linear regression were calculated by plotting $\log(A_{490}^{STD\ 0\mu g}/A_{490}^{STD})$ *vs* protein amount. Total protein amount in the samples tested was calculated by comparison of the $\log(A_{490}^{STD\ 0\mu g}/A_{490}^{Sample})$ with the BSA protein standards.

3.5.4 *Immunoprecipitation*

For the method development work, see chapter 4.II Method development for "combined" elastin and collagen quantification.

An aliquot of the OAE*p* underwent immunoprecipitation to separate the collagen and elastin components, as elastin will interfere with the collagen analysis. Unless stated otherwise all centrifugation steps were performed at 1,000xg for 1 min, and all the incubations were performed at 4^0C with gentle end-over-end mixing.

For the capture of the elastin proteins solubilized to α-elastin in section 3.6.1, 100 µL of the pooled OAE was neutralized to pH 7-8 with 1M NaOH. The sample was then further diluted with 2x TBS Buffer for a final protein content of between 30-50 µg, as determined with the NIPA™ assay (see section 3.6.3). Prior to analysis a pre-clearing step was conducted to remove any proteins and ligands that bind non-specifically to the beaded support. Briefly: 80 µL of Control Agarose Resin slurry was incubated with 300 µL of the neutralized OAE*p* solution for 1 hour. The flow-

through was collected by centrifugation of the spin column into a new collection tube.

The immunoprecipitation procedure was carried out in four steps, using the Pierce® Classic IP Kit (Thermo Fisher Scientific Inc., Rockford, USA):

I. Antibody capture in agarose beaded support: 7 μg of the specific [10B8] anti-elastin antibody (Abcam, Cambridge, UK), 30 μL of Pierce Protein A/G Agarose resin slurry and 150 μL of 1x TBS Buffer were incubated in a spin column for 5 hours at 4ºC. The flow-through was collected and analysed for protein content (section 3.6.3) to confirm the successful binding of the antibody to the agarose beads.

II. Formation of the immune complex: 250 μL of the pre-clear solution was added to the complex agarose beaded support-antibody and incubated overnight (15-17 hours) at 4ºC.

III. Elution of the collagen and proteins fraction: all non-elastin proteins, including collagen, were collected by centrifugation of the non-antibody-bound fraction. The resin was further washed three times with 1x TBS Buffer and finally with 100 μL of conditioning buffer.

IV. Elution of the immune complex: the spin column was incubated in a heating plate with 100 μL of elution buffer for 10 minutes at 70ºC with gentle mixing. The immune complex was collected through centrifugation of the eluate.

The collagen and protein fractions collected at step III were analysed for elastin content by the Fastin™ Elastin Assay (see section 3.6.2) to verify that the IP was successful, i.e. no elastin should be detected in the collagen/proteins fraction; and the collagen content was estimated by a hydroxyproline assay (see below, section 3.6.5).

Chicken tendon was used as a positive quality control of the immunoprecipitation assay, and was carried out simultaneously with the aorta samples.

3.5.5 *Collagen quantification*

A hydroxyproline (OH-Pro) assay was used to estimate the total amount of collagen in the aorta matrix. The eluted fractions collected in section 3.6.4 – step III., containing collagen and other matrix proteins, were pooled together and freeze dried for 48 h to concentrate the protein amount. The residue obtained after freeze drying was hydrolysed by vapour phase HCl in a microwave digestion system (CEM Discover System, Matthews, Nc, USA). The digestion was carried out under inert, anaerobic conditions (15 psig nitrogen pressure); at a constant temperature of 150ºC and 150 W for 15 min. Vapour phase HCl was generated from 10 mL 6M HCl added into the reaction vessel.

The hydrolysed samples were reconstituted with 50% isopropanol and carefully transferred into eppendorf tubes. In a 96-well plate, 10 µL of sample or standard solution was mixed with a buffered chloramine-T reagent and the oxidation was allowed to proceed for 5 min at room temperature. The chromophore was developed with the addition of 0.1 mL Erlich's Reagent followed by incubation for 30 min at 60ºC[53]. The absorbance was measured at 540 nm in a microplate reader. The hydroxyproline content was determined by comparison with *trans*-4-hydroxy-L-proline standards (Sigma-Aldrich Company Ltd., Dorset, UK) prepared in the concentrations range 0 to 0.5 mg/mL.

Gelatine (Sigma-Aldrich Company Ltd., Dorset, UK) was used as a quality and positive control for the OH-Pro assay, and was carried out simultaneously with the samples.

Total collagen content was expressed as µg of collagen per mg dry weight, assuming that collagen contains an average of 13.5% w/w OH-Pro[48].

3.6 Statistical analysis

The statistical analysis was carried out using the GraphPad Prism statistical package (version 5.04 for Windows, GraphPad Software, San Diego California USA). All measurements were performed at least in duplicates ($n \geq 2$). Experimental results are shown as mean ± SD and, where appropriate medians and ranges, are also presented. The ROUT algorithm of the GraphPad software for outliers was used on all datasets to identify potential outliers.

The normality of the variables was tested via D'Agostino & Pearson omnibus normality test. Because not all the variables were normally distributed, and due to the variable sample size and small age distribution of the subjects, non-parametric test were carried out for all statistical analysis. For comparison of the elemental contents between genders a non-parametric two-tailed *t* test: Mann-Whitney test, was used. Spearman correlation coefficients were calculated between aorta element concentrations with age or gender. Associations with BMI were also investigated as some subjects were overweight and this is a known risk factor for cardiovascular diseases. Linear models were fitted to the data. Subgroup analyses were performed only if the interaction was significant. The level of significance was set at $P < 0.05$.

Element concentrations below the limit of quantification were not rejected, or changed, so that the distributions would not be distorted, which is important for correlation analysis and calculation of median values.

4.I Mineral and biochemical study of human aortas

4.I.1 Results

4.I.1.1 Population characteristics

Baseline characteristics for the study population are presented in Table 5. Overall 40 aorta specimens were collected from 21 male and 19 female organ donors. Median age, BMI and water content were similar for male and female subjects.

Table 5 - Descriptive characteristics of the healthy organ donors.

	Males (n = 21)			**Female (n = 19)**		
	Mean ± SD	Median	Range	Mean ± SD	Median	Range
Age (years)	59 ± 13.4	64	25 – 79	66 ± 7.9	64	54 – 83
Weight (kg)	80 ± 8.1	80	62 – 90	74 ± 21.5	68	50 – 130
Height (m)	1.72 ± 0.09	1.72	1.58 – 1.83	1.60 ± 0.06	1.59	1.45 – 1.73
BMI (kg/m²)	27.3 ± 3.5	27.4	21.6 – 36.1	27.8 ± 6.6	26.7	19.7 – 45.0
Water† (%)	71.4 ± 4.5	72.2	61.7 – 78.7	73.6 ± 4.3	74.8	67.0 – 82.4

†Calculated as percentage of the difference between the initial and the freeze dried sample weight.

As previously mentioned (see Materials and Methods, section 3.4) the aortas were generally from healthy individuals, but less than 5% had a diagnosed cardiovascular disease. Indeed, discernible aortic lesions were observed in three aorta samples. Two presented visible calcified areas (Figure 20 (c) & (d)). The other specimen showed no signs of calcified plaques, but revealed clear changes in the aortic wall with increased arterial wall thickness (Figure 20 (b)), one of the recognized indicators of aortic stiffness. Lesion areas were analysed separately for elemental composition (Appendix A).

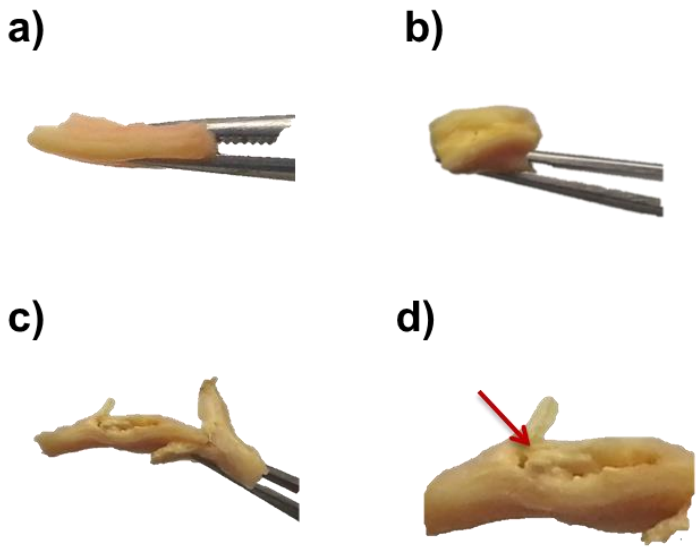

Figure 19 - Representation of a normal looking aorta (a) and aortas with discernible wall lesions (b-c). b) Aorta with increase wall thickness and luminal enlargement characteristic of a stiffened aorta. c) & d) Aorta displaying calcified plaques, d) Close-up view of the calcified area and plaque (red arrow) in the aortic wall.

4.I.1.2 Aorta mineral composition

Table I.2 shows the results of the metallomic study of the aorta specimens by ICP-OES. The trace-elements B, Mn and Si were only detected in 60, 48 and 90%, respectively, of the 40 samples analysed. The mean concentrations of the elements found are shown in Table 6 with relevant values from literature (see discussion).

Table 6 - Essential and trace-element concentrations (per dry tissue weight) in human aorta specimens analysed in this study with reference values from literature population studies.

	Units	All subjects			Reference			
		Mean ± SD	Range	n	Mean	Age range	n	Year
Al	μg/g	8.3 ± 3.0	3.48 – 14.27	21†	10	55 - 92	26	2000[54]
B	μg/g	6.8 ± 4.9	0.38 – 22.7	24	n.a			
Cu	μg/g	4.1 ± 2.2	1.16 – 13.86	39	4.35 ‡	16 - 80	200	1987[55]
Fe	μg/g	45.7 ± 27.9	15.0 – 118.2	40	125	55 - 92	26	2000[54]
Mn	μg/g	1.1 ± 0.4	0.11 – 1.79	17	n.a			
Si	μg/g	14.1 ± 11.7	0.75 – 44.8	35	12.5	55 - 92	26	2000[54]
Zn	μg/g	70.9 ± 19.4	29.7 – 125.1	40	85.0 ‡	16 - 80	200	1987[55]
Ca	mg/g	9.3 ± 5.2	2.64 – 23.81	40	10.25	0 - 99	71	1997[56]
K	mg/g	7.1 ± 5.1	0.71 – 16.9	22†	4.06	72	1	1985[57]
Mg	mg/g	0.9 ± 0.4	0.26 – 2.23	40	0.81	20 - 40	20	2011[58]
Na	mg/g	6.2 ± 4.4	1.76 – 17.1	22†	n.a			
P	mg/g	3.4 ± 1.3	1.01 – 6.90	40	11.49	0 - 99	71	1997[56]

†Only 22 aorta samples were analysed for Al, K and Na content
‡Values corrected for matrix effect
n.a: data not available

Age- and gender-related alterations

Correlations with age and gender were studied for the different elements studied in the aortas and these are shown in Table 7. Significant (*P*-value < 0.05) gender-related distributions in the elements concentrations were found for Cu and Na (Figure 21). Age-related changes in these elements (Cu & Na) were investigated between genders (Figure 22). For the other elements, as there were no gender differences in concentrations, male and female data were combined to investigate correlation with age.

Significant age-dependent alterations in the elements concentrations were only found for Al, Ca and P (Figure 23). See Appendix B for other (non-significant) associations with age and gender.

Table 7 - Correlation with age and gender for the different elements in the aortic wall.

	Age interaction		Association with age				Association with gender		Male vs Female
			Male		Female		Male	Female	
	r^2†	*P*-value†	r^2†	*P*-value‡	r^2	*P*-value	Mean ± SD	Mean ± SD	*P*-value‡
Al	0.802	0.003	ND	ND	ND	ND	8.70 ± 3.1	7.67 ± 2.9	0.538
B	0.378	0.069	ND	ND	ND	ND	5.52 ± 3.2	7.70 ± 5.8	0.151
Cu	0.251	0.055	0.051	0.827	0.396	0.103	3.39 ± 1.3	5.03 ± 2.7	0.023
Fe	0.433	0.008	ND	ND	ND	ND	44.2 ± 24.8	52.9 ± 39.1	0.989
Mn	0.049	0.428	ND	ND	ND	ND	0.94 ± 0.56	1.22 ± 0.25	0.093
Si	0.188	0.280	ND	ND	ND	ND	12.5 ± 8.5	15.9 ± 14.5	0.779
Zn	-0.008	0.962	ND	ND	ND	ND	67.4 ± 18.2	74.8 ± 20.5	0.432
Ca	0.336	0.034	ND	ND	ND	ND	9.23 ± 5.43	9.46 ± 5.1	0.871
K	0.235	0.293	ND	ND	ND	ND	8.52 ± 4.8	4.53 ± 4.8	0.260
Mg	0.126	0.466	ND	ND	ND	ND	0.85 ± 0.32	0.76 ± 0.33	0.278
Na	-0.226	0.312	- 0.286	0.321	- 0.464	0.243	4.63 ± 3.6	9.04 ± 4.33	0.011
P	0.320	0.044	ND	ND	ND	ND	3.59 ± 1.4	3.14 ± 1.3	0.330

†*P*-value and Spearman's correlation coefficient (r^2) indicates whether the parameter varies with age independent of gender (Spearman's correlation).
‡*P*-value indicates whether the parameter varies between gender independent of age (Mann-Whitney *t* test).
ND – not determined

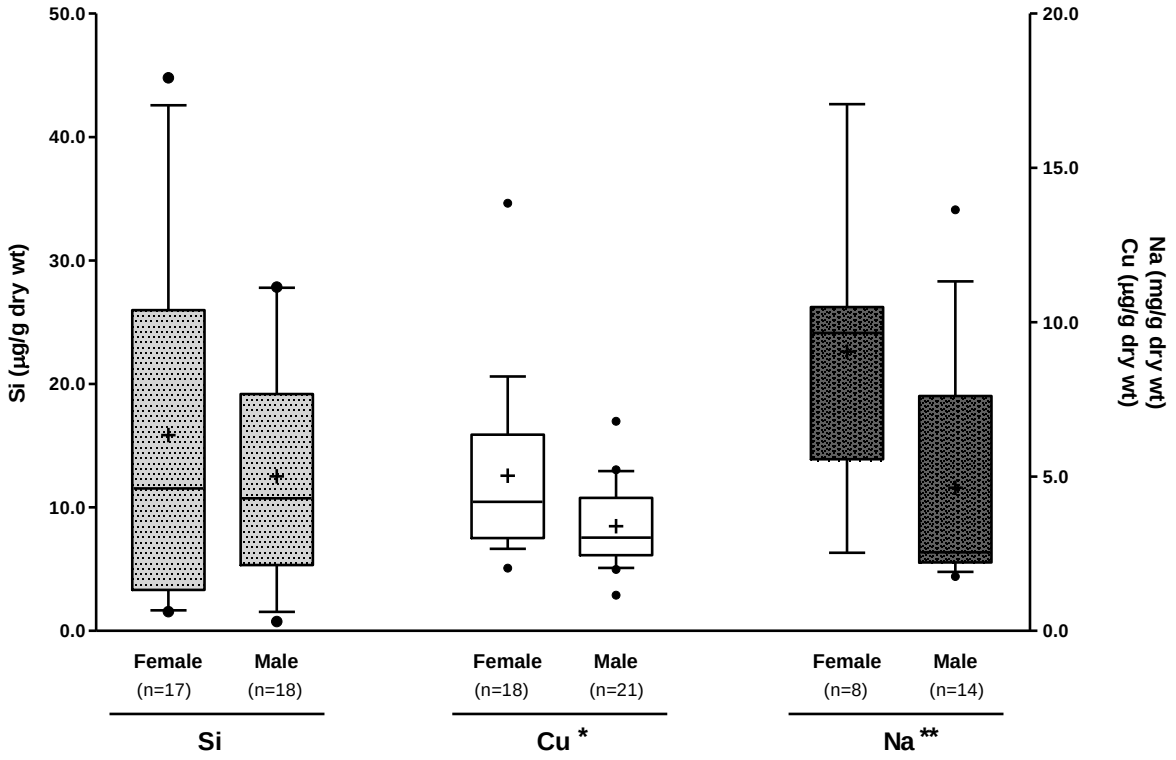

Figure 20 - Gender distribution of Si, Cu and Na in the human aorta samples. Data is shown as box-plots, where the horizontal lines indicate 10th, 25th, 50th (or median), 75th and 90th percentiles; the plus signal shows the mean, *n* represents the number of subjects. Female vs Male: **P*-value = 0.023; ***P*-value = 0.011 (Mann-Whitney *t* test).

Despite the differences in mean Cu and Na concentrations between genders, no significant age-related variations in these elements were observed for either males or females separately or when combined (Figure 22). Furthermore, by separating the data between genders, the number of subjects per group decreases and no conclusion can be made from the analytical test.

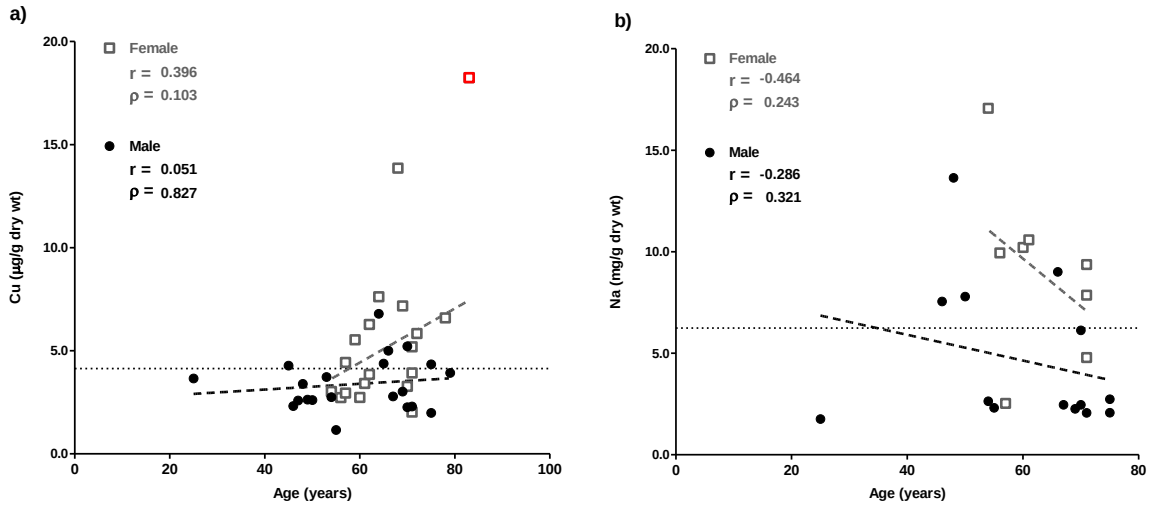

Figure 21 - Association of age for Cu (a) and Na (b) levels in the aorta samples from male and female subjects. Concentrations are represented for each subject and the dashed lines show the correlations with age. The thin horizontal dotted line shows the mean concentration for the element. Outliers are highlighted in red and were not included when carrying out the correlations. Spearman's correlation coefficients (r^2) and *P*-value are shown.

A strong exponential positive relationship between Al concentrations in the aorta and age was found (Figure 23 (b)). Other statistically significant positive associations with age were found for Fe, Ca and P (Figure 23 (c-e)). In this study, Zn levels were found to not vary with age (Figure 23 (f)). Silicon content did not vary significantly with age, although there appears to be an increase with age (Figure 23 (a)).

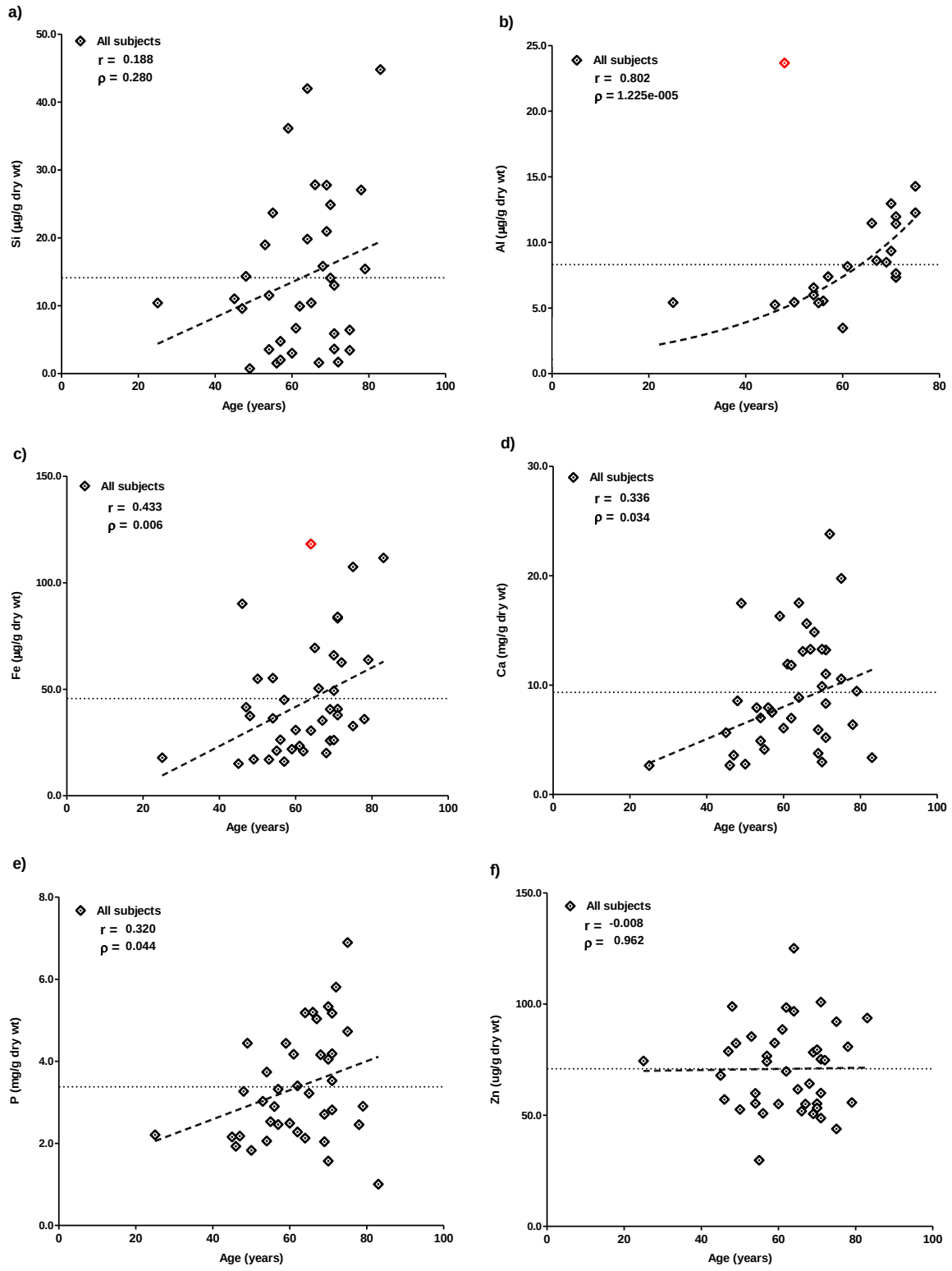

Figure 22 - Changes in Si (a), Al (b), Fe (c), Ca (d), P (e) and Zn (f) concentrations in the aorta. Concentrations are represented for each subject and the dashed lines show the correlations with age. The thin horizontal dotted line shows the mean concentration for the element. Outliers are highlighted in red and were not included when carrying out the correlations. Spearman's correlation coefficients (r^2) and *P*-value are shown. Note: removing the value at 25 years did not affect the correlation shown.

4.1.1.3 Aorta structural composition

Elastin concentration in the aortic wall was determined in 39 of the 40 specimens collected, with an average of 225.1 ± 62.8 mg per g dry weight.

Differences in elastin content and correlation with age (male plus female samples) are displayed in Figure 24. Mean elastin concentrations did not differ between males and females (Figure 24 (a)). The elastin content of the aortic walls did not significantly change with ageing. Although a slight decrease in the elastin concentration after 66 years was observed (Figure 24 (b)).

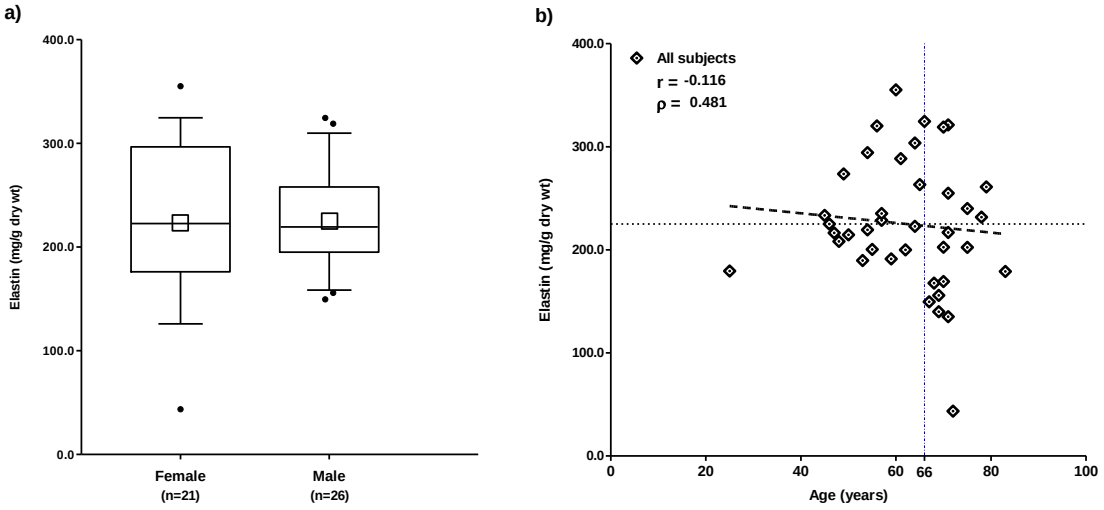

Figure 23 - Association of elastin with gender (a) and with age (b). a) Data is shown as box-plots, where the horizontal lines indicate 10th, 25th, 50th (or median), 75th and 90th percentiles; the open square show the mean, *n* represents the number of subjects. Elastin content did not correlate with gender (Mann-Whitney *t* test: P-value = 0.989). b) **.** Concentrations are represented for each subject and the dashed lines show the correlations with age. The thin horizontal dotted line shows the mean concentration for the element. The vertical dashed blue line at 66 years is only indicative. Spearman's correlation coefficients (r^2) and *P*-value are shown.

4.1.1.4 Elemental and structural interactions

Correlations between aorta element concentrations with elastin concentrations and with BMI were investigated. There were 13 statistically significant correlations ($r > 0.500$, $p < 0.05$ and $n > 15$) of the total 225 tested (Note: these are tabulated in Appendix C). However, the relevant interactions are shown in Figure 25, 26 and 27. Copper and sodium correlations are gender dependent (Figure 26), as significantly different mean concentrations were found between genders (Table 7). No correlation was found between BMI and element levels or BMI and elastin content.

Element vs Element

There were statistically significant positive correlations between Ca and P concentrations in the aorta, and between the following elements: Al and Ca, Al and P, Al and Mg, Mg and Ca, Mg and P and B and Zn (Figure 25). The strongest correlation coefficient was found between Ca and P. Relatively close correlations were found between Al – Ca and Al – P and, Mg – Ca and Mg – P, respectively. Notably, no significant correlations between Si and Al or, between Fe and Al were observed. While not significant, a negative correlation was obtained between Si and P levels in the human aorta (Figure 25 (b)).

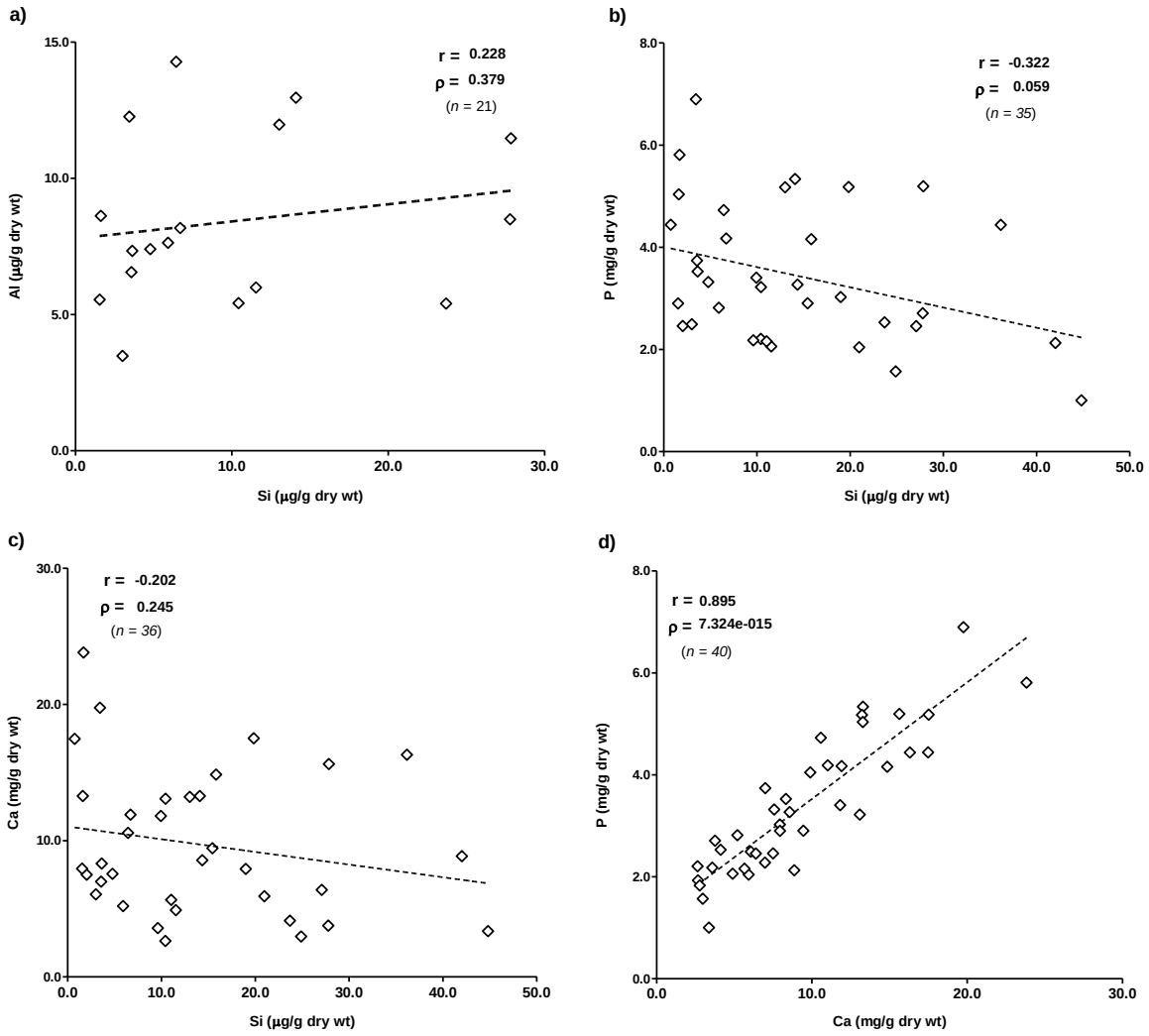

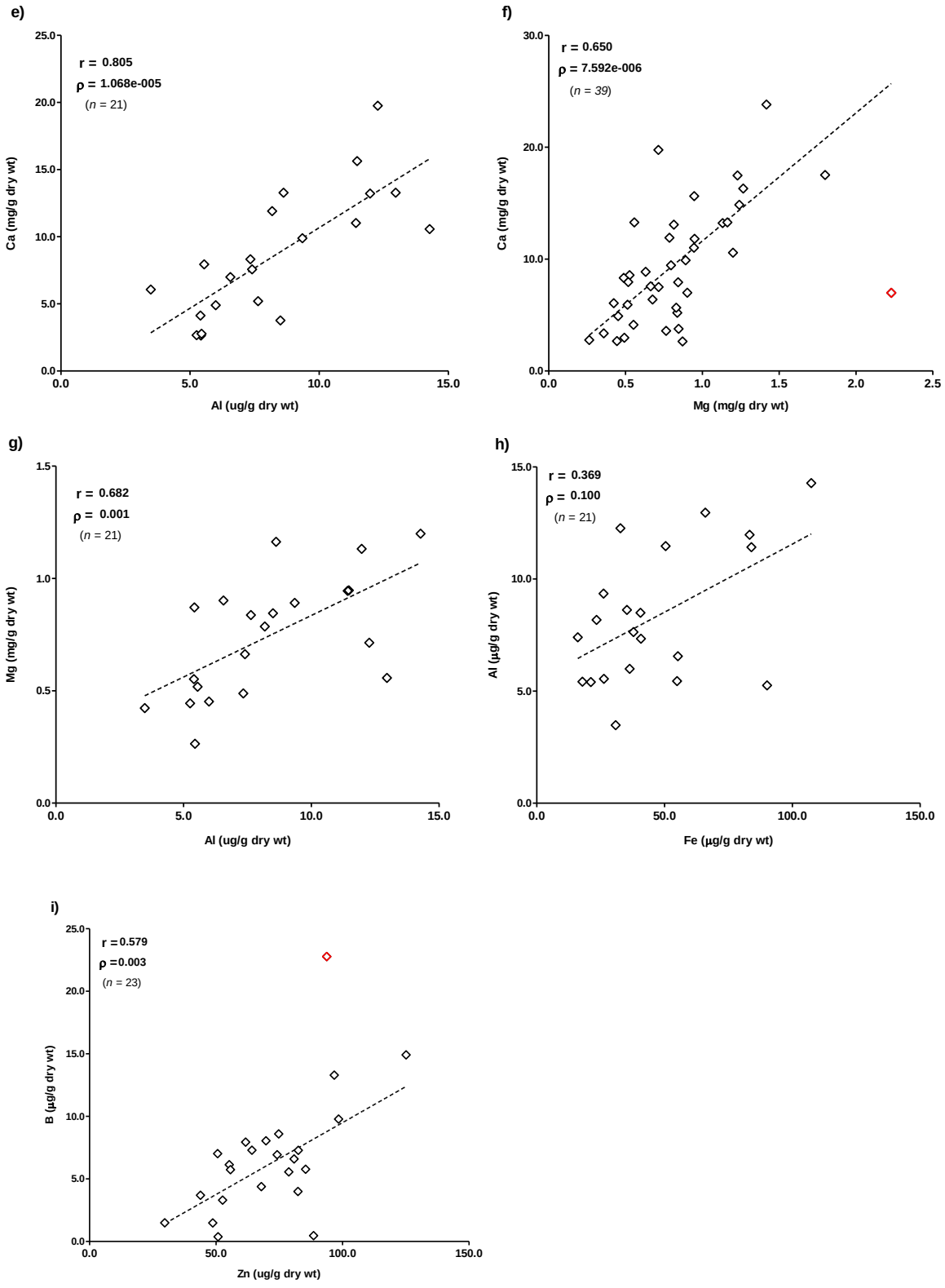

Figure 24 - Correlations between element concentrations in the human aorta samples. a) Si vs Al, b) Si vs P, c) Si vs Ca, d)Ca vs P, e) Al vs Ca, f) Mg vs Ca, g) Al vs Mg, h) Zn vs B and i) Fe vs Al. Outliers are highlighted in red and were excluded from the fitted linear model. Spearman's correlation coefficient (r^2), corresponding *P*-value (ρ) and number of data points excluding the outliers (*n*) are shown.

Statistically significant correlations were also found between Cu and Si and, Cu and Mg in female and between Cu and Zn in male aorta samples (Figure 26 (a - c)). A strong negative correlation was found between Na and K in the male aorta samples (Figure 26 (d)). Silicon levels in the aorta were not significantly correlated to any element with the exception of Cu in female aorta samples (Figure 26 (a)).

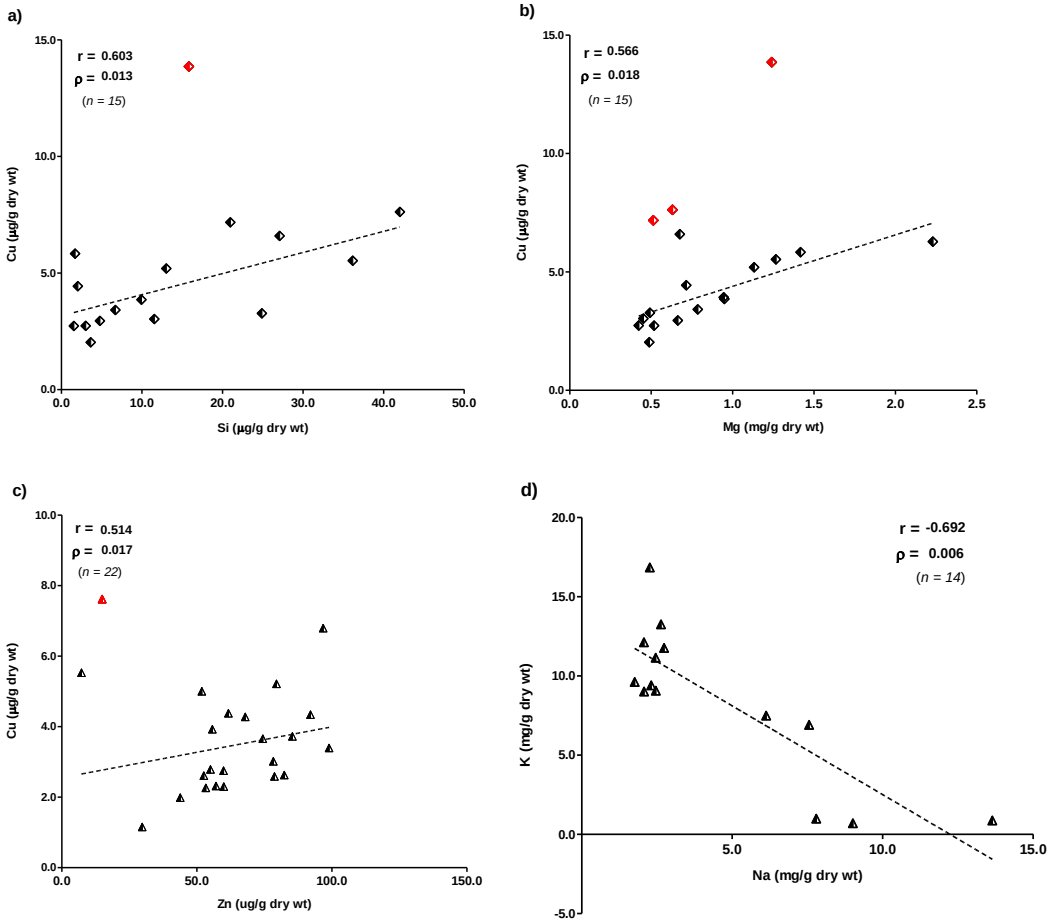

Figure 25 - Correlations with Cu and Na concentrations of the human aorta samples. a) Si vs Cu in females, b) Mg vs Cu in females, c) Zn vs Cu in males and d) Na vs K in males. Outliers are highlighted in red and were excluded from the fitted linear model. Spearman's correlation coefficient (r^2), corresponding *P*-value (ρ) and number of data points excluding the outliers (*n*) are shown.

Element vs Elastin

Three statistically significant correlations were found between the element and elastin concentrations in the aorta samples. The strongest correlation (r^2 = -0.615, *P* = 0.009) was obtained between elastin and copper in samples from the female donors (Figure 27 (f)). Interestingly, a positive correlation was found between elastin and Cu concentrations in the samples from the male donors, but with less significance (r^2 =

0.455, $P = 0.038$). K and Na concentrations were also correlated with the elastin in the human aorta, but in opposing directions (Figure 27 (b) & (c)). Elastin levels did not correlate with the Si, Zn or Ca concentrations in the aorta samples.

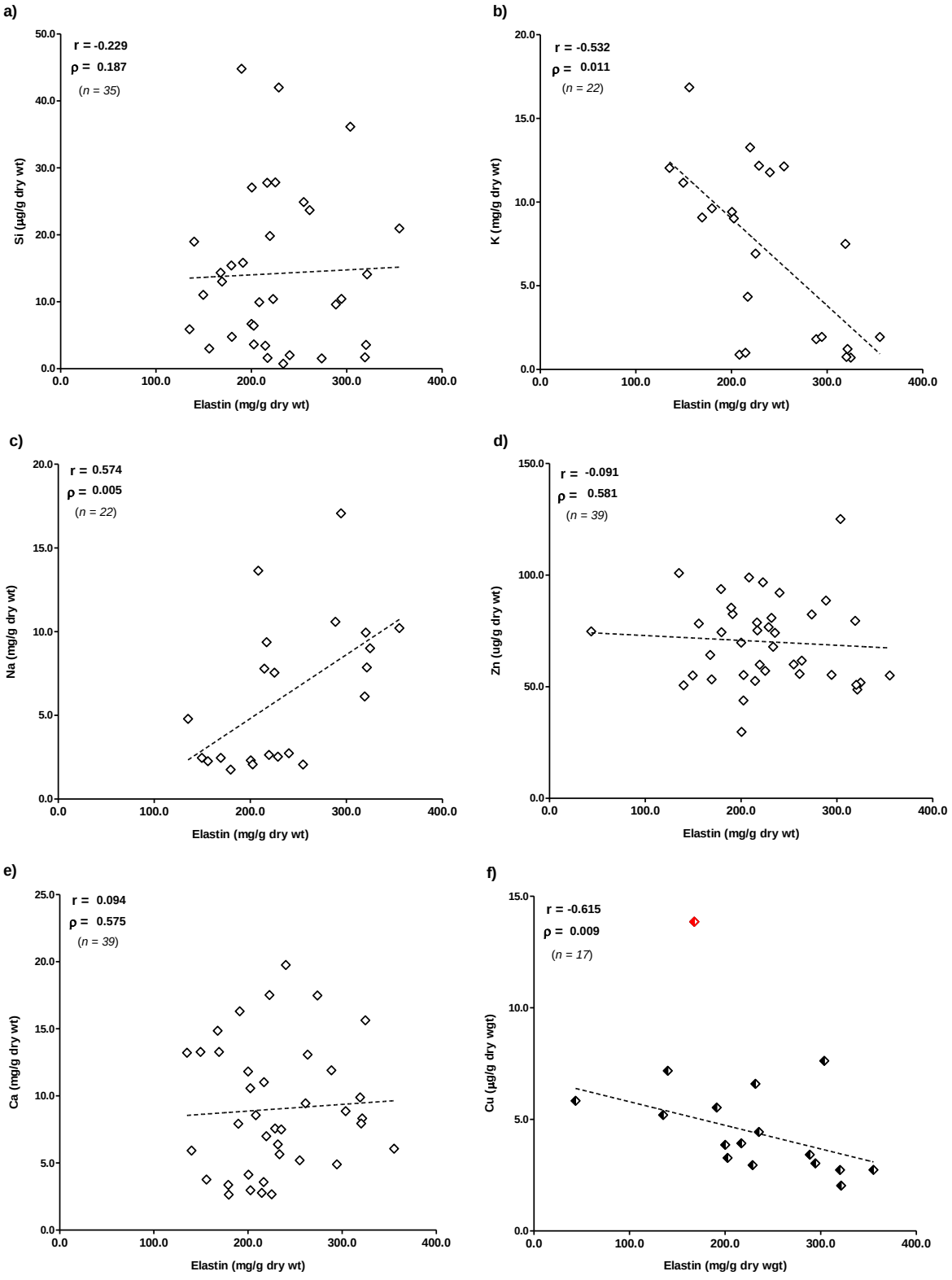

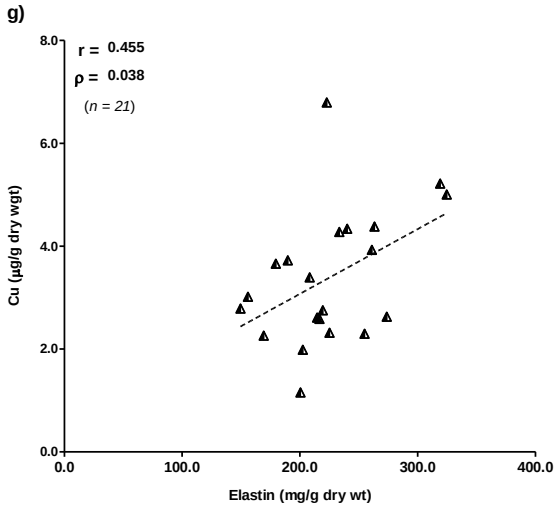

Figure 26 - Correlations between elastin and elements concentrations in the human aorta samples. a) Elastin vs Si, b) Elastin vs K, c) Elastin vs Na in all subjects, d)Elastin vs Zn, e) Elastin vs Ca, f) Elastin vs Cu in females and g) Elastin vs Cu in males. Outliers are highlighted in red and were excluded from the fitted linear model. Spearman's correlation coefficient (r^2), corresponding *P*-value (ρ) and number of data points excluding the outliers (*n*) are shown.

4.I.2 Discussion

The distribution of silicon in animal tissues and the nature of the Si interactions with ECM components, have led to the supposition of an essential role for Si in vascular health. As to enlighten possible associations between silicon and aortic health, the aim of this project was to determine the age- and gender-related changes in silicon levels of the human aorta, and to assess if these changes can be correlated with changes in elastin content. Silicon levels in the aorta samples were not found to vary significantly with age or with gender. The silicon concentration in the aorta was not significantly correlated to any element with the exception of Cu in female aorta samples, and although not significant, a negative correlation was obtained between Si and P levels. Moreover elastin levels did not correlate with the Si concentrations in the aorta samples.

One of the challenges experienced when performing this study was obtaining representative samples of a normal healthy population. Moreover, with the increasing life expectancy observed in the past century, acquiring a wide age range from both female and male donors was even more problematic. In this study, the mean age of the donors was ≥ 59 years and the majority were not diagnosed with a cardiovascular disease (> 95%). Additionally BMI values were within the reported mean of the UK adult population[59] (BMI: men = 27.2 kg/m^2; women = 27.1 kg/m^2). Still, the small number of samples and the low age range of the population studied should allow a critical analysis of the levels of Si, other elements and elastin in the human aorta.

Since the first published paper in 1974 by Loeper *et al.*[3] suggesting a protective role for Si in aortic health, only one study has measured the silicon content of the human aorta. Minami and colleagues[54] determined the Si levels (and other elements) in five human arteries. The aorta Si concentrations found in this study (14.1 μg/g dry weight) is similar to the results reported by Minami's group (12.5 μg/g dry weight). Earlier studies suggested the potential involvement of Si in aortic health based on observations in which the Si content in connective tissues, especially the aorta, were

richer than other soft tissues[3, 14]. Little is known about the Si content in human soft tissues, with the exception of blood[16] (0.037 – 0.377 μg/g wet wt) and women breast tissues[60] (64 μg/g dry wt). In this study, the Si content found in the aorta was 35% lower than that reported in human breast tissues. Moreover, the human aorta was previously reported to have the lowest Si level among human arteries[54], aorta (12.5 μg/g dry wt) < basilar < femoral < coronary < radial (115 μg/g dry wt). Minami's results suggest that high Si levels are, in fact, found in connective tissues, such as arteries, compared with soft tissues, e.g. human breast. However, Carlisle[14] proposal that the highest Si concentrations are found in the aorta should be re-evaluated, as low Si levels were observed in the present study compared to the Si levels found in human breast tissue and radial arteries.

Some studies assessing the concentration of silicon in humans have demonstrated a decrease of silicon concentration with age[3, 61] and associations between silicon and endocrine balance[17, 18]. Distinctive associations between bone mineral density in post-menopausal women, compared with pre-menopausal women and post-menopausal women taking hormone replacement therapy[18]; suggested that the hormonal effect on Si is associated with tissue incorporation and cellular utilization of this element. Older men and post-menopausal women (< 54 years) were investigated in this study, thus it was not surprising that no age dependent or gender-related behaviour was found for the silicon concentrations in the aortic wall.

The aorta and other large elastic arteries progressively stiffen throughout life in a process called arteriosclerosis. Aortic stiffness is largely determined by the aortic wall structure, especially by the modification, natural (ageing) or induced (disease), of ECM components, namely elastin and collagen fibres[20]. When expressed as the tissue dry weight, the elastin concentration ranged between 135.1 to 355.1 mg/g, with a mean of 225.1 mg/g. The elastin values are in agreement with those observed in the human aorta for the same age range (50 – 90 years), where values between 113 – 371 mg/g[62, 63] have been reported.

The analysis of the elastin burden in the whole aorta (i.e. all three layers: intima, media and adventitia present) revealed no age-related changes, although a slight visual descending trend was observed for older subjects (< 66 years). There is no consensus in literature as to whether the concentration of elastin increases or remains unchanged in the ageing aorta[62, 63]. Cattel and colleagues[62] have highlighted the need to distinguish between changes in the absolute amount of a tissue component (per length) versus changes in its concentration (per mass). In Cattel's study, aortic elastin concentrations increased with age, whilst the absolute amount of this protein decreased. Conversely, Spina and co-workers[63] have reported a decrease in the elastin concentrations and the maintenance of a constant amount of elastin in the ageing aorta. These conflicting observations are possibly related to the different methodologies used by the different groups. In fact, Spina determined the elastin content through quantification of the elastin specific cross-linking residues (desmosine and isodesmosine) that have been recurrently shown to decrease with senescence[64, 65]; suggesting that changes in the elastic properties and stiffening observed in the ageing aorta may not be due to the degradation of the elastin in itself, but to alterations in the structure of the protein network.

In addition to the proteolytic mechanisms, the structure of elastic fibres in ageing tissues may also be altered by calcification. Calcium accumulates in the ageing blood vessel walls and is strongly bound to the microfibrillar component of elastic fibres[22]. Loeper and Fragny observed that Si partially inhibits lipid deposition through the preservation of elastin fibres and mucopolysaccharides integrity which enhances the impermeability of the vessel wall to lipid and calcium deposition[3]. Despite evidence of increased calcification in the ageing aorta (Ca/P vs age: $P > 0.0001$), and the decrease in elastin content with ageing, no significant correlations were found between the elastin content and the Ca concentrations in the subjects studied (Elastin vs Ca: $P = 0.575$). Nevertheless, the negative interactions observed between Si and Ca and more strongly between Si and P suggest a protective effect for Si in preventing the calcification of the aortic wall (Figure 25 (b-c)). The role of

silicon as calcium/phosphorus-antagonist has also been previously reported in a Si supplementation study in horses[66].

Birchall has proposed that the essentiality of Si was not due to the direct action of the element on biological functions, but related to its ability to interact with other elements by limiting the bioavailability of aluminium and promoting copper utilization[67]. Minami and colleagues have investigated the Al and Si contents in the human aorta, reporting an age dependent accumulation of Al with a significant positive interaction with Si[54]. In the present study, an exponential increased in Al concentrations with age, but no correlation between Al and Si were observed. Although the number and age range of subjects are similar between both studies, differences in the methodology for trace element quantification may explain the variations between observations.

Although a small number of subjects were studied, a strong Cu and Si interaction (P = 0.01) was shown and implications of the silicon-facilitated copper utilization in promoting cardiovascular health have been pointed by several authors[38, 39]. Copper is an essential trace metal in humans, which is critical for connective tissue formation, iron metabolism, and free radical detoxification. The role of copper in connective tissue formation is largely recognized to its participation as a co-factor in the crosslinking of elastin and collagen by lysyl oxidase[40], a copper-containing enzyme. In other *in vitro* studies, Cu/Zn SOD activity was positively correlated with aortic stiffness and was suggested to play a crucial role in preventing atherosclerosis and maintaining the cardiovascular health[30]. Although in this study, no correlation was found between elastin and ageing, increased Cu/Zn SOD activity in aortic stiffness may explain the negative correlation between the copper content and the elastin burden observed in this study.

Elastin and collagen are the two main structural components of the aorta and major determinants of aortic health and mechanical properties. A biochemical assay was developed to measure collagen content, but due to operational problems,

collagen content in the aorta samples was not measured. Aorta mechanical testing, e.g. elasticity, was performed by Dr. Ian Wilkinson at Addenbrooke's Hospital. However the results were not shown in this thesis as the data was not available when writing this report.

Other correlations with aortic health

The mean concentrations of the different elements were compared with the data collected from population studies and similarities were found between Al, Cu, Si, Zn, Ca, Mg and K levels (Table 6). The P and Fe concentrations were significantly lower in this study when compared with the referenced values in literature. Furthermore, a wide scatter distribution was also observed for the Fe concentration in the aortic wall. Fe contaminations from blood residues present in some samples are a possible explanation for this variation[55].

The mean concentrations of the different elements differ between male and female subjects, with generally higher levels in female donors (Table 7). However, variations in the aortic wall mineral composition were mostly independent of the specimen gender, with the exception of Cu and Na levels.

The relationship between macro- and trace element concentrations in human tissues and the pathogenesis of cardiovascular disease have been investigated in many epidemiological studies[68-70]. In the present thesis and considering the amount of subjects, there was a surprisingly large number of correlations between elements, most of which have been reported previously.

Ca, P and Mg accumulation in senescence and their strong interaction in human aortas have been shown in several studies[54, 71]. Additionally the accumulation of Al was suggested to be associated with the increasing calcification of the ageing aortic wall, with Al being adsorbed on to the calcium phosphate mineral formed[54, 72]. Supporting these observations, strong correlations with ageing and between Ca, P, Mg and Al concentrations were also observed in this study.

Among essential trace elements, Cu and Zn play a particular role in biological systems and are positively correlated in the aorta[70]. A disturbance of the trace elements balance in the human body creates possible risks of cardiovascular diseases. For example, the remodelling and homeostasis of the ECM is mediated primarily by a large group of zinc-dependent endopeptidases, the MMPs and their inhibitors[73]. Increased expressions of MMPs, such as MMP-2 and MMP-9 have been reported to be involved in the thinning and degradation of vascular elastin[65]. Even so, no correlations between the Zn content and age or between the zinc and elastin concentrations were found in this study.

Boron is a trace element playing an important role in mineral and hormonal metabolisms, cell membrane functions, and enzyme reactions[74]. Boron is thought to be implicated in the turnover of the ECM by modulating the production of MMP-2 and MMP-9[75], which provides a plausible explanation for the significant and positive correlation between boron and zinc concentrations.

In the present study Fe was found to increase with senescence. Although iron is an essential element for many physiological processes, iron overload has been associated with increased cardiovascular risk. Excess iron can lead to tissue damage by promoting the generation of ROS, affecting the bioavailability of nitric oxide (NO) and thus impairing vasorelaxation[76]. ROS may also enhance the susceptibility of elastic fibres to subsequent elastase-mediate degradation, but the influence of oxidation on the structure and functions of elastic fibres is still poorly understood[77].
The homeostasis of sodium and potassium plays an important role in the blood vessel and general cardiovascular health. Sodium was found to have a strong negative correlation with potassium, and opposing associations between these elements and elastin concentration were identified (Figure 27 (b-c)). Supporting the current study findings, other investigators have demonstrated that excessive salt intake increased hypertension and that this effect is counteracted by potassium supplementation[78]. Additionally, in animal and cellular studies, Na and K were found to modulate elastin synthesis. In spontaneously hypertensive rats,

supplemented with NaCl, the aortic elastin was found to be slightly elevated when compared to the control[79]. Conversely, in chick VSMCs, high medium concentrations of potassium were found to decrease elastin synthesis[80].

4.I.3 Conclusion

The circumstantial evidence supporting the conviction of silicon essentiality in the maintenance and preservation of the ECM health in animals is extensive. However, postulating a silicon requirement for humans is difficult because only limited data is available. If beneficial effects can be established, then silicon supplementation may play a major role in the vascular aging to promote health and longevity.

Aging effects and mutual correlations between the 12 elements analysed and the elastin burden in healthy human aortas were investigated. Many significant correlations and clear aging effects were found. It is worth emphasizing that despite the small number of samples, the results of the present study are mostly in agreement with the previous findings and reports in literature on minerals and aortic/cardiovascular health.

Earlier studies had suggested that the Si content in the aorta is higher than in other connective tissues, conversely low levels of silicon in human aortas were found in male and female subjects aged over 54 years compared to reported Si levels in other human arteries (e.g. radial artery).

Silicon levels did not appear to be markedly affected by either age or elastin content contrary to the strong literature evidence that Si affects ECM synthesis. Suggesting, that Si does not have a major effect on aortic health and maintenance of the ECM architecture once its formation is completed (elastin expression occurs only during late gestation until the end of childhood).

Results from the present study support the suggestion that silicon affects factors that are involved in progression of aortic stiffness, including the utilization of copper, essential in preventing oxidative damage to adult elastin fibres, and decreasing the adsorption of phosphorus to the matrix proteins involved in the calcification of the aortic wall.

4.II Method development for 'combined' elastin and collagen quantification

4.II.1 Background

Elastin and collagen are the two main structural components of the aorta and major determinants of aortic health and mechanical properties[25].

The matured cross-linked elastin produced during late fetal and early postnatal development is extremely stable and has a slow turnover rate with a longevity comparable to the human lifespan[25]. The aorta specimens analysed in this work were collected from human organ donors between the ages of 25 – 83 years, thus elastin in these samples will be grossly in form of mature/insoluble elastin.

In mature human aorta collagen type I and type III are the most abundant, but other isoforms of collagen are also present, e.g. collagen type IV, V and VIII[25]. Methods for the determination of collagen in tissue samples can be generally classified into two large groups. One group is based on immunochemical approach and the distinct chemical and physical properties of the different collagen types, where particular types of collagen can be individually analysed[81]; and the other comprises everything else, e.g. radiolabeling, chromatography and colorimetric assay, for the determination of total collagen content[82].

In animal tissues, 4-hydroxyproline (OH-Pro) is a major component of collagen, comprising around 13.5% of the protein amino acid composition. The protein with the next highest OH-Pro content is elastin with 2%[48]. For this reason, the colorimetric OH-Pro assay is considered the gold standard and is customarily used to estimate the total collagen content with a reliable degree of accuracy[48]. However, even though the OH-Pro content in human elastin is only 2%, the elastin content in the aortic media is considerable higher than collagen, especially in younger specimens (< 50 years old - Figure 27); imparting significance to elastin input in the total OH-Pro of the tissue lysate. Traditionally, collagen contents are estimated from the total OH-

Pro concentration after subtraction of the elastin OH-Pro contribution, determined by the desmosine and isodesmosine content of the tested sample[63]. However, the processes for the accurate quantification of these two crosslinking amino acids (desmosine and isodesmosine) in elastic tissues are complex, expensive, and require more sample than the amount that is available[83].

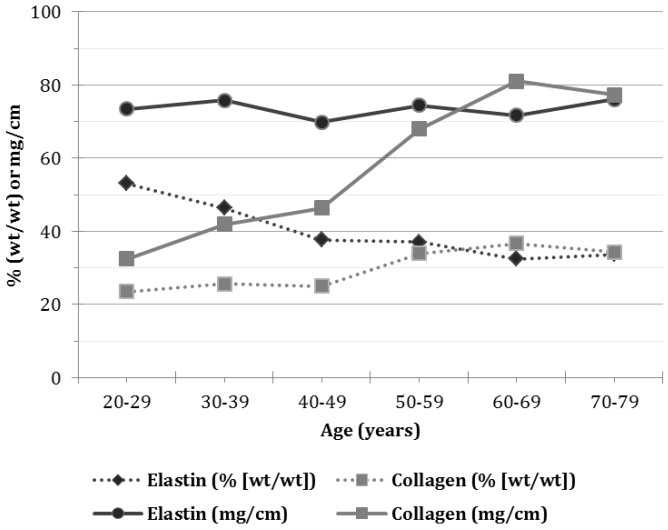

Figure 27 - Relative (% [wt/wt]) and absolute (mg/cm) elastin and collagen concentrations of the human upper thoracic aortic media. Produced from Spina, 1983[63].

The aim of this developmental work was to devise a simplified method for the accurate measurement of the total collagen and elastin contents in human aortas using a single specimen for both assays. For this purpose, the immunoprecipitation assay principles were applied to isolate elastin from collagens to quantify total elastin and collagen contents.

Pig feet cartilage and chicken tendon were used to optimise the immunoprecipitation process and, elastin and collagen assays.

4.II.2 Elastin and collagen extraction

Techniques for extraction and purification of mature elastin and collagen from connective tissues take advantage of the proteins unique and contrasting structural and chemical properties[84]. Two methods were investigated to extract elastin and

collagen from the test materials. These were the NaOH and oxalic acid extraction methods.

4.II.2.1 NaOH treatment

Mecham[85] and Daamen[45] undertook a comparison of the most commonly used methods for purifying elastin. The results presented on the traditional hot alkali procedure showed that the final product still contained some non-elastinous material of microfibrillar nature, but the bright field microscopy revealed the absence of collagenous material[45].

Elastin is insoluble when treated with 0.1M NaOH at 95ºC, and collagen is solubilized in the supernatant fraction. The residue and collagenous fractions (supernatant) were analysed by sodium dodecyl sulphate polyacrylamide gel electrophoresis (SDS-PAGE) and compared with the results obtained by Daamen and co-workers (Figure 28). Results indicated major protein contaminations in the elastin residue and high variability between samples. This procedure proved to be unreliable, time consuming and due to the viscous appearance of the insolubilized elastin above the supernatant, subject to elastin contaminations in the collagenous fraction during collection.

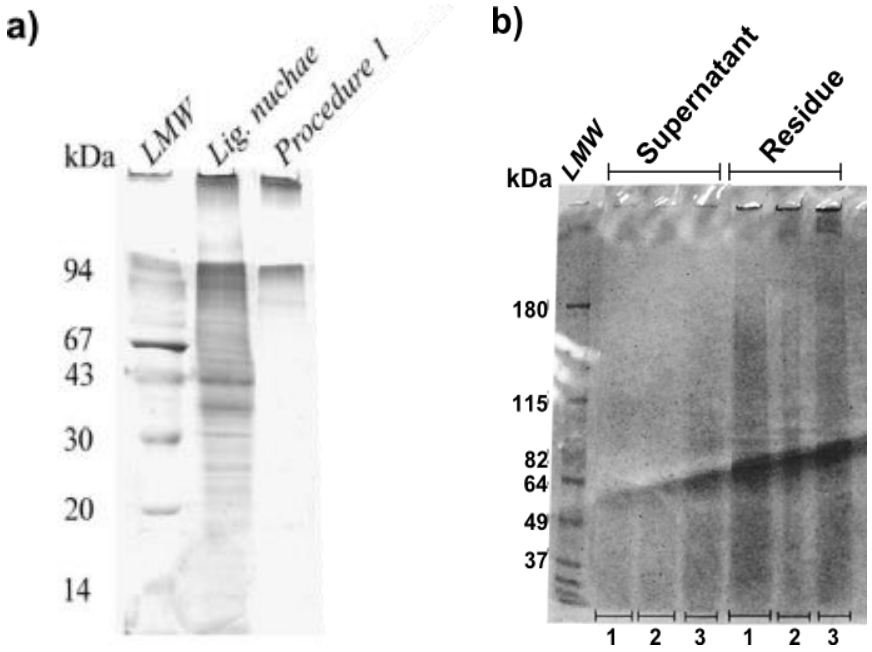

Figure 28 - SDS-PAGE electrophoresis of elastin preparations purified by hot alkali procedure. a) Representation of the reference lanes in Daamen et.al[45] experiments. LMW: Lane marker weights (kDa). Lig nuchae: Horse ligamentum nuchae source of insoluble elastin. Procedure 1: Elastin treated with 0.1 M NaOH heated at 95ºC for 45 min. b) Electrophoresis results of the supernatant and corresponding elastin residues fractions collected after treating three (1-3) samples of pig feet cartilage with 0.1M NaOH heated at 90ºC for 45 min. Note that only soluble contaminants (collagen and proteins) and/or elastin breakdown products will enter the gel. Insoluble elastin, which represent the vast majority of the residue, will not permeate the gel and will be visible at the top of the gel.

4.II.2.2 Hot Oxalic Acid Treatment

Insoluble native collagen must be pre-treated before it can be converted into a form suitable for extraction, such as gelatine. Food and waste industries use weak acids, such as oxalic acid and acetic acid, to obtain gelatine from limed split wastes and fish skin[51]. Moreover oxalic acid treatment of elastic matrixes promotes the extraction and reduction of mature insoluble elastin to soluble fragments easily analysed by a colorimetric assay (Fastin™ Elastin assay, see Introduction section 2.3.2.1).

The protocol for the extraction of elastin and collagen from the aortic tissue was optimized for the following parameters:

I. Minimum sample weight required
II. Wet or freeze dried sample
III. Tissue homogenization technique

IV. Acid volume

V. Number of extraction cycles

VI. Extraction time

VII. Storage of the extracts

Of all the methods investigated, elastin and collagen purification was more efficient if the tissues were dried and minced as fine as possible before the extraction steps (data not shown). Complete extraction of the elastin and collagen components of the elastic matrix was obtained with 3 cycles of heating the test homogenized samples in hot (95 - 100°C) oxalic acid (0.25 M) for one hour (Table 8). Insoluble elastin was extracted in the form of soluble cross-linked polypeptides elastin fragments (α-elastin), while collagen was partially hydrolysed to small peptides of molecular of various molecular weights.

The oxalic acid extracts (1st, 2nd and 3rd extractions) were pooled together (OAE*p*) for the separation of the elastin and collagen proteins (see below).

Table 8 - Elastin and collagen extraction. Descriptive analysis of the hot oxalic acid extractions and corresponding protein and elastin quantitative analysis performed on 3 samples of chicken tendon, with an average wet weight of 9.86 mg. Results are present as mean values of three samples. Elastin and protein content are expressed as μg in the volume of oxalic acid extract (OAE).

	1st Extraction	2nd Extraction	3rd Extraction	4th Extraction
Hot oxalic acid treatment				
Acid Volume (mL)	1.0	0.5	0.5	0.5
Tissue Homogenization	Yes	No	No	No
Temperature (ºC)	102	98	100	100
Time (min)	60	60	60	60
Solid residue	Yes	Yes	No	No
OAE				
pH	1-2	1-2	1-2	1-2
Volume (mL)	0.97	0.47	0.49	0.51
Elastin (μg)	177.30	27.70	2.04	0.0
Total protein† (μg)	720.91	76.79	14.17	0.0

†Total protein as determined by NIPA assay. Through this method elastin and gelatine protein amount recovery is 60-70% and 40-45%, respectively.

4.II.3 Collagen and elastin separation

To accurately determine the absolute amount of collagen in the aortic ECM, an immunoprecipitation step was developed to remove the soluble elastin fragments present in the pooled extract solution obtained by the hot oxalic acid treatment (OAE*p*) (see above). By immobilizing the α-elastin fragments present in solution, all the collagens types, also solubilized during the acid extraction, are eluted collectively, allowing the total collagen quantification by OH-Pro without the interfering signal of the elastin's OH-Pro.

4.II.3.1 Elastin Immunoprecipitation

The Thermo Scientific Pierce Classic IP kit was preferred to perform the immunoprecipitation of the elastin fragments obtained after the hot oxalic acid extraction. The kit uses high-capacity Protein A/G agarose affinity resin and a

microcentrifuge spin column format that helps to ensure effective washing and separation of samples from the beaded agarose resin.

The mouse monoclonal anti-elastin antibody [10B8] from Abcam, Cambridge, UK was selected for the immobilization of α-elastin according to the following criteria:

I. Specificity for elastin and elastin peptides.
II. Tested successfully for IP applications.
III. Species reactivity, i.e. human reactivity.
IV. Isotype with strong binding affinity for Protein A/G.
V. Monoclonal antibody.
    a. Compared to polyclonal antibodies, monoclonal antibodies have less batch variability, e.g. the results from monoclonal antibodies are highly reproducible between experiments.
    b. Its specificity makes monoclonal antibodies extremely efficient for binding antigens within a mixture of related molecules and less likely to cross-react.

The immunoprecipitation procedure was developed based on the protocol and reagents provided within the Thermo Scientific Pierce Classic IP kit. The conditions for the immobilization of the elastin fragments solubilized in the acid extracts were optimized by examining the effect of various critical parameters such as extract pre-clearing, minimum antibody and maximum protein loading, order of assembly of the immobilized antibody/antigen complex and buffers compositions and interference with the quantitative assays (hydroxyproline and Fastin™ Elastin assays) (Table 9).

Table 9 - Optimal conditions for IP assay.

	Optimal Conditions
Order of assembly	Beads – Antibody – Antigen
Antibody	[10B8]
Volume (µL)	7
Sample	
pH	7-8
Pre-clearing	Yes
Volume (µL)	250
Total protein† (µg)	30-50
Wash buffer interference ‡	
Lysis/Wash Buffer	Yes
TBS wash Buffer (1x)	No

† As determined by NIPA assay.
‡ Buffer interference with control assay: Fastin Elastin Assay.

Antigen yield was highest when first binding 7 µg of antibody to 30 µL of Protein A/G beaded support, followed by the incubation of the immobilized antibody with the 250 µL of the previously pre-cleared and neutralized tissue extract (Table 9). Sample pre-clearing is an optional step designed to remove proteins and ligands that bind non-specifically to the beaded support. This involves adjusting the pH of the sample (oxalic acid extracts) to neutral pH (pH 7-8). IP Lysis/Wash buffer provided with the IP kit was found to interfere with the Fastin™ Elastin assay. Moreover collagen elution was more effective when using the wash detergent-free 1xTBS buffer.

A representative scheme of the final elastin immunoprecipitation protocol is displayed in Figure 29 and the protein and elastin quantitative analysis of the different fractions collected with the IP assay are summarize in the Table 10.

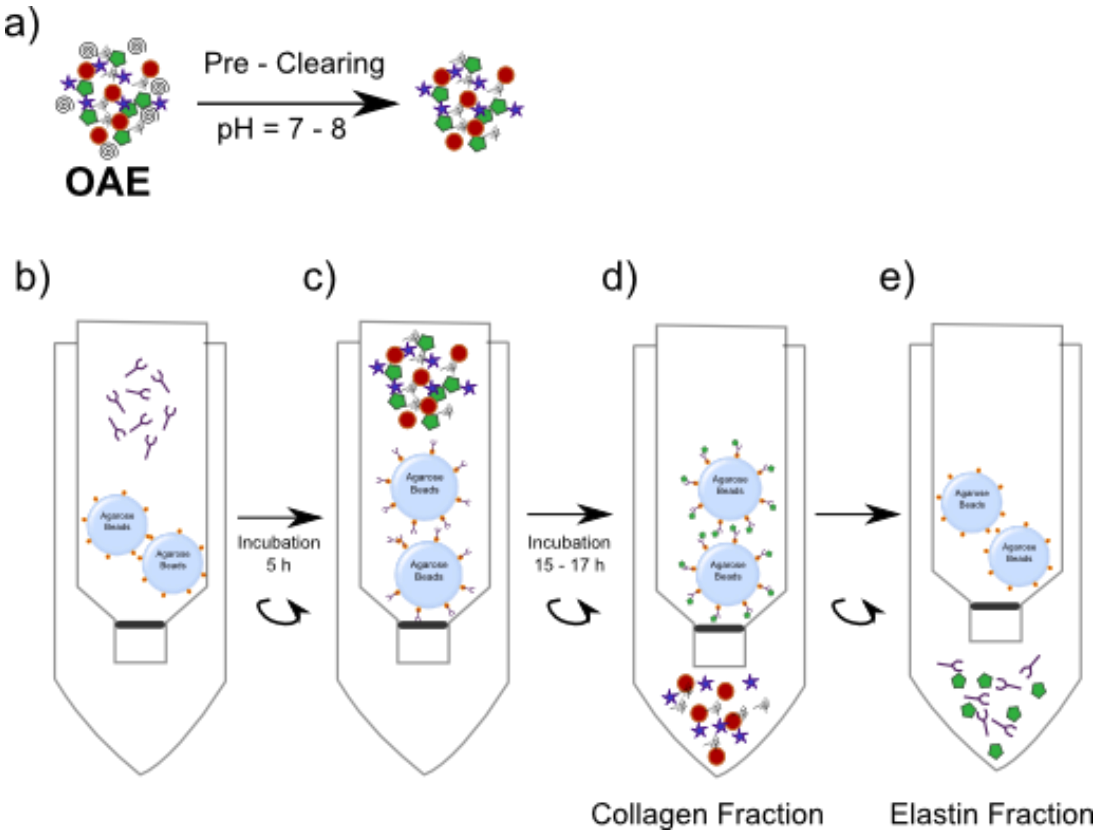

Figure 29 - Immunoprecipitation assay procedure. a) Sample pre-clearing step to reduce non-specific binding of protein to the agarose beads: adjust the pH of sample to 7-8. b) Formation of the antibody – beads complex: incubation for 5h at 4ºC of the Pierce protein A/G agarose beads with the monoclonal antibody. Centrifuge and discard supernatant. c) Formation of the immune complex: incubation for 15 -17h at 4ºC of the antibody – beads complex with the pre-cleared solution. d) Collected collagen fractions: centrifuge and collect the unbound collagenous fraction. Wash the spin column and collect the eluate solution, twice. e) Collect elastin fractions: incubate for 10 min at 97ºC, the immune complex with the Pierce elution buffer. Centrifuge and collect the elastin fraction. Repeat the incubation with the elution buffer twice.

Prior to the IP assay, the various OAEs collected were pooled together (OAE_P), analysed for elastin and protein content with the Fastin™ Elastin assay and NIPA assays, respectively, and a suitable sample volume (≈100 μL) was calculated for the adequate protein loading concentration into the immunoprecipitation assay (optimal concentration of 30 – 50 μg) (Table 10). The sample was further diluted to a total volume of 250 μL with 1xTBS buffer and the IP assay carried out as previously described (Figure 29). The multiple collagen and elastin fractions collected were analysed for elastin and total protein content by Fastin™ Elastin assay and NIPA assay, respectively (Table 10).

The results from Table 10, suggested a high affinity of the antibody for the elastin protein, as less than 1 μg of elastin was detected in the collagenous fractions.

Differences between the calculated elastin concentration loaded in the column (7.2 – 13.6 μg) and the total elastin recovered (5.3 – 12.2 μg) are probably related to instrumental errors (pipetting and tube transferences).

Table 10 - Elastin and total protein analysis of the collagen and elastin fractions collected from the IP assay developed. IP assay performed on OAE obtained from chicken tendon, n=3 samples/specimens.

	Elastin (μg)	**Total Protein† (μg)**
OAE_P (100 μL)	7.2 – 13.6	42.6 – 50.1
Collagen Fraction		
1st eluate	< 1.0	20.2 – 23.6
2nd eluate	0.0	7.4 – 9.0
3rd eluate	0.0	< 1.8
Elastin fraction		
1st eluate	4.3 – 6.0	NP
2nd eluate	< 4.3	NP
3rd eluate	0.0	NP
Recovery (%)	**70 - 80**	**~65‡**

†As determined by NIPA assay. Through this method elastin and gelatine protein amount recovery is 60-70% and 40-45%, respectively.
‡Total protein recovery will always be lower than 100% as the elastin should be collected in the immobilized fraction
NP: assay not performed

4.II.4 Collagen assay

The collagenous fractions collected in the immunoprecipitation assay (Table 10: collagen fraction = 1st and 2nd eluate), where pooled together for further collagen analysis by the hydroxyproline assay. The pooled samples were freeze dried for 48 h to concentrate the protein amount.

The OH-Pro assay procedure was based on the vapour-phase HCl microwave hydrolysis of the freeze dried residue and subsequent determination of the free hydroxyproline in the hydrolysed sample. Chloramine-T was used to oxidize the free hydroxyproline for the production of a pyrrole, and the addition of Ehrlich's reagent resulted in the formation of a chromophore that can be measured at 540 nm.

As 4-hydroxyproline (OH-Pro) is a major component of collagen that comprising around 13.5% of the protein amino acid composition, the total collagen content of the tissue lysate is determined assuming that this protein contains an average of 13.5% w/w of OH-Pro residues[48].

A complete protocol of the developed assay for the determination of collagen and elastin contents can be found in Appendix D.

4.II.5 Conclusion

This project was successful in establishing a new biochemical method that allows the analysis and quantification of elastin and collagen using one single specimen. This allowed a significant reduction in the amount of sampled used while still obtaining accurate data on the elastin and collagen contents of the human aorta, using cost effective techniques. Disadvantages to the new protocol include its susceptibility to experimental errors due to the usage of low volumes and sample loss due to material transference between the various tubes. Measures can be adopted to reduce these problems such as careful homogenization of the sample solutions before handling and the recording of the weights of the sample volumes used in the assays.

5 Future Research

Silicon is the third most abundant trace-element in the human body. Considering the abundance of silicon, both in the nature and in humans, it is expected that it should play an important role in human and animal health. The Si potential involvement in atherosclerosis has been suggested by several authors. However, when the role of trace elements in various diseases is discussed, it is not only essential to know the concentrations of these elements in tissues under disease, but also in normal conditions, which has not received adequate attention. Additional insights into the Si biological mechanisms of action and its role in cardiovascular health, along with larger studies on both animals and humans are required.

In this study, due to instrumental problems and time constrictions, collagen was not determined and association between Si and collagen and aortic performance, e.g. elasticity, may provide crucial information and must be investigated, this being a subject for future complementary studies.

Whether Si has a biological role in man is not known, but large evidence from animal and *in vitro* studies have continuously suggested that Si contributes to the synthesis and architecture of the ECM matrix proteins, and is uniquely localized in active growth areas in young bones of animals[86]. Human studies have also implied a higher requirement of Si in newborns and developing foetus, serum Si levels where found higher in infants compared to older children and adults[49, 87]. Knowing that elastin expression occurs over a narrow window of development, beginning in mid-gestation and continuing at high levels through the postnatal period with minimal synthesis in the adult life[25], a question stands up: could the essential role of Si in the maintenance of the resilience and architecture of the aortic ECM matrix be connected to its early development? Could the Si levels in foetus and young children aorta be correlated with longevity and lower cardiovascular incidence? From this viewpoint, supplementation of the regular diet with bioavailable form of silicon in pregnant

women may, therefore, have a long-term therapeutic potential including prevention of degenerative processes. Further research is needed to determine the role of silicon in the developing foetus and long-term outcomes.

6 References

1. Seaborn, C.D., Nielsen, F.H. Silicon: A nutritional beneficence for bones, brains and blood vessels? Nutrition Today. 1993; 28 (4).
2. Carlisle, E.M. Silicon. Nutrition Reviews. 1975; 33 (9).
3. Loeper, J. & Fragny, M. The physiological role of the silicon and its antiatheromatous action. In Biochemistry of silicon and related problems. New York (1978): Plenum Press; 281-296
4. Schwarz, K. Silicon, fibre, and atherosclerosis. The Lancet. 1977; 309 (8009): 454-457.
5. McNaughton, S.A.; Bolton-Smith, C.; Mishra, G.D.; Jugdaohsingh, R. & Powell, J.J. Dietary silicon intake in post-menopausal women. British Journal of Nutrition. 2005; 94 (5): 813-817.
6. Carlisle, E.M. Silicon as an esential trace element in animal nutrition. In Silicon biochemistry. Sussex (1986): John Wiley & Sons Ltd.;
7. Martin, K.R. The chemistry of silica and its potential health benefits. The Journal Of Nutrition, Health & Aging. 2007; 11 (2): 94-97.
8. Jugdaohsingh, R.; Anderson, S.; Tucker, K.; Elliott, H.; Kiel, D.; Thompson, R. & Powell, J. Dietary silicon intake and absorption. The American Journal of Clinical Nutrition. 2002; 75 (5): 887-893.
9. Powell, J.; McNaughton, S.; Jugdaohsingh, R.; Anderson, S.; Dear, J.; Khot, F.; Mowatt, L.; Gleason, K.; Sykes, M.; Thompson, R.; Bolton-Smith, C. & Hodson, M. A provisional database for the silicon content of foods in the united kingdom. The British journal of nutrition. 2005; 94 (5): 804-812.
10. Reffitt, D.M.; Jugdaohsingh, R.; Thompson, R.P.H. & Powell, J.J. Silicic acid: Its gastrointestinal uptake and urinary excretion in man and effects on aluminium excretion. Journal of Inorganic Biochemistry. 1999; 76 (2): 141-147.
11. Adler, A.J.; Etzion, Z. & Berlyne, G.M. Uptake, distribution, and excretion of 31silicon in normal rats. American Journal of Physiology - Endocrinology And Metabolism. 1986; 251 (6): E670-E673.
12. Jugdaohsingh, R. Silicon and bone health. Journal of Nutrition Health and Aging. 2007; 11 (2): 99-110.
13. Schwarz, K. Significance and functions of silicon in warm-blooded animals. In Biochemistry of silicon and related problems. New York (1978): Plenum Press; 207-230
14. Carlisle, E.M. Essentiality and function of silicon. In Biochemistry of silicon and related problems. New York (1978): Plenum Press; 231-254
15. Schwarz, K. A bound form of silicon in glycosaminoglycans and polyuronides. Proceedings of the National Academy of Sciences of the United States of America. 1973; 70 (5): 1608-1612.

16. Jugdaohsingh, R.; Sripanyakorn, S. & Powell, J. Silicon absorption and excretion is independent of age and sex in adults. The British journal of nutrition. 2013; 1-7.
17. Charnot, Y. & Peres, G. Silicon, endocrine balance and mineral metabolism (calcium and magnesium). Biochemistry of Silicon and Related Problems. 1978; 269-280.
18. Jugdaohsingh, R.; Tucker, K.L.; Qiao, N.; Cupples, L.A.; Kiel, D.P. & Powell, J.J. Dietary silicon intake is positively associated with bone mineral density in men and premenopausal women of the framingham offspring cohort. Journal of Bone and Mineral Research. 2004; 19 (2): 297-307.
19. Macdonald, H.M.; Hardcastle, A.C.; Jugdaohsingh, R.; Fraser, W.D.; Reid, D.M. & Powell, J.J. Dietary silicon interacts with oestrogen to influence bone health: Evidence from the aberdeen prospective osteoporosis screening study. Bone. 2012; 50 (3): 681-687.
20. Vlachopoulos, C.; Alexopoulos, N. & Stefanadis, C. Aortic stiffness: Prime time for integration into clinical practice? Hellenic Journal of Cardiology. 2010; 51 (5): 385-390.
21. Boudoulas, K.D.; Vlachopoulos, C.; Raman, S.V.; Sparks, E.A.; Triposciadis, F.; Stefanadis, C. & Boudoulas, H. Aortic function: From the research laboratory to the clinic. Cardiology. 2012; 121 (1): 31-42.
22. Sawabe, M. Vascular aging: From molecular mechanism to clinical significance. Geriatrics & Gerontology International. 2010; 10 S213-S220.
23. Warfield, L.M. in Arteriosclerosis and Hypertension: with Chapters on Blood Pressure, Edn. 3 rd (C. V. Mosby Company, St. Louis; 1920).
24. Briet, M.; Boutouyrie, P.; Laurent, S. & London, G.M. Arterial stiffness and pulse pressure in ckd and esrd. Kidney International. 2012; 82 (4): 388-400.
25. Wagenseil, J.E. & Mecham, R.P. Vascular extracellular matrix and arterial mechanics. Physiological Reviews. 2009; 89 (3): 957-989.
26. O'Connell, M.K.; Murthy, S.; Phan, S.; Xu, C.; Buchanan, J.; Spilker, R.; Dalman, R.L.; Zarins, C.K.; Denk, W. & Taylor, C.A. The three-dimensional micro- and nanostructure of the aortic medial lamellar unit measured using 3d confocal and electron microscopy imaging. Matrix Biology. 2008; 27 (3): 171-181.
27. Ushiki, T. Collagen fibers, reticular fibers and elastic fibers. A comprehensive understanding from a morphological viewpoint. Archives of Histology and Cytology. 2002; 65 (2): 109-126.
28. Moore, J. & Thibeault, S. Insights into the role of elastin in vocal fold health and disease. Journal of Voice. 2012; 26 (3): 269-275.
29. Jacob, M.P. Extracellular matrix remodeling and matrix metalloproteinases in the vascular wall during aging and in pathological conditions. Biomedicine & Pharmacotherapy. 2003; 57 (5–6): 195-202.
30. Umeji, K.; Umemoto, S.; Itoh, S.; Tanaka, M.; Kawahara, S.; Fukai, T. & Matsuzaki, M. Comparative effects of pitavastatin and probucol on oxidative stress, cu/zn superoxide dismutase, ppar-γ, and aortic stiffness in

hypercholesterolemia. American Journal of Physiology - Heart and Circulatory Physiology. 2006; 291 (5): H2522-H2532.
31. Dawson, E.B.; Frey, M.J.; Moore, T.D. & McGanity, W.J. Relationship of metal metabolism to vascular disease mortality rates in texas. The American Journal of Clinical Nutrition. 1978; 31 (7): 1188-1197.
32. Nakashima, Y.; Kuroiwa, A. & Nakamura, M. Silicon contents in normal, fatty streaks and atheroma of human aortic intima: Its relationship with glycosaminoglycans. The British Journal of Experimental Pathology. 1985; 66 (1): 123-127.
33. Najda, J.; Gminski, J.; Drozdz, M. & Flak, A. The effect of silicon (si) on lipid parameters in blood serum and arterial wall. Biological Trace Element Research. 1991; 31 (3): 235-247.
34. Maehira, F.; Motomura, K.; Ishimine, N.; Miyagi, I.; Eguchi, Y. & Teruya, S. Soluble silica and coral sand suppress high blood pressure and improve the related aortic gene expressions in spontaneously hypertensive rats. Nutrition Research. 2011; 31 (2): 147-156.
35. Carlisle, E. In vivo requirement for silicon in articular cartilage and connective tissue formation in the chick. The Journal of nutrition. 1976; 106 (4): 478-484.
36. Reffitt, D.M.; Ogston, N.; Jugdaohsingh, R.; Cheung, H.F.J.; Evans, B.A.J.; Thompson, R.P.H.; Powell, J.J. & Hampson, G.N. Orthosilicic acid stimulates collagen type 1 synthesis and osteoblastic differentiation in human osteoblast-like cells in vitro. Bone. 2003; 32 (2): 127-135.
37. Birchall, J.D. The essentiality of silicon in biology. Chemical Society Reviews. 1995; 24.
38. Najda, J.; Gmiński, J.; Drózdz, M. & Danch, A. Silicon metabolism. The interrelations of inorganic silicon (si) with systemic iron (fe), zinc (zn), and copper (cu) pools in the rat. Biological Trace Element Research. 1992; 34 (2): 185-195.
39. Emerick, R.J. & Kayongo-Male, H. Silicon facilitation of copper utilization in the rat. The Journal Of Nutritional Biochemistry. 1990; 1 (9): 487-492.
40. Rucker, R.B.; Kosonen, T.; Clegg, M.S.; Mitchell, A.E.; Rucker, B.R.; Uriu-Hare, J.Y. & Keen, C.L. Copper, lysyl oxidase, and extracellular matrix protein cross-linking. The American Journal of Clinical Nutrition. 1998; 67 (5): 996S-1002S.
41. Greenwald, S. Ageing of the conduit arteries. The Journal of pathology. 2007; 211 (2): 157-172.
42. Jugdaohsingh, R.; Calomme, M.R.; Robinson, K.; Nielsen, F.; Anderson, S.H.C.; D'Haese, P.; Geusens, P.; Loveridge, N.; Thompson, R.P.H. & Powell, J.J. Increased longitudinal growth in rats on a silicon-depleted diet. Bone. 2008; 43 (3): 596-606.
43. Nóbrega, J.A.; Pirola, C.; Fialho, L.L.; Rota, G.; de Campos Jordão, C.E.K.M.A. & Pollo, F. Microwave-assisted digestion of organic samples: How simple can it become? Talanta. 2012; 98 (0): 272-276.

44. Hou, X. & Jones, B. Inductively coupled plasma-optical emission spectrometry. In Encyclopedia of analytical chemistry. (2006): John Wiley & Sons, Ltd;
45. Daamen, W.; Hafmans, T.; Veerkamp, J. & Van Kuppevelt, T. Comparison of five procedures for the purification of insoluble elastin. Biomaterials. 2001; 22 (14): 1997-2005.
46. Rutherfurd, S. & Gilani, G. Amino acid analysis. In Current protocols in protein science. (2001): John Wiley & Sons, Inc.;
47. Ignat'eva, N.Y.; Danilov, N.A.; Averkiev, S.V.; Obrezkova, M.V.; Lunin, V.V. & Sobol', E.N. Determination of hydroxyproline in tissues and the evaluation of the collagen content of the tissues. Journal of Analytical Chemistry. 2007; 62 (1): 51-57.
48. Kliment, C.; Englert, J.; Crum, L. & Oury, T. A novel method for accurate collagen and biochemical assessment of pulmonary tissue utilizing one animal. International journal of clinical and experimental pathology. 2011; 4 (4): 349-355.
49. Jugdaohsingh, R.; Anderson, S.H.C.; Lakasing, L.; Sripanyakorn, S.; Ratcliffe, S. & Powell, J.J. Serum silicon concentrations in pregnant women and newborn babies. British Journal of Nutrition. 2013; 1-7.
50. Hall, D. & Czerkawski, J. The reaction between elastase and elastic tissue. 4. Soluble elastins. The Biochemical journal. 1961; 80 (1): 121-128.
51. Gómez-Guillén, M.; Giménez, B.; López-Caballero, M. & Montero, M. Functional and bioactive properties of collagen and gelatin from alternative sources: A review. Food Hydrocolloids. 2011; 25 1813-1827.
52. Honório, A.; de Lurdes Pinto, M.; Gonçalves, C. & Bairos, V. Elastin in the avian lungs. The Open Chemical and Biomedical Methods Journal. 2009; 2 18-23.
53. Hofman, K.; Hall, B.; Cleaver, H. & Marshall, S. High-throughput quantification of hydroxyproline for determination of collagen. Analytical Biochemistry. 2011; 417 (2): 289-291.
54. Minami, T.; Tohno, S.; Utsumi, M.; Moriwake, Y.; Yamada, M. & Tohno, Y. Selective accumulations of aluminum in five human arteries. Biological Trace Element Research. 2001; 79 (1): 29-38.
55. Aalbers, T.G.; Houtman, J.P. & Makkink, B. Trace-element concentrations in human autopsy tissue. Clinical Chemistry. 1987; 33 (11): 2057-2064.
56. Tohno, Y.; Tohno, S.; Minami, T.; Utsumi, M.; Moriwake, Y.; Nishiwaki, F.; Yamada, M.; Yamamoto, K.; Takano, Y.; Okazaki, Y. & Yamamoto, H. Age-related changes of mineral contents in the human aorta and internal thoracic artery. Biological Trace Element Research. 1998; 61 (2): 219-226.
57. Cichocki, T.; Heck, D.; Jarczyk, L.; Rokita, E.; Strzałkowski, A. & Sych, M. Elemental composition of the human atherosclerotic artery wall. Histochemistry and Cell Biology. 1985; 83 (1): 87-92.
58. Hanć, A.; Komorowicz, I.; Iskra, M.; Majewski, W. & Barałkiewicz, D. Application of spectroscopic techniques: Icp-oes, la-icp-ms and chemometric

methods for studying the relationships between trace elements in clinical samples from patients with atherosclerosis obliterans. Analytical and Bioanalytical Chemistry. 2011; 399 (9): 3221-3231.
59. 2012, Health survey for england - 2011, health, social care and lifestyles: Chapter 10 - Adult anthropometric measures, overweight and obesity. The Health and Social Care Information Centre [National Statistics]. http://www.hscic.gov.uk/home
60. McConnell, J.P.; Moyer, T.P.; Nixon, D.E.; Schnur, P.L.; Salomao, D.R.; Crotty, T.B.; Weinzweig, J.; Harris, J.B. & Petty, P.M. Determination of silicon in breast and capsular tissue from patients with breast implants performed by inductively coupled plasma emission spectroscopy. Comparison with tissue histology. Am J Clin Pathol. 1997; 107 (2): 236-246.
61. Van Dyck, K.; Robberecht, H.; Van Cauwenbergh, R.; Van Vlaslaer, V. & Deelstra, H. Indication of silicon essentiality in humans: Serum concentrations in belgian children and adults, including pregnant women. Biological Trace Element Research. 2000; 77 (1): 25-32.
62. Cattell, M.A.; Anderson, J.C. & Hasleton, P.S. Age-related changes in amounts and concentrations of collagen and elastin in normotensive human thoracic aorta. Clinica Chimica Acta. 1996; 245 (1): 73-84.
63. Spina, M.; Garbisa, S.; Hinnie, J.; Hunter, J.C. & Serafini-Fracassini, A. Age-related changes in composition and mechanical properties of the tunica media of the upper thoracic human aorta. Arteriosclerosis, Thrombosis, and Vascular Biology. 1983; 3 (1): 64-76.
64. Watanabe, M.; Sawai, T.; Nagura, H. & Suyama, K. Age-related alteration of cross-linking amino acids of elastin in human aorta. The Tohoku journal of experimental medicine. 1996; 180 (2): 115-130.
65. Fritze, O.; Romero, B.; Schleicher, M.; Jacob, M.; Oh, D.-Y.; Starcher, B.; Schenke-Layland, K.; Bujan, J. & Stock, U. Age-related changes in the elastic tissue of the human aorta. Journal of Vascular Research. 2012; 49 (1): 77-86.
66. O'Connor, C.I.; Nielsen, B.D.; Woodward, A.D.; Spooner, H.S.; Ventura, B.A. & Turner, K.K. Mineral balance in horses fed two supplemental silicon sources. Journal of Animal Physiology and Animal Nutrition. 2008; 92 (2): 173-181.
67. Birchall, J.D.; Bellia, J.P. & Roberts, N.B. On the mechanisms underlying the essentiality of silicon — interactions with aluminium and copper. Coordination Chemistry Reviews. 1996; 149 (0): 231-240.
68. Dubick, M.A.; Hunter, G.C.; Casey, S.M. & Keen, C.L. Aortic ascorbic acid, trace elements, and superoxide dismutase activity in human aneurysmal and occlusive disease. Proceedings of the Society for Experimental Biology and Medicine. Society for Experimental Biology and Medicine. 1987; 184 (2): 138-143.
69. Iskra, M.; Patelski, J. & Majewski, W. Relationship of calcium, magnesium, zinc and copperconcentrations in the arterial wall and serum in atherosclerosis

obliterans and aneurysm. Journal of Trace Elements in Medicine and Biology. 1997; 11 (4): 248-252.
70. Aalbers, T.G. & Houtman, J.P.W. Relationships between trace elements and atherosclerosis. Science of The Total Environment. 1985; 43 (3): 255-283.
71. Tohno, Y.; Tohno, S.; Moriwake, Y.; Azuma, C.; Ohnishi, Y. & Minami, T. Accumulation of calcium and phosphorus accompanied by increase of magnesium and decrease of sulfur in human arteries. Biological Trace Element Research. 2001; 82 (1-3): 9-19.
72. Minami, T.; Ichii, M.; Tohno, Y.; Tohno, S.; Utsumi, M.; Yamada, M. & Okazaki, Y. Age-dependent aluminum accumulation in the human aorta and cerebral artery. Biological Trace Element Research. 1996; 55 (1-2): 199-205.
73. Sherratt, M.J. Tissue elasticity and the ageing elastic fibre. AGE. 2009; 31 (4): 305-325.
74. Hakki, S.; Dundar, N.; Kayis, S.; Hakki, E.; Hamurcu, M.; Kerimoglu, U.; Baspinar, N.; Basoglu, A. & Nielsen, F. Boron enhances strength and alters mineral composition of bone in rabbits fed a high energy diet. Journal of trace elements in medicine and biology : organ of the Society for Minerals and Trace Elements (GMS). 2013; 27 (2): 148-153.
75. Chebassier, N.; El Houssein, O.; Viegas, I. & Dréno, B. In vitro induction of matrix metalloproteinase-2 and matrix metalloproteinase-9 expression in keratinocytes by boron and manganese. Experimental Dermatology. 2004; 13 (8): 484-490.
76. Day, S.; Duquaine, D.; Mundada, L.; Menon, R.; Khan, B.; Rajagopalan, S. & Fay, W. Chronic iron administration increases vascular oxidative stress and accelerates arterial thrombosis. Circulation. 2003; 107 (20): 2601-2606.
77. Cantor, J.; Shteyngart, B.; Cerreta, J.; Ma, S. & Turino, G. Synergistic effect of hydrogen peroxide and elastase on elastic fiber injury in vitro. Experimental Biology and Medicine. 2006; 231 (1): 107-111.
78. Adrogué, H. & Madias, N. Sodium and potassium in the pathogenesis of hypertension. The New England journal of medicine. 2007; 356 (19): 1966-1978.
79. Et-taouil, K.; Schiavi, P.; Lévy, B.I. & Plante, G.E. Sodium intake, large artery stiffness, and proteoglycans in the spontaneously hypertensive rat. Hypertension. 2001; 38 (5): 1172-1176.
80. Tokimitsu, I. & Tajima, S. Inhibition of elastin synthesis by high potassium salt is mediated by ca2+ influx in cultured smooth muscle cells in vitro: Reciprocal effects of k+ on elastin and collagen synthesis. Journal of Biochemistry. 1994; 115 (3): 536-539.
81. Katsuda, S.; Okada, Y.; Minamoto, T.; Oda, Y.; Matsui, Y. & Nakanishi, I. Collagens in human atherosclerosis. Immunohistochemical analysis using collagen type-specific antibodies. Arteriosclerosis, Thrombosis, and Vascular Biology. 1992; 12 494-502.
82. Lareu, R.; Zeugolis, D.; Abu-Rub, M.; Pandit, A. & Raghunath, M. Essential modification of the sircol collagen assay for the accurate quantification of

collagen content in complex protein solutions. Acta biomaterialia. 2010; 6 (8): 3146-3151.
83. Simona, V.; Laura, A.; Maurizio, L.; Jan, S.; Begoña, C. & Paolo, I. Progress in the methodological strategies for the detection in real samples of desmosine and isodesmosine, two biological markers of elastin degradation. Journal of Separation Science. 2007; 30 202-213.
84. Venturi, M.; Bonavina, L.; Annoni, F.; Colombo, L.; Butera, C.; Peracchia, A. & Mussini, E. Biochemical assay of collagen and elastin in the normal and varicose vein wall. Journal of Surgical Research. 1996; 60 (1): 245-248.
85. Mecham, R.P. Methods in elastic tissue biology: Elastin isolation and purification. Methods. 2008; 45 (1): 32-41.
86. Sripanyakorn, S.; Jugdaohsingh, R.; Thompson, R.P.H. & Powell, J.J. Dietary silicon and bone health. Nutrition Bulletin. 2005; 30 (3): 222-230.
87. Dyck, K.; Robberecht, H.; Cauwenbergh, R.; Vlaslaer, V. & Deelstra, H. Indication of silicon essentiality in humans. Biological Trace Element Research. 2000; 77 (1): 25-32.

APPENDIX

CONTENTS

Appendix A : Elements of lesions areas in the human aorta

A.1 Background

To elucidate the mineral and structural composition of the ageing human aorta, this thesis investigated age- and gender-related changes of minerals and elastin in aortas from male and female organ donors. It was established that the accumulation of calcium, phosphorus and aluminium occurs with advancing age. Relationships among the element concentrations were investigated and significant direct correlations were found between calcium, phosphorus, magnesium and aluminium levels. In contrast, inverse correlations were found between silicon and phosphorus contents, suggesting a possible preventive role for silicon in the maintenance of aortic health. However, mechanisms are not clear.

During the sampling of the aortas, three specimens were identified as being abnormal. Increased aortic wall thickness was observed in one sample and, visible calcified areas in two others (Results - Figure I.1). For easier identification, the first sample is classified as stiff aorta, and the latter as calcified aortas.

In the present Appendix, the mineral concentrations and the elastin contents in the lesion and lesion-surrounding sites of the stiff and calcified aortas were investigated and compared with the average results from the normal aortas.

A.2 Results and Discussion

Abnormal aortas were identified in three subjects; all were male, and the ages were as follow: stiff aorta = 70 year old male and calcified aortas = 55 and 70 years old males. Due to the limited number of samples (n=3), no statistical analysis was performed in the data presented below.

Table A.1 and A.2 show the mineral and elastin content, respectively, of the stiff and calcified aortas in the lesion and surrounding area, separately, and compared with the control aortas (normal). No manganese or boron was detected

when analysing both the lesion and the surrounding sites of the abnormal aortas by ICP-OES.

Table A.1 - Content of elements in the stiff and calcified lesions and surrounding lesion free areas of the abnormal aorta samples, and mean concentrations in normal aorta samples. Values expressed as mg/g dry weight for the elements: Ca, P, Mg, Na and K; and expressed as μg/g dry weight for the elements: Al, Cu, Si, Fe and Zn.

	Stiff (*n*=1)		**Calcified (*n*=2)**		**Normal (*n*=40)**
	Lesion	Surrounding	Lesion	Surrounding	Mean ± SD
Ca	2.21	9.89	142.20	8.70	9.3 ± 3.0
P	1.29	4.05	34.80	3.93	3.4 ± 1.3
Mg	0.14	0.89	1.21	0.55	0.9 ± 0.4
Na	2.78	6.13	3.10	2.38	6.2 ± 4.4
K	4.00	7.50	6.36	9.24	7.1 ± 5.1
Al	1.78	9.35	87.28	9.18	8.3 ± 3.0
Cu	1.20	5.22	1.68	1.71	4.1 ± 2.2
Si	ND	ND	5.87	18.89	14.1 ± 11.7
Fe	8.58	26.15	71.09	43.55	45.7 ± 27.9
Zn	22.94	79.51	75.44	41.52	70.9 ± 19.4

ND – not detected

Table A.2 - Content of the elastin concentrations in the stiff and calcified lesions and surrounding lesion free areas of the abnormal aorta samples, and mean concentrations in normal aorta samples. Values expressed as mg/g dry weight.

	Stiff (*n*=1)		**Calcified (*n*=2)**		**Normal (*n*=40)**
	Lesion	Surrounding	Lesion	Surrounding	Mean ± SD
Elastin	120.38	316.38	74.66	101.24	225.1 ± 62.8

A.2.1Stiff aorta

The element contents of the stiff lesion were much lower than in its surrounding areas, but the values were still within the range previously established for the control aortas (Table A.1). The elastin content of the stiff area (lesion) was only slightly below the previously defined range for normal aortas, but when comparing the elastin levels between the lesion and the lesion-surrounding sites, a decrease in almost 3-folds was observed (Table A.2).

A.2.2 Calcified aorta

Tables A.1 and A.2 show the content of the calcified aortas in the lesion and surrounding area plus the mean concentrations of control aortas (n = 40). Elemental concentrations in the calcified and surrounding areas determined in this study were found to be very similar to a published reported by Tohno and colleagues[2], where the authors investigated the concentrations of some elements (Ca, P, S, Mg, Fe, Zn, Pb and Al) in calcified and calcification surrounding sites of the thoracic aorta.

Generally, higher element concentrations were found for the calcified lesions when compared with the surrounding sites where the results were similar to the control samples. As expected, the contents of calcium, phosphorus and aluminium are extremely high in the calcified areas, compared with the surrounding and control samples. However, magnesium, sodium, potassium and copper contents did not seem to be largely altered by the calcification of the aorta. Interestingly, in calcified sites, Si content was approximately 4- and 3-times lower than in surrounding sites and mean content in normal aortas, respectively; endorsing the previous observation in this thesis than Si may have a role in aorta calcification.

Elastin content in the calcified and surrounding sites was identical (Calcified: 74.66 ± 28.2 mg/g & Surrounding: 101.24 ± 86.1 mg/g), but approximately half of the amount found in the control samples. In fact, Bobryshev et. al[3] examined the association of calcified deposits with ECM components, such as elastin, and observed that calcification requires a pre-existing structural base such as altered elastin fibres and that the co-localization of calcified deposits and elastin fibres was followed by destruction of the elastin.

A.3 Conclusion

Data from the elemental and structural composition of the stiff, non-calcified sample were in agreement with literature studies proposing that the macroscopic increase in wall thickness observed in the ageing arteries is associated with increased

collagen expression as a repair mechanism for the degeneration in the elastin fibres[1] (hypothesis not study in this project).

Vascular stiffening is a universal change associated with advancing age and develops from a complex interaction between structural and cellular elements of the vessel wall. These vascular alterations are influenced by the mineral status of the organism. Stiffness does not seem to occur uniformly along the aortic wall, which is evidenced by the clear differences between the elemental concentration in the lesion sites and the surrounding areas. Moreover, the elemental analysis indicated a very different and characteristic mineral profile between abnormal aortas dependent on the presence of calcified deposits in the arterial wall.

The data shown in this Appendix support the findings in the main thesis for a Si preventive role in ECM calcification.

A.4 References

1. Wagenseil, J.E. & Mecham, R.P. Vascular Extracellular Matrix and Arterial Mechanics. Physiological Reviews. 2009; 89 (3): 957-989.

2. Tohno, S.; Tohno, Y.; Minami, T.; Moriwake, Y.; Azuma, C. & Ohnishi, Y. Elements of Calcified Sites in Human Thoracic Aorta. Biological Trace Element Research. 2002; 86 (1): 23-30.

3. Bobryshev, Y.; Lord, R. & Warren, B. Calcified Deposit Formation in Intimal Thickenings of the Human Aorta. Atherosclerosis. 1995; 118 (1): 9-21.

Appendix B : Elements age and gender correlations

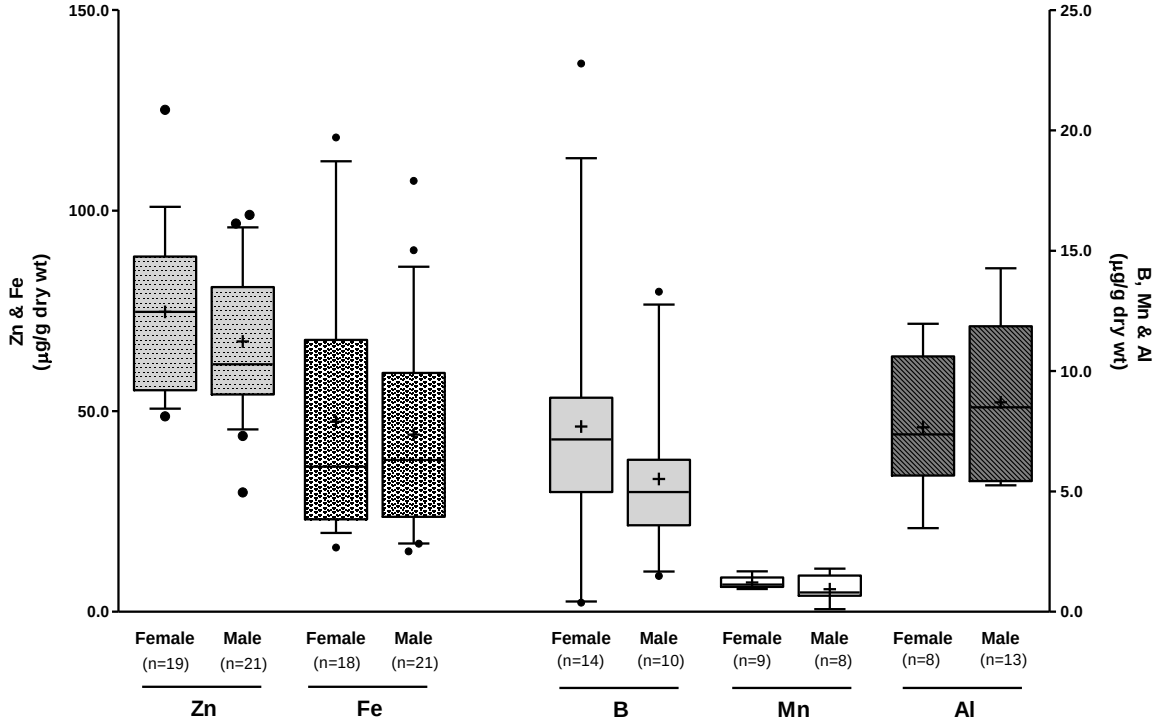

Figure B.1 - Gender distribution of Zn and Fe (left Y axis) and, B, Mn and Al (right Y axis) in the human aorta samples. Data is shown as box-plots, where the horizontal lines indicate 10th, 25th, 50th (or median), 75th and 90th percentiles; the plus signal shows the mean, n represents the number of subjects (female and male) in this study.

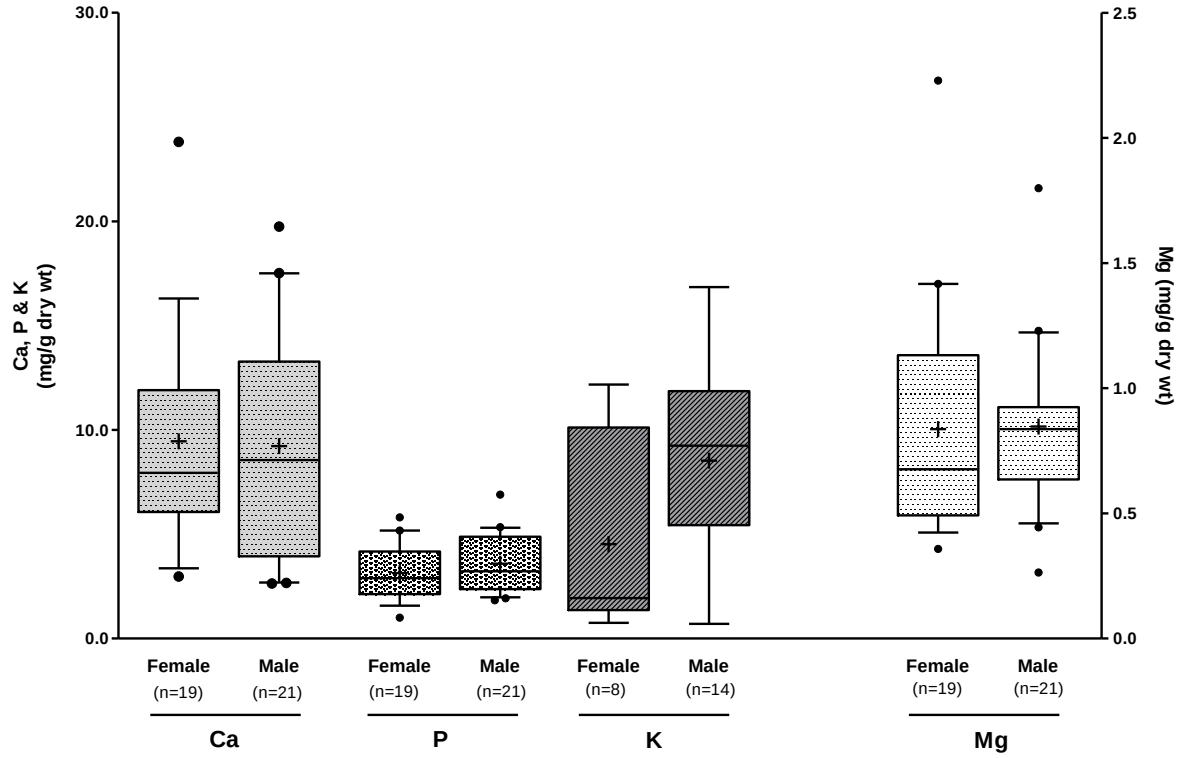

Figure B.2 - Gender distribution of Ca, P and K (left Y axis) and, Mg (right Y axis) in the human aorta samples. Data is shown as box-plots, where the horizontal lines indicate 10th, 25th, 50th (or median), 75th and 90th percentiles; the plus signal shows the mean, n represents the number of subjects (female and male) in this study.

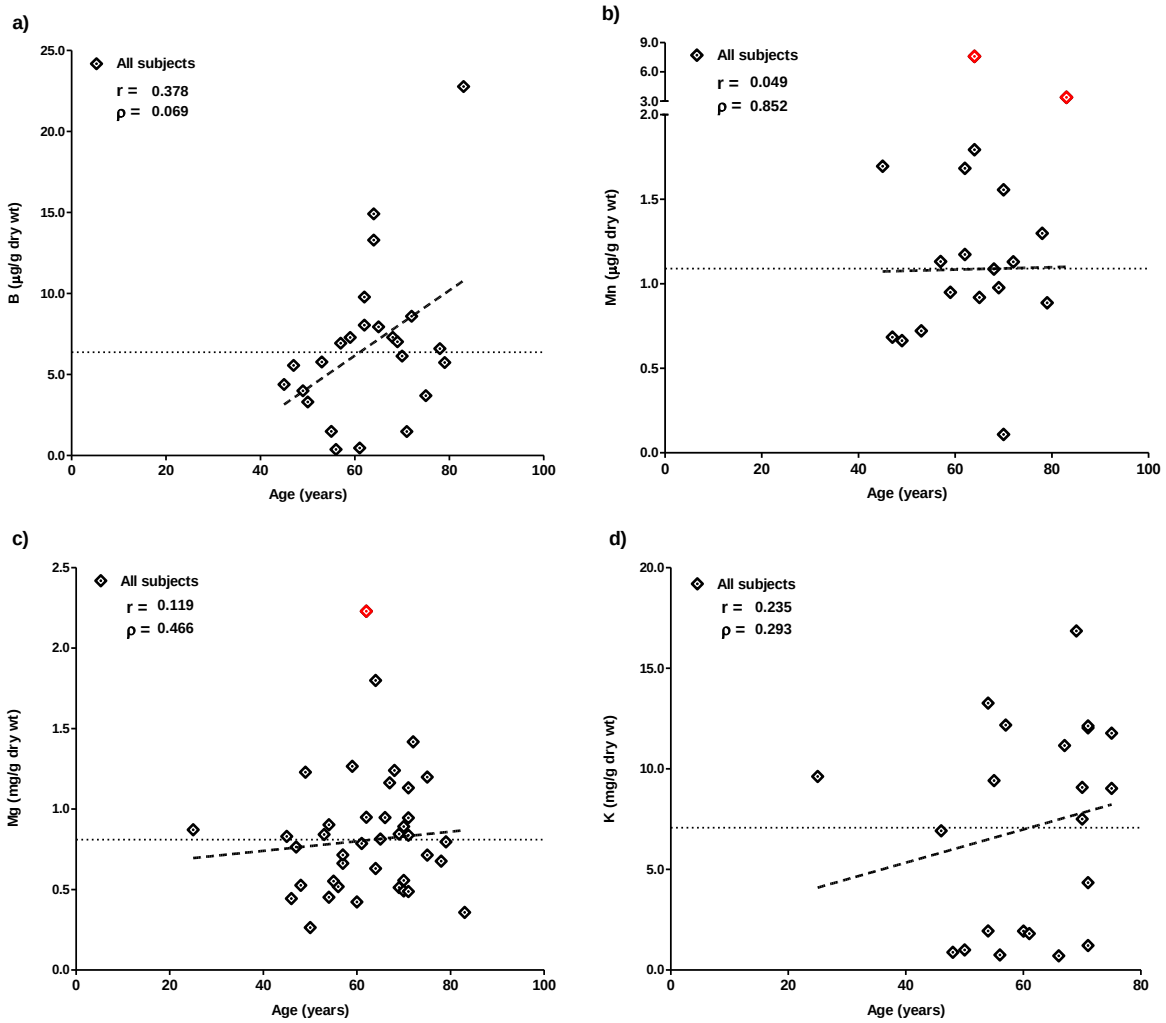

Figure B.3 - Changes in B (a), Mn (b), Mg (c) and K (d) concentrations in the aorta. Concentrations are represented for each subject and the dashed lines show the correlations with age. The thin horizontal dotted line shows the mean concentration for the element. Outliers are highlighted in red and were not included when carrying out the correlations. Spearman's correlation coefficients (r^2) and *P*-value are shown. Note: removing the value at 25 years did not affect the correlation shown.

Appendix C : Elements, elastin and BMI correlations

Table C.1 - Correlations between element concentrations, elastin concentrations and BMI in the human aorta samples. Spearman's correlation coefficient (r^2), corresponding *P*-value.

	Si	Zn	B	Mn	Cu	Fe	Al	Mg	Ca	P	Na	K	Elastin	BMI
Si														
P-value														
Zn	**0.211**													
P-value	*0.223*													
B	**0.495**	**0.579**												
P-value	*0.019*	*0.003*												
Mn	**0.288**	**0.211**	**0.471**											
P-value	*0.279*	*0.417*	*0.066*											
Cu	**0.438**	**0.523**	**0.805**	**0.542**										
P-value	*0.010*	*0.001*	*< 0.0001*	*0.025*										
Fe	**0.154**	**-0.103**	**0.270**	**-0.203**	**-0.131**									
P-value	*0.385*	*0.534*	*0.213*	*0.451*	*0.435*									
Al	**0.228**	**0.270**	**0.086**	**ND**	**0.321**	**0.369**								
P-value	*0.379*	*0.236*	*0.919*	*ND*	*0.156*	*0.100*								
Mg	**-0.108**	**0.279**	**0.298**	**0.109**	**0.378**	**-0.149**	**0.682**							
P-value	*0.536*	*0.086*	*0.167*	*0.688*	*0.019*	*0.372*	*0.001*							
Ca	**-0.202**	**0.226**	**0.217**	**-0.203**	**0.378**	**-0.003**	**0.805**	**0.650**						
P-value	*0.245*	*0.161*	*0.308*	*0.434*	*0.018*	*0.985*	*<0.0001*	*<0.0001*						
P	**-0.322**	**0.106**	**-0.071**	**-0.297**	**0.096**	**-0.019**	**0.882**	**0.694**	**0.895**					
P-value	*0.059*	*0.514*	*0.741*	*0.248*	*0.560*	*0.907*	*<0.0001*	*<0.0001*	*<0.0001*					
Na	**-0.067**	**0.089**	**-0.886**	**ND**	**0.283**	**-0.002**	**-0.197**	**-0.456**	**0.162**	**-0.089**				
P-value	*0.791*	*0.695*	*0.033*	*ND*	*0.202*	*0.994*	*0.391*	*0.033*	*0.471*	*0.695*				
K	**-0.049**	**0.351**	**0.486**	**ND**	**0.003**	**-0.039**	**0.204**	**0.418**	**-0.107**	**0.128**	**-0.755**			
P-value	*0.848*	*0.110*	*0.356*	*ND*	*0.990*	*0.863*	*0.375*	*0.053*	*0.636*	*0.570*	*<0.0001*			
Elastin	**-0.322**	**-0.083**	**-0.401**	**-0.041**	**-0.041**	**-0.006**	**-0.256**	**-0.229**	**0.094**	**-0.010**	**0.574**	**-0.532**		
P-value	*0.064*	*0.620*	*0.064*	*0.909*	*0.812*	*0.970*	*0.263*	*0.167*	*0.575*	*0.952*	*0.005*	*0.011*		
BMI	**-0.264**	**0.062**	**-0.342**	**-0.073**	**-0.064**	**-0.064**	**0.119**	**-0.080**	**0.150**	**0.067**	**0.063**	**-0.112**	**0.207**	
P-value	*0.132*	*0.709*	*0.110*	*0.948*	*0.664*	*0.703*	*0.606*	*0.633*	*0.361*	*0.684*	*0.782*	*0.619*	*0.219*	

Table C.2 - Correlations with Cu and Na concentrations in female and male human aorta samples. Spearman's correlation coefficient (r^2), corresponding *P*-value are shown

	Cu Females	Cu Males	Na Females	Na Males
Si	**0.603**	**0.298**	**0.036**	**0.118**
P-value	*0.013*	*0.229*	*0.963*	*0.735*
Zn	**0.472**	**0.514**	**-0.190**	**0.121**
P-value	*0.048*	*0.017*	*0.665*	*0.681*
B	**0.692**	**0.830**	ND	ND
P-value	*0.009*	*0.005*	*ND*	*ND*
Mn	**-0.333**	**0.952**	ND	ND
P-value	*0.385*	*0.001*	*ND*	*ND*
Cu			**-0.024**	**0.385**
P-value			*0.977*	*0.175*
Fe	**-0.005**	**-0.313**	**-0.095**	**0.191**
P-value	*0.985*	*0.167*	*0.840*	*0.513*
Al	**0.786**	**0.165**	**-0.452**	**0.027**
P-value	*0.028*	*0.590*	*0.267*	*0.929*
Mg	**0.566**	**0.312**	**-0.476**	**-0.367**
P-value	*0.018*	*0.169*	*0.243*	*0.197*
Ca	**0.265**	**0.412**	**-0.357**	**0.253**
P-value	*0.287*	*0.064*	*0.389*	*0.383*
P	**-0.024**	**0.286**	**-0.524**	**0.099**
P-value	*0.926*	*0.209*	*0.197*	*0.737*
Na	**-0.024**	**0.385**		
P-value	*0.977*	*0.175*		
K	**0.643**	**-0.130**	**-0.476**	**-0.692**
P-value	*0.096*	*0.659*	*0.243*	*0.006*
Elastin	**-0.615**	**0.455**	**0.429**	**0.464**
P-value	*0.009*	*0.038*	*0.299*	*0.095*
BMI	**0.488**	**0.231**	**0.381**	**0.143**
P-value	*0.047*	*0.313*	*0.360*	*0.626*

Appendix D : Elastin and collagen assay

D.1 Protocol for the Pierce Classic IP Kit

A. Tissue Lysis

1. Cut the tissue in ~10 mg pieces and freeze dry it.
2. Add 400 μL of 0.25M oxalic acid to the tissue and homogenize with an electric homogenizer, speed 4 for 1 min.
3. Rinse the blade with 600 μL of 0.25M oxalic acid.
   (Further extractions with 500 μL of 0.25M oxalic acid)
4. Incubate for 1 hour at 90ºC with plate agitation.
5. Centrifuge at ~11 000 rpm for 20 minutes to pellet the cell debris (centrifuge 5804R G03).
6. Carefully transfer the supernatant to a new tube for further analysis:
   a. Elastin quantification:
      50 μL of supernatant → Fastin Elastin Assay
   b. Protein quantification:
      50 μL of supernatant →NIPA assay
      (The amount of total protein per IP reaction is 30–50 μg)
   c. Immunoprecipitation assay (**OSA*p***):
      100 μL of supernatant + 52 μL NaOH 1M (freshly prepared) + 250 μL of 1x TBS Buffer
      pH: 7-8 (If further dilutions are necessary use 1x TBS buffer)

B. Pre-clear lysate using the Control Agarose Resin

1. Add 80 μL of the Control Agarose Resin slurry into a spin column.
2. Centrifuge column to remove storage buffer.
3. Add 100 μL of clearing solution to the column, centrifuge and discard the flow-through.
4. Add 300 μL of OSA*p* to the column containing the resin and incubate at 4ºC for 1 hour with gentle end-over-end mixing.
5. Centrifuge column at 4 000 rpm for 1 minute. Discard the column containing the resin and save the flow-through, which will be added to the immobilized antibody.

C. Capture of the antibody in the resin

1. Gently swirl the bottle of Pierce Protein A/G Agarose to obtain an even suspension. Using a cut pipette tip, add 30 μL of the resin slurry into a column.

2. Place column into a microcentrifuge tube and centrifuge at 4 000 rpm for 1 minute. Discard the flow-through.
3. Wash resin twice with 100 µL of cold 1x TBS Buffer. Discard the flow-through after each wash.
4. Gently tap the bottom of the spin column on a paper towel to remove excess liquid and insert the bottom plug.
5. Add 7 µL of antibody [10B8] to the spin column, plus 150 µL of 1x TBS Buffer. Attach the screw cap and incubate for 5 hours at 4^{0}C with gentle end-over-end mixing.
6. Loosen the screw cap, remove bottom plug and place the column in a collection tube. Centrifuge column and save the flow-through. **(Antibody fraction)**
7. Wash resin twice with 200µL of cold 1x TBS Buffer. Discard the flow-through after each wash.

D. Preparation of the Immune Complex

1. Add 250 µL of the pre-cleared solution (see section B.) to the spin column.
2. Incubate overnight (15-17 hours) at 4^{0}C with gentle end-over-end mixing.

   ---
3. Loosen the screw cap, remove bottom plug and place the column in a collection tube. Centrifuge column and save the flow-through. **(Collagen + Proteins)**
4. Add 200 µL of 1x TBS Buffer and centrifuge and save the flow-through. **(Collagen + Proteins 2**)
5. Wash the resin three times with 200 µL 1x TBS Buffer and centrifuge after each wash. Discard the flow-through after each wash.
6. Wash the resin once with 100 µL of 1X Conditioning Buffer. Centrifuge.

E. Elution of the Immune Complex

Low-pH elution:

1. Place the spin column into a new collection tube and add 100µL of Elution Buffer.
2. Cap the column and incubate for 10 minutes at 70^{0}C with gentle mixing.
3. Centrifuge the tube and collect the flow-through. **(Elastin)**
4. Perform 2 additional elutions.
5. Analyse each eluate separately to ensure that the antigen has completely eluted.

D.2 Protocol for the Hydroxyproline Collagen Determination

A. Preparation of the Reagents

1. **HYP Stock Solution**
    a. In 25 mL of 1 mM HCl add:
        i. HYP: 0.130g
    b. Store in 1mL aliquots at -20^{0}C
2. **Buffer Solution**
    a. In 10 mL of UHP water add:
        i. Sodium Acetate: 0.574g
        ii. Trisodium Citrate: 0.588g
        iii. Citric Acid: 0.0945g
    b. Adjust pH to 6,0.
    c. On the day of the assay:
        i. Dilute 3 mL of Isopropanol 50% in 2mL of buffer solution
3. **Oxidant Solution**
    a. On the day of the assay, in 1mL of buffer add:
        i. Chloramine T: 0.085g
4. **Erlich's Reagent**
    a. In 6 mL of perchloric acid 70% add:
        i. pDABA: 4.03g

    (this solution cannot be older than 4 days)
    b. On the day of the assay:
        i. Dilute 1 mL of pDABA in 3 mL of Isopropanol 50%

B. Freeze Drying

1. Pool together the collagenous fractions collected in the immunoprecipitation assay.
2. Transfer and freeze dry overnight in the glass vials of the microwave (MW) system.

C. Microwave Vapour Digestion

1. Prepare 10 mL of 6 M HCl and add it to the container of the MW system.
2. Place the samples in the container and leave it at -80^{0}C for 30 min.

a. MW digestion parameters - Temp: 150^{0}C; Power: 150 W; Time: 15 min.

D. Sample Reconstitution

1. Transfer the sample to an eppendorf tube by carefully adding a total volume of 200 μL of 50%isopropanol and pipetting the suspended residue.
2. Vortex until dissolution, and spin down the solution using a centrifuge.

E. Hydroxyproline Standards

Table D.1 – Hydroxyproline standards preparation and final amino acid (OH-Pro) concentration.

	HYP stock (μL)	Isopropanol 50% (μL)	Concentration (mg/mL)
C0	0	500.00	0
C1	3.85	496.15	0.04
C2	11.54	488.46	0.12
C3	23.08	476.92	0.24
C4	18.46	461.54	0.40
C5	48.08	451.92	0.50

F. Hydroxyproline Assay

1. In a 96 well-plate add:
    a. 10 μL of sample/standard solution
    b. 30 μL of buffer solution
    c. 10 μL of oxidant solution
2. Shake and leave at room temperature for 5 min.
3. Add 0.1 mL of Erlich's reagent.
4. Shake and incubate for 30 min at 60^{0}C.
5. Cool to RT for 10 min.
6. Read OD at 540 nm.

Appendix E : Silicon levels in the human skin

E.1 Background

Skin is the most extended and heaviest organ of the human body, acting as a barrier between the internal and external environment. Nutrition is one the most important factors that is involved in modulating skin health, and several studies have attempted to improve skin health by changing or manipulating the diet[1].

Human skin ageing is accompanied by many clinical signs, the most evident of which are dryness, colour changes, wrinkles and loss of firmness. These clinical manifestations reflect morphological and structural changes in the skin that can be broadly categorized as either photoageing or intrinsic ageing[2]. The first is the result of UV exposure. The second is similar to that occurring in most internal organs, including the aorta, and is clinically associated with irreversible tissue degeneration, with a marked decrease in collagen, glycosaminoglycans and proteoglycans, and elastin fibres degeneration[3].

High levels of silicon were found in rat connective tissues such as bone, aorta and skin[4]. Even though numerous observational studies have suggested the beneficial effects of silicon on skin health, no concrete evidence exists of the silicon mechanism of action of silicon in skin. Human supplementation studies, for example, have reported that when Si was administered orally a positive effect was observed in the skin surface and mechanical properties with significant improvement in the thickness and turgor of the skin and wrinkles[5, 6].

The only study investigating the silicon content of human skin dates back to 1927 and used gravimetric and colorimetric assays to determine the Si content. Brown and colleagues reported that silicon concentrations varied between 7.5 – 9.0 mg/g dry weight with a positive, although not significant, trend to decrease with

ageing[7]. However, the age of the study and the quantification method raises concerns about the validity of the values reported.

In this Appendix, the analytical results from a pilot study in human punch skin biopsies (VMS samples), obtained from and in collaboration with Dr Ian Wilkinson, are presented. Skin tissue bank samples (TB samples) were also obtained to evaluate possible ionic contaminations during skin sample collection and to assess the validity of the analytical method.

The main aim of this pilot study was to establish the changes in silicon levels in human skin with ageing and between genders.

Sample preparation and analytical methodologies were developed and optimized by Dr. Sylvaine Bruggraber in the BMR group at MRC-HNR, Cambridge, UK. At the same institution, samples were analysed for sodium, potassium, calcium and silicon content by ICP-OES by Miss Julia Schmidt and myself separately.

E.2 Methodology

E.2.1 Sample acquisition

H**u**man skin biopsies and skin tissue bank samples were provided by Dr Ian Wilkinson and Dr Viknesh Selvarajah from Addenbrooks' Hospital, Cambridge, UK. VMS skin biopsies were approximately 4-5 mm deep and sampled both the epidermis and dermis. They were collected from the lower back under local anaesthesia.

E.2.2 Elemental Analysis

The skin element concentrations of Na, K, Ca and Si were determined via ICP-OES (Jobin Yvon Horiba – ULTIMA 2000-2).

For element determination, samples were digested according to the following procedure: the skin samples were freeze dried overnight (Mini Lyotrap,

LTE scientific, Ldt, Greenfield, Oldham, UK) until constant weight. The dried material was accurately weighted to determine water content loss and then digested with 1:1 (v/v) mixture of high purity (69%) HNO_3 and high purity (40%) H_2O_2. The samples were incubated overnight at room temperature followed by a second incubation overnight in a water bath at 40°C. All samples were digested to completeness and diluted with 450 µL of a sample diluent consisting of 1% HNO_3 and 200 ppb strontium (Sr) as an internal standard. For the Na and K analysis and aliquot (100 µL) of previously digested and diluted samples were further diluted with water to a final volume of 1000 µL.

Sample blanks for control of the digestion process were prepared in a similar manner and analysed collectively with the samples. Two sets of multi-element standards (Na/K and Ca/Si) were prepared from 1,000 ppm aqueous stock solutions, with final concentrations per element ranging from 0 to 10 ppm in a diluent matched to the digested solution (9% (v/v) HNO_3 for Ca/Si standards; and 1.7% (v/v) HNO_3 for Na/K standards).

Peak profiles were used and the elements were measured at: 588.995 nm for Na, 766.490 nm for K, 393.366 nm for Ca, 251.611 nm for Si and 346.446 nm for Sr. The running conditions for the digested skin samples by ICP-OES are summarized in Table E.1.

Table E.1 - Running conditions of ICP-OES for the analysis of skin samples.

Analytical Conditions	Na/K	Ca/Si
RF power (W)	1000	1000
Plasma gas (L min^{-1})	12	10
Sheath gas (L min^{-1})	2	2
Auxiliary gas (L min^{-1})	0.0	0.0
Speed pump (rates min^{-1})	8	8
Nebulisation flow rate (L min^{-1})	0.02	0.02
Plasma stabilization time (s)	10	10
Number of replicates	3	3

Matrix effects were corrected using pooled sample-based standards (PSBS). Briefly, after elemental analysis by ICP-OES the remainder of the digested samples were pooled into two new tubes, one for Na/K analysis and the other for Ca/K analysis. Aliquots of the pooled samples were spiked with different concentrations (0 – 10 ppm) of the standard solutions, previously prepared for ICP-OES analysis.

The TB samples were digested and analysed by a similar procedure described above for the VMS samples. The TB samples were larger than the VMS samples, therefore the volumes of acid (HNO_3 + H_2O_2) and diluents were adjusted accordingly to the difference in weights.

Element concentration was measured in mg or µg of dry sample mass and corrected for matrix effect. The limits of quantification for the samples were restricted by the background levels of the elements analysed in the sample blanks of each batch: $\mathrm{LOQ} = \mathrm{mean}_{\mathrm{Blank}} + 3\mathrm{SD}_{\mathrm{Blank}}$.

E.3 Results

The demographic distribution of the punch skin biopsies (VMS) and the skin tissue bank (TB) samples analysed are described in Table E.2. Skin TB samples were collected from patients undergoing breast surgery and only female subjects were available.

Table E.2 - Subjects demographic data of the samples analysed in this study.

	VMS	**TB**
N	47	17
Gender		
Male	24	0
Female	23	17
Age		
Mean	43	43
Range	19 – 68	19 – 72

E.3.3 VMS vs TB

A total of 47 VMS and 17 TB skin samples were collected and analysed with an average dry weight of 8.5 ± 4.6 mg and 22.6 ± 10.6 mg, respectively. Na, K, Ca and Si concentrations (males and females) are shown in Table E.3 separately for the VMS and TB samples. When comparing the VMS and TB samples, VMS Ca and Si concentrations were significantly lower than TB samples.

In some VMS samples the Ca (n = 8) and Si (n = 6) contents were below the detection limit and thus the elements concentration was not determined. Moreover a Si contamination in one batch of the VMS samples was identified, and the results for this set of samples (n = 12) was not included here.

Table E.3 - VMS and TB skin samples concentrations of Na, K , Ca and Si. Mean values ± SD, range and total number of subjects.

	VMS‡			TB⍰		
	Mean ± SD	Range	n	Mean ± SD	Range	n
Na (mg/g)	7.10 ± 2.36	1.46 – 11.85	47	8.54 ± 2.35	5.46 – 13.74	17
K (mg/g)	2.55 ± 0.88	1.23 – 4.77	47	2.00 ± 0.62	0.93 – 3.49	17
Ca (mg/g)	0.32 ± 0.06 †*	0.18 – 0.49	40	0.70 ± 0.24	0.38 – 1.12	17
Si (µg/g)	9.67 ± 8.31 †**	1.57 – 36.15	30	16.13 ± 7.69	7.09 – 30.53	17

†Mean VMS vs TB: *P = 0.002; **P < 0.0001 (Mann-Whitney t test).
‡Female + male donors/cohort.
⍰Female donors/cohort

E.3.4 Age and gender variations

The elemental distribution per gram dry weight of tissue of the VMS skin samples as a function of age and gender were plotted in Figure E.1. Excluding silicon, similar behaviours were observed in the elements content between ageing males and females; sodium and potassium concentrations decreased and calcium concentration increased with ageing. Conversely, silicon levels appear to decrease in ageing males and increase in ageing females. No significant impact of age was found in the female and male element concentrations with the exception of Si in females (r = 0.736 and P = 0.01).

a)

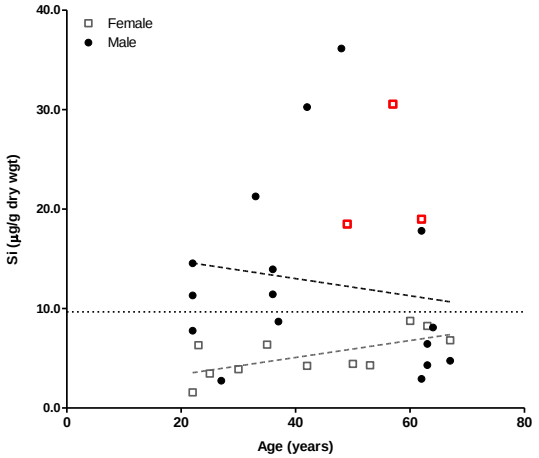
Female
Male
Si (µg/g dry wgt)
40.0
30.0
20.0
10.0
0.0
0
20
40
60
80
Age (years)

b)

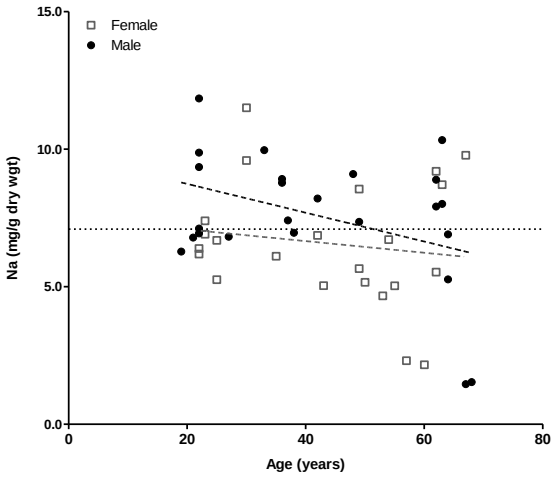
Female
Male
Na (mg/g dry wgt)
15.0
10.0
5.0
0.0
0
20
40
60
80
Age (years)

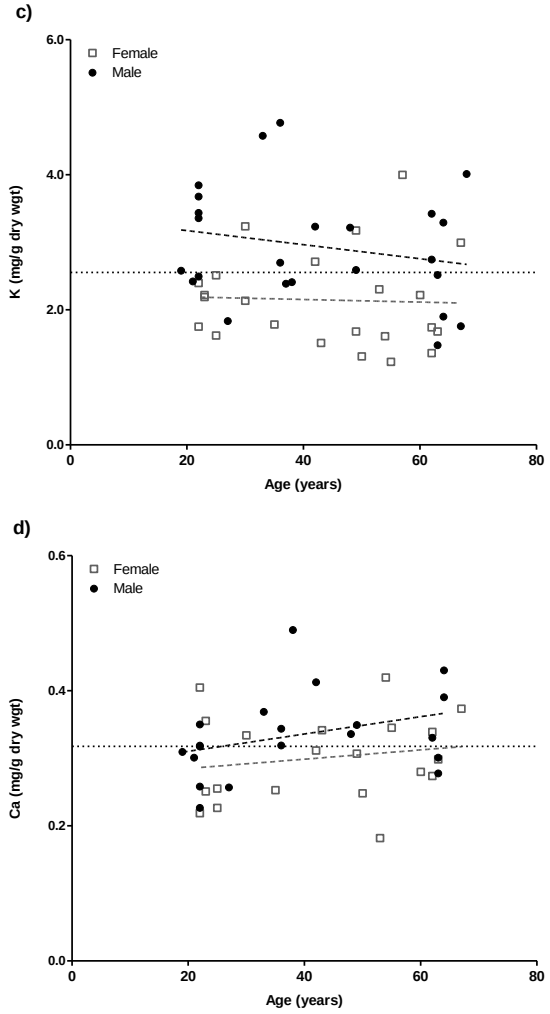

Figure E.1 - Age-related changes in Si (a), Na (b), K (c) and Ca (d) contents in VMS skin samplesfrom male and female donors. Concentrations are presented for each subject and the dashed lines show the best fit line through the data points (male and female) separately .The thin horizontal dotted line shows the mean element concentration (male and female). Outliers are highlighted in red and were not included when carrying out the correlation between the element content, ageing and gender (Spearman's correlation).

Overall, the mean element concentrations in male VMS skin samples were higher than in females. However, only for Na, K and Si where these differences statistically significant, $P = 0.03$ for Na; $P = 0.0007$ for K and $P = 0.02$ for Si (Figure E.2).

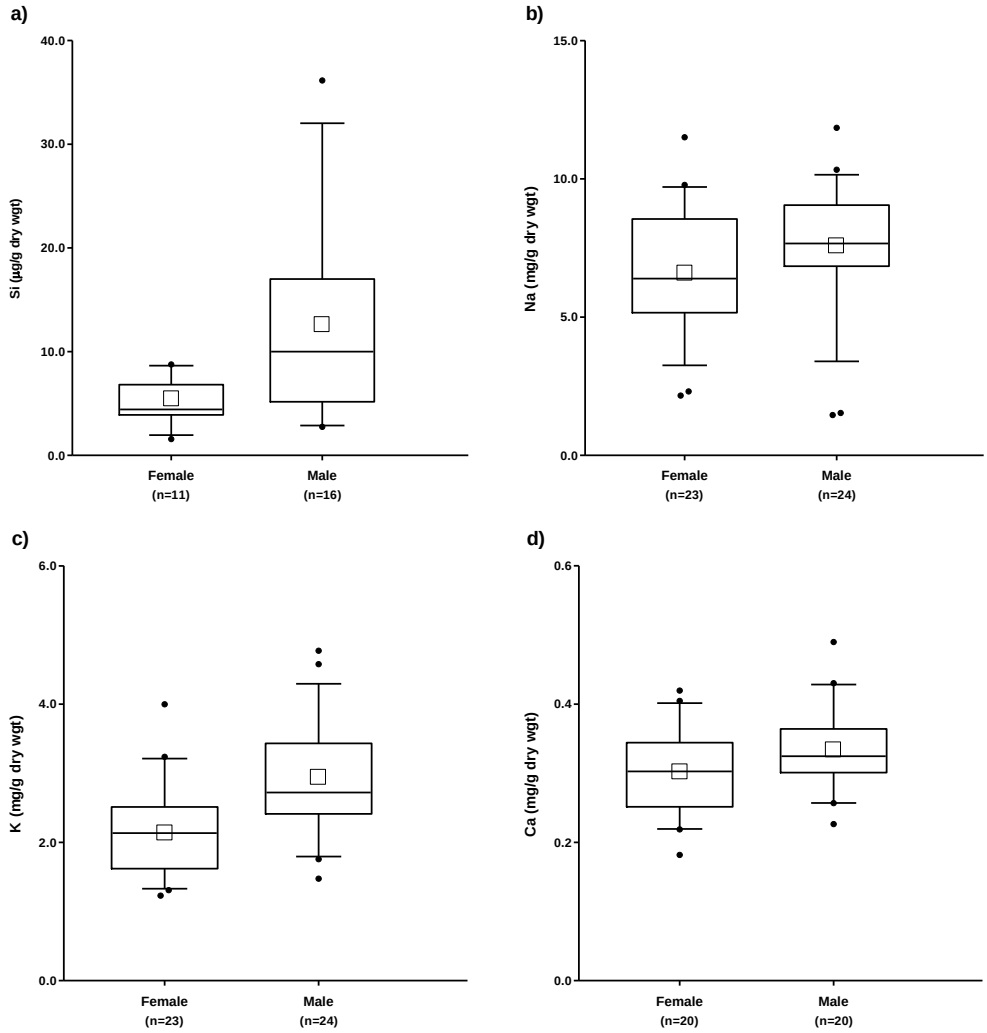

Figure E.2 - Gender differences in Si (a), Na (b), K (c) and Ca (d) concentrations in VMS skin tissue samples. Data is shown as box-plots, where the horizontal lines indicate 10th, 25th, 50th (or median), 75th and 90th percentiles; the open squares show the mean, *n* represents the number of subjects, female and male, considered in this study. Na, K and Si concentration were significantly higher in males compared with females (Na: $P = 0.03$, K: $P = 0.0007$ and Si: $P = 0.02$; Mann-Whitney *t* test).

E.3.5 Contaminations & method validity

The TB samples were analysed and compare with the VMS samples to evaluate possible contaminations during the collection and to assess the validity of the analytical method. Comparison between TB and VMS data (Figure A.3) was only performed for samples from female donors, on account that TB samples were only collected from female donors and considering the gender differences observed with the VMS samples (Figure E.2).

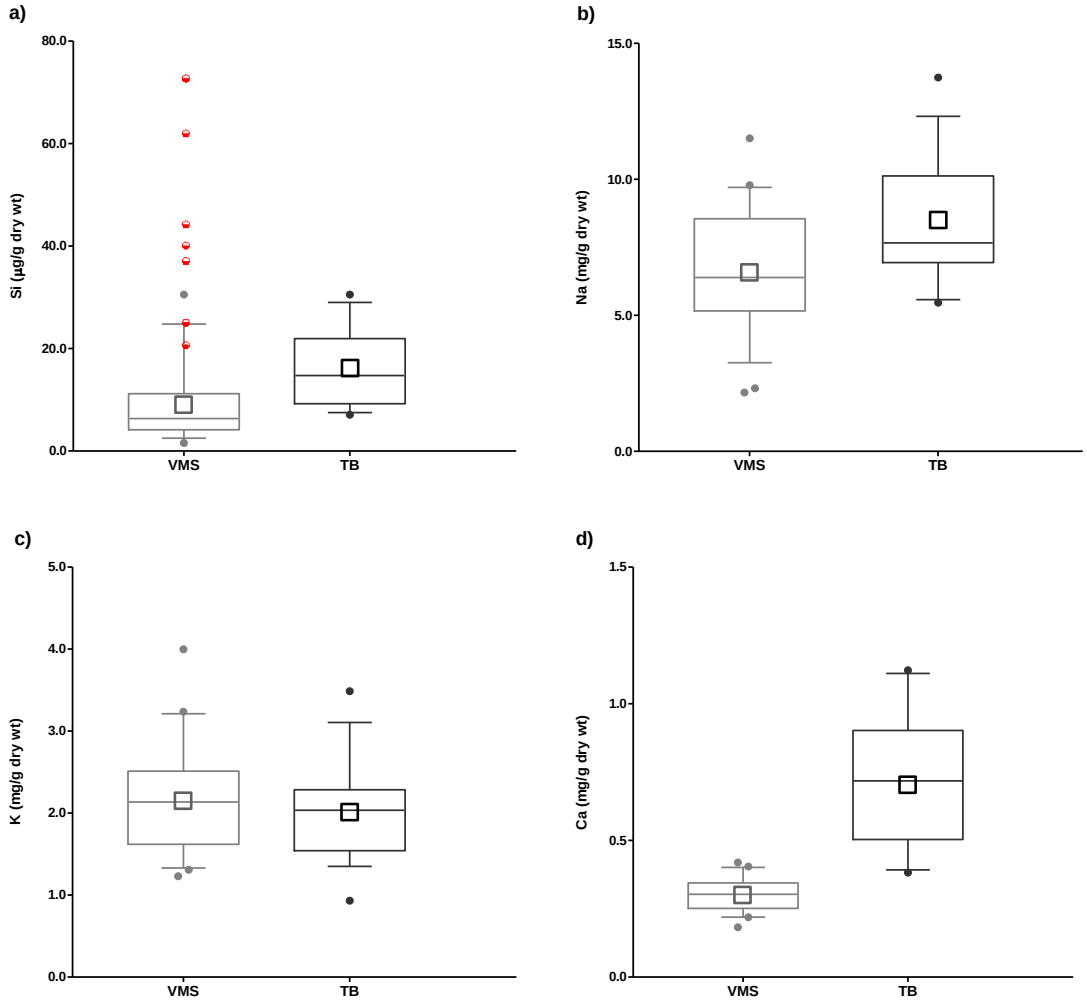

Figure E.3 – Comparison of the VMS and TB samples for Si (a), Na (b), K (c) and Ca (d). TB and VMS elemental concentrations are presented for each female patient. Data is shown as box-plots, where the horizontal lines indicate 10th, 25th, 50th (or median), 75th and 90th percentiles; the open square shows the mean. In red are the VMS samples with suspected contamination.

The results represented in Figure A.3 mirrors the results previously reported of the mean differences between the TB and VMS samples (male plus female) (Table E.3), with marked differences in calcium and silicon concentrations with advancing age between the two groups/cohorts. Despite the differences in the absolute Si and Ca levels, the same trend with senescence is maintained between VMS and TB samples for these two elements.

The Si results from the contaminated VMS sample batch were clearly higher and with a wider concentration range when comparing to previous non-

contaminated batches. Subsequently, the contamination source was identified as being the sponge antiseptic applicator used for the collection of that specific batch of samples.

E.4 Discussion and Conclusion

The present pilot study investigated the effect of ageing and gender on Na, K, Ca and Si concentrations of the human skin. The results obtained suggested that males have generally higher skin Na, K and Si concentrations than females. This gender difference has also been previously reported in other human tissues for other trace elements[8].

Skin silicon levels in female donors were found to increase significantly with ageing in the VMS cohort, and although the trend was reproduced in the TB cohort, the increase was less pronounced and not statistically significant. The reduced number of admissible samples in the VMS cohort was too small (n = 11); some samples were not considered because the Si levels were below the analytical quantification limit and others were excluded due to sample contamination. For these reasons this information has to be carefully considered and a greater number of subjects/samples should be analysed before asserting any definite conclusions made.

Calcium levels were also found to increase with ageing. Aging of the skin involves dermal changes and this is associated with damage to elastic and collagen fibres. No literature information is available but, much like other connective tissues, progressive increase in Ca tissue levels may be associated with advancing age and ECM degradation/calcification.

Essential elements such as Na, K and Ca reported a more constricted range and a limited distribution in concentration between subjects when compared to Si, which may in part result from homeostatic regulation mechanisms for these essential elements. Silicon is a ubiquitous element and may be affected by

environmental factors, such as cosmetics and dietary factors, so a wider scatter in Si concentrations observed both in TB and VMS samples was to be expected. Surprisingly, males presented a wider scatter than females in both skin groups. Considering the body area were the samples were collected (VMS: lower back and TB: breast area) it is unlikely that VMS samples, contrary to TB samples, were contaminated by residues from cosmetic usage. In fact, Si intake in males has been proved to be higher due to beer consumption, a highly bioavailable source of Si, which may account for the wider distribution in Si levels in the VMS skin samples from males[9].

Trace-element determination, in most clinical specimens, represents a considerable challenge. Na and K occur in mg/g concentration in human skin. Therefore, with the adequate precautions against sample contamination during the collection and analysis, there are no other major analytical problems in the determination of these two elements. This is reflected by the similar results between the VMS and TB cohorts, which experience totally different collection procedures (VMS: punch skin biopsies and TB: breast surgery skin sample). Conversely, Ca and especially Si occur in lower levels in the human skin, being more susceptible to environmental sample contaminations. Although dramatic differences in absolute Ca and Si concentrations were observed between VMS and TB cohorts, the maintenance of the trend with ageing and the lower concentration range for these elements in the VMS cohort, suggests that the sample size difference between VMS (n = 47) and TB (n = 17) samples may be involved in the overall higher results for TB samples. Alternatively, and most likely, the difference in levels represent true differences in skin levels from two areas of the body: breast vs lower back.

In conclusion, the results present in this Appendix may not provide absolute values on skin silicon and calcium levels, however an increase in silicon levels with age in females was noted. These preliminary results need to be followed up in more detail and the subject number increased, both for male and female donors. No age-related changes were observed in the sodium and potassium concentrations, but males have a higher content of these elements when compared to female donors.

It is also important to reiterate the importance of careful sample collection and handling to prevent environmental contaminations, especially in elements with low tissue concentrations, such as calcium and silicon.

E.5 References

1. Boelsma, E.; van de Vijver, L.P.; Goldbohm, R.A.; Klöpping-Ketelaars, I.A.; Hendriks, H.F. & Roza, L. Human Skin Condition and Its Associations with Nutrient Concentrations in Serum and Diet. The American Journal of Clinical Nutrition. 2003; 77 (2): 348-355.

2. El-Domyati, M.; Attia, S.; Saleh, F.; Brown, D.; Birk, D.E.; Gasparro, F.; Ahmad, H. & Uitto, J. Intrinsic Aging Vs. Photoaging: A Comparative Histopathological, Immunohistochemical, and Ultrastructural Study of Skin. Experimental Dermatology. 2002; 11 (5): 398-405.

3. Bailey, A.J. Molecular Mechanisms of Ageing in Connective Tissues. Mechanisms of Ageing and Development. 2001; 122 (7): 735-755.

4. Adler, A.J.; Etzion, Z. & Berlyne, G.M. Uptake, Distribution, and Excretion of 31silicon in Normal Rats. American Journal of Physiology - Endocrinology And Metabolism. 1986; 251 (6): E670-E673.

5. Lassus, A. Colloidal Silicic Acid for Oral and Topical Treatment of Aged Skin, Fragile Hair and Brittle Nails in Females. The Journal of international medical research. 1993; 21 (4): 209-215.

6. Barel, A.; Calomme, M.; Timchenko, A.; De Paepe, K.; Paepe, K.; Demeester, N.; Rogiers, V.; Clarys, P. & Vanden Berghe, D. Effect of Oral Intake of Choline-Stabilized Orthosilicic Acid on Skin, Nails and Hair in Women with Photodamaged Skin. Archives of Dermatological Research. 2005; 297 (4): 147-153.

7. Brown, H. The Mineral Content of Human Skin. Journal of Biological Chemistry. 1927; 75 (3): 789-794.

8. Rahil-Khazen, R.; Bolann, B.J.; Myking, A. & Ulvik, R.J. Multi-Element Analysis of Trace Element Levels in Human Autopsy Tissues by Using Inductively Coupled Atomic Emission Spectrometry Technique (Icp-Aes). Journal of Trace Elements in Medicine and Biology. 2002; 16 (1): 15-25.

9. Jugdaohsingh, R. Silicon and Bone Health. Journal of Nutrition Health and Aging. 2007; 11 (2): 99-110.